Fatigue Properties and Reliability of SnAgCu-Bi Solder Joints in Varying Stress Amplitudes

by

Minghong Jian

A dissertation submitted to the Graduate Faculty of
Auburn University
in partial fulfillment of the
requirements for the Degree of
Doctor of Philosophy

Auburn, Alabama
May 1, 2021

Keywords: Fatigue, Reliability, Solder Joint, Isothermal Aging, Varying Amplitude

Approved by

Sa'd Hamasha, Chair, Associate Professor of Industrial and Systems Engineering
John Evans, Charles D. Miller Endowed Chair Professor of Industrial and Systems Engineering
Sean Gallagher, Associate Professor of Industrial and Systems Engineering
Michael Bozack, Professor of Physics

Abstract

The eutectic Sn-Pb solder alloys are widely used in the electronic packaging industry. However, they are being replaced by new near-eutectic solder alloys because of environment and health concerns associated with lead. The performance of solder alloys can be improved by adding extra elements, such as nickel (Ni), bismuth (Bi), antimony (Sb), iron (Fe), indium (In), and aluminum (Al). Although much research has been done about mechanical, thermal, and fatigue properties of these solder alloys using the accelerated tests, the performance of individual solder joints under realistic service condition needs better understanding. Because the stress amplitude of solder joint will be frequently changed during its real service life, it is necessary to test the solder alloys under the varying amplitude condition in the accelerated test. Our study is focusing on the fatigue performance of individual SAC-Bi solder joints with isothermal aging under varying stress amplitude condition. Background introduction and literature review will be introduced in Chapter 1, Chapter 2, and Chapter 3. Chapter 4 will focus on explaining the experiment design and analysis method of our study.

In Chapter 5, three kinds of individual SAC-Bi solder joints along with SAC305 (Sn-3.0%Ag-0.5%Cu) were tested with Organic Solderability Preservative (OSP) surface finish under four single stress amplitudes condition. In this research, their fatigue properties were compared in aspect of inelastic work, plastic strain, and microstructure. Their characteristic fatigue life was investigated using Morrow Energy model and Coffin-Manson model. Typically, SAC-Q and SAC-I showed more fatigue resistance than SAC305 and SAC-R. SAC-Q and SAC-I showed similar fatigue performance, so we believe that the addition of Ni and Sb does not influence fatigue

performance of SAC-I individual solder joints and Bi is the main reason. Also, a power equation of characteristic life versus stress amplitudes was fitted and we were able to find any characteristic life associated with a specific stress amplitude, which was a good reference for the following study in varying stress amplitude test.

In Chapter 6, we focused on the fatigue performance of SAC-Bi solder alloys (SAC305, SAC-Q, and SAC-R) under varying stress amplitude conditions. Typically, all the individual SAC-Bi solder joints were failed earlier than expected according to common damage accumulation model. SAC-Q showed better fatigue resistance than SAC305 and SAC-R under varying stress amplitude conditions. Hysteresis loops (Inelastic Work & Loading Slope) under varying stress amplitude conditions were analyzed. And they were compared with the case of single stress amplitude conditions. Basically, inelastic work was observed to step up after every switch between mild stress cycles and harsh stress cycles. Loading slope was observed to step down after every switch between mild stress cycles and harsh stress cycles.

In Chapter 7, we focused on the aging effect on the fatigue of SAC-Bi solder alloys (SAC305, SAC-Q, and SAC-R). After aging for 10 hours and 1000 hours aging under 125℃, all the solder alloys' fatigue life were reduced under single stress amplitude test, especially SAC305. SAC305's characteristic life under each single stress amplitude test would drop up to 60%. However, SAC-Q and SAC-R were seldomly influenced by aging in single stress amplitude test. Bi was believed as the main reason considering their compositions. Similar phenomena were observed under varying stress amplitude test. SAC305's characteristic life (Switches) was significantly reduced after 10 hours aging and 1000 hours aging under 125℃. We could see a decreasing trend of characteristic life (Intervals), though that decrease was not significant. The more important is, all

the solder alloys after aging were failed earlier than expected using common damage accumulation model. It indicates that a more accurate fatigue model is essential for individual solder joints under varying stress amplitude conditions.

In Chapter 8, we focused on the fatigue modeling of aged individual SAC-Bi solder joint under varying stress amplitude conditions. Because the “Step-up” phenomena of inelastic work were observed, we got a modified fatigue model based on the common damage accumulation model. In the proposed model, amplification factor was considered to quantify the amplification of inelastic work after every switching between mild and harsh stress cycles under varying stress amplitude conditions. For SAC-Bi solder alloys (SAC305, SAB-Q, and SAC-R), the amplification factor would increase linearly with the crack initiation and dramatically rise after crack propagation until total failure. The cut-off points were analyzed for all the cases and the results indicated that SAC-Q’s amplification factor would increase linearly in 83% of its total life, significantly higher than the cases of SAC305 and SAC-R. Additionally, we were surprised that the aging time would not significantly influence the cut-off point for different SAC-Bi solder alloys. Finally, the proposed fatigue model was showing better estimation of damage accumulation, when comparing with the common damage accumulation models.

Acknowledgements

I would like to sincerely appreciate to my advisor Dr. Sa'd Hamasha. I am extremely thankful for his years of help, guidance, and support during my academic career. Without his inspiration and encouragement, it is impossible for me to complete all the graduate study. Also, I would like to extend my appreciation to my committee members, Dr. Michael Bozack, Dr. John L. Evans, Dr. Sean Gallagher, Dr. Elvan Ceyhan for their valuable suggestions and time. Meanwhile, I would like to thank all my lab-mates, co-workers, and friends: Dr. Sinan Su, Mohamed El Amine Belhadi, Xin Wei, Dr. Francy John Akkara, Dr. Anto Raj and Dr. Raed Alathamneh.

In addition, I would like to appreciate my parents, Mr. Haiquan Jian and Mrs.Chun Liu. I still remember it was you that rise me up, educated me, inspired my interest of engineering, gave me the opportunities to study abroad and endlessly support my decisions.

Of course, I am indebted to my wife, Mrs. Zhaohui Jin. I feel very lucky to meet you in my life. You always gave me your smart suggestions and help me to make the right decisions all the time. I truly appreciate your understanding, accompany, and support.

Finally, I would like to offer my best respect to Auburn University and Industrial & System Engineering Department!

War Eagle!

Table of Contents

List of Tables

List of Figures

List of Abbreviations

IC	Integrated Circuit
I/O	Inputs/Outputs
FC	Flip Chip
PCB	Printed Circuit Board
THT	Through-Hole technology
THC	Through-Hole component
SMT	Surface-Mounting technology
SMC	Surface-Mounting component
SQT	Statistical Quality Control
ALT	Accelerated Life Test
SOT	Small Outline Transistor
CTE	Coefficient of Thermal Expansion
SMD	Solder Mask Defined
NSMD	Non-Solder Mask Defined
OSP	Organic Solderability Preservative
ENIG	Electroless Nickel Immersion Gold
ImAg	Immersion Silver
HASL	Hot Air Solder Leveling
IMC	Intermetallic Compounds
LCF	Low Cycle Fatigue
HCF	High Cycle Fatigue

Chapter 1 General Introduction

1.1 Electronic Packaging

Electronic packaging is defined as the combination of engineering and manufacturing technologies required to convert an electronic circuit into a manufactured assembly [1]. Also, the electronic circuit is called an Integrated Circuit (IC), which is an assembly of electronic components in which there are many electronic devices and their interconnections. Generally, the electronic packaging is classified into 4 levels as below:

Level 0: Gate-to-gate interconnections on the silicon die

Level 1: Chips or ICs packaging

Level 2: Assembly multiple chips or ICs packaging on Printed Circuit Board (PCB)

Level 3: Assembly multiple PCBs on the motherboards or backplanes

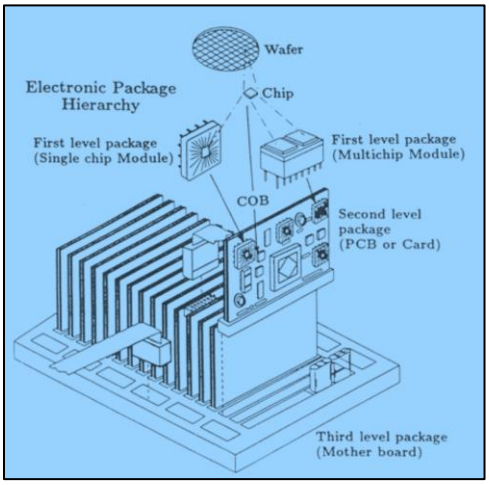

Figure 1-1 Classification of Electronic Packaging Structure

In Figure 1-1, the chips will be assembled on the packages normally by some technologies like the wire bonding technology, the tape automated bonding technology and the Flip-Chip (FC) technology in Level 1. Then the packages with the chips are connected with the PCBs in Level 2. The commonly used technologies are Through-Hole technology (THT) and Surface-Mounting technology (SMT). Finally, the PCBs with many chip packages will be installed on the motherboards in Level 3. All these assemblies and packaging technologies are made for providing better protections, heat dissipations, signal distributions and power distributions for the electronic product [2].

1.2 Reliability of Electronic Product and Packaging

Generally, reliability is defined as the ability of a system or product to perform its designed functions under stated conditions for a specific time. In the case that most of electronic products are applied under the extreme, complex, and varying conditions, electronic products must run stably and continually according to the desired design with thousands of electronic packages inside of them. Once any of electronic packages fails, electronic product cannot function properly. Therefore, high performance and high reliability of packaging are required since modern electronics' demand of more functions and lower volumes are increasing. Normally, a reliability test is conducted to assess the reliability of electronic product and packaging, such like thermal cycling test, vibration test, drop test, aging test, etc. Most of reliability tests' conditions will be designed more extreme than realistic service life, and thus more failures will be generated in limited time and costs. After that, reliability analysis will be done to identify the weakest part of electronic product, and to assess failure probability, and to predict expected service life of

electronic product. Based on the demand on reliability of electronic product, people classified electronic product into three categories [3]:

Class 1: General Electronic Products. Includes products suitable for applications where the major requirement is function of the completed assembly.

Class 2: Dedicated Service Electronic Products. Includes products where continued performance and extended life is required, and for which uninterrupted service is desired but not critical. Typically, the end-use environment would not cause failures.

Class 3: High Performance Electronic Products. Includes products where continued high performance or performance-on-demand is critical, equipment downtime cannot be tolerated, end-use environment may be uncommonly harsh, and the equipment must function when required, such as life support or other critical systems.

1.3 Surface Mounting Technology and Reliability of Surface Mounting Packages

Electronic product with more functions and less volume implies the requirement of more Inputs/Outputs (I/O) and less assembly volumes in electronic packaging. Therefore, SMT were widely used and gradually replacing THT. And the SMT's reliability is always a hot topic. Before discussing it, we need to briefly introduce what is the SMT.

Comparing to THT in which the components with leads are inserted into circuit boards, SMT is used to mount electronic components on the surface of printed circuit boards or substrates [4]. However, SMT cannot be available for all the components and it is normally used with THT together. Therefore, there form three types of SMT assembly [4]:

Type I: Only contains surface mount component.

Type II: Combination of Type I and Type III.

Type III: Only discrete surface mount components glued to the bottom side.

Though SMT gives more flexibilities and possibilities in the electronic packaging, the limitations of this technology deserve people's attentions. For example, if a board has thermal problems, SMT will aggravate thermal concentration since it increases the numbers of components per area. Also, the initial investment of manufacturing and testing equipment is essential to implement this technology [4]. Besides, many plastic components are prone to absorb moisture, and the absorbed moisture will expand and crack the package during the reflow soldering process (above 200℃) in SMT. What is more, the main issue of SMT is the package and connection reliability. The increasing number of solder joints will significantly reduce electronic system's reliability. It means that higher reliability requirement for each solder joint is prerequisite condition of high reliability of electronic system using SMT. In other words, the reliability of solder joints will determine the reliability of Surface-Mounting packages, and thus it will generally determine the reliability of an electronic product or system. Thus, many researchers are making efforts to improve the reliability of SMT by controlling the manufacturing/assembling process and improving the properties of solder material. For instance, Statistical Quality Control (SQC) are applied to minimize the defects in manufacturing and assembling. Various elements are added to develop new solder alloys with better performance.

1.4 Reliability of Solder Joints and Varying Amplitude Loading Test

As it is said, solder joints play critical roles for SMT, electronic product, and system, because solder joints serve both mechanical and electronic support for electronics [5, 6, 7]. However, heat and temperature variations will reduce the reliability of solder joints due to mismatched Coefficient of Thermal Expansion (CTE) between the components and substrates [8]. Besides, moisture, shock and vibration in the realistic service condition will simultaneously induce more forces that will accelerate the breakdown of weakest solder joints [8]. To specify solder joints' endurance to these forces, the reliability models are widely used to quantify the characteristic fatigue life of solder joints in electronic industry. However, same solder alloy will not form identical solder joints even if they are going through identical reflow process. The main reason is randomly formed grain orientation of each solder joint. Therefore, large amount of data will be needed, but it will spend much time and money. Therefore, to assess the reliability of solder joint, solder joints are normally tested in the Accelerated Life Test (ALT) by aggravating the service conditions for discovering more failures and defects in a short time. Furthermore, electronic product will fail once any of solder joints within the electronics fails. Thus, many researchers are more interested in when the first failure will happen. It indicates when the electronic product will fail, and it will normally refer to the time until 1% cumulative failure [9].

So far, many electronics were designed and manufactured by referring to the results of single stress amplitude reliability test. We believe that electronic products and systems will perform better in reality when they perform better in single stress amplitude reliability test. However, the realistic service conditions are different from that of single stress amplitude reliability test, because service conditions in real life will keep varying according to temperature, vibration, and humidity, etc.

Therefore, many studies focus on not only single stress amplitude test but varying stress amplitude test. In general, varying stress amplitude can be categorized into, the Simple Variable Amplitude Load histories, the Block Load histories, and the Random Load histories (See Figure 1-2). Normally, the Random Load histories are recorded and stored by specific transducers, but it is not always straightforward to implement the test with random load. Thus, the Random Load histories will usually be simplified to the Block Load histories or Simple Variable Amplitude Load histories. The main difference between the single and varying load histories is the load interaction and sequence effect on the reliability of solder joints. Therefore, the benchmark based on the single stress test can be misleading without full understanding of loading history and it is essential to exam solder joint under varying stress amplitude cycling.

	Load type	Representation
Random Loading	Spectrum	
Block Loading	low-high	
	high-low	
	low-high-low	
Simple Loading	Single OL	
	Sequence of OL's	
	Periodic sequence of OL's	
	Single UL	
	Sequence of UL's	
	Periodic sequence of UL's	
	OL - UL	
	UL - OL	
	Periodic OL - UL	
	Periodic UL - OL	

Figure 1-2 Categories of Varying Amplitude Loading

1.5 Fatigue Properties and Doped Solder Alloy

Solder alloy is the main composition of solder joints in electronic and thus the properties of solder alloys, especially the fatigue properties, will be the key for the reliability performance of solder joints in the realistic service life. The fatigue failure is one of the most common failures in electronic products, which is defined as the failure of a material caused by the repeated loads much less than the strength of the material. Basically, the kind of force endured by solder joints under the realistic service condition is usually not as high as the strength limit of solder joints. However, it will lead to stress concentrations at the weakest part of solder joints, and then initializes cracks, and eventually propagates the cracks until fatigue failure. When some electronic products are required to work under large variations of temperature and vibrations, both thermal fatigue properties and mechanical fatigue properties of solder joints are important for electronic products' reliability. Besides, most of electronic components will produce large amount of heat and the working temperature of some electronic products will be high. It indicates that solder alloys must also provide excellent fatigue properties under aging conditions.

For extending the service life of solder joints and improving some specific properties of solder joints, various elements have been applied to form high performance alloys, which is called solder doping. In the past, the most popular solders were lead-based alloys due to their outstanding chemical, physical, thermal, and mechanical properties [10]. However, the whole industry was looking for substitute material because of the critical effect of lead on human health and environment [10, 11, 12, 13, 14, 15]. In the beginning, Sn was kept and people were using Cu, Ag, Zn, Al, etc., instead of Pb to form new binary solder alloys. However, it has been proved that the multiple-component alloys are able to provide more desired mechanical and physical properties

than the binary solder alloys [10, 16, 17]. In general, the new solder alloys with additional elements to the Sn-based system are supposed to satisfy the following requirements [10]:

1) Reduce the surface tension of pure Sn to improve the wettability.
2) Enable quick formation of Intermetallic Compounds (IMC) between solder and substrate by diffusion.
3) Improve upon the ductility of Sn.
4) Prevent the transformation of b-Sn to a-Sn, which causes unwanted volume change and degrades structural integrity and reliability of solder.
5) Keep the melting temperature around 183 degree with eutectic or near-eutectic composition, in instances where the liquid phase can transform into two or more solid phases.
6) Improve mechanical properties (e.g., creep, thermo-mechanical fatigue, vibration, and mechanical shock, sheared and thermal ageing).
7) Prevent the occurrence of excessive tin whisker growth.

1.6 Problem Statement

The reliability of solder joint is often the bottleneck and limit of electronics' reliability. ALTs are widely used in many studies to assess solder joints and electronic packaging's reliability. Generally, better performance of solder joints in ALTs is assumed to indicate better performance under realistic service condition. However, it is not always true because the results of ALTs are used for extrapolating the performance under realistic service conditions. In ALTs, accelerate factors will be quite different with various factors such as, alloys, dimensions, surface finishes, test parameters, etc. The aim of ALT is to generate more failures and defects with limited time and

resources, but the result of ALTs may be misleading if we ignore some critical factors. Better ALTs are required to be designed to assess the reliability of electronic packaging under realistic service conditions.

In addition, many studies were using bulk material instead of individual solder joints in the ALTs. However, it has been approved that crack propagations, energy accumulation models, and distribution of precipitates are different between the bulk materials and individual solder joints [18, 19]. Despite same solder alloy and reflow process, individual SAC solder joints will vary a lot with each other because of random grain orientation and anisotropy of microstructure. Moreover, single stress/strain amplitude is applied in common ALTs, while realistic service conditions are more complex. It is not necessarily true that solder joints' fatigue will keep consistent in the single stress amplitude test and real service life. It is essential to find a method to correctly interpret ALT's result and better predict the reliability of electronic assembly in real service condition.

Many models were proposed to extrapolate ALT's result to real service conditions. One of the most famous models is Miner's rule. It is based on damage accumulation concept, but its critical problem is that it assumes that the loading history has no effect on fatigue. However, it has been proved that characteristic fatigue life predictions are incredible if ignoring the interaction effect of the varying stress amplitudes [19]. Therefore, it is urgent to find a more accurate fatigue model to predict fatigue life of solder joints, especially in varying stress amplitude cycling.

Sn-Ag-Cu is one of the most popular commercial solder alloys in the market. Much research was done based on the Sn-Ag-Cu alloy due to its low melting temperature, good mechanical properties, and low costs [13, 20]. And many kinds of element, such like Sb, Bi, Ni, Al, Fe, etc., have been

doped into Sn-Ag-Cu system to strengthen some properties of alloys. Many studies have investigated their fatigue performance under thermal cycling and mechanical cycling. But limited research has been done related to the fatigue of solder joints under varying isothermal mechanical cycling conditions. And it is not clear how individual solder joints, especially SAC-Bi, perform under isothermal varying stress amplitude conditions.

Additionally, a limited amount of research has investigated how aging influences the fatigue of individual SAC-Bi solder joint under varying amplitude stress conditions. Generally, aging cannot be entirely avoided in solder joints' real service life. And we had no idea how doped Bi would influence the fatigue of aged SAC solder joints under both single and varying stress amplitude conditions.

1.7 Research Objectives

The motivation of this research is to improve the understanding of aged individual SAC-Bi solder joints' reliability under varying stress amplitude conditions. Therefore, it was firstly expected to figure out how aged individual SAC-Bi solder joints would perform under single stress amplitude conditions. Secondly, we were interested in the fatigue of individual SAC-Bi solder joints and the effect of aging on SAC-Bi solder joints under varying stress amplitude condition. At last, we were looking for a fatigue model to estimate fatigue life of aged individual SAC-Bi solder joints under varying stress amplitude conditions. To answer the questions above, the following objectives would be achieved in this research:

1. Develop the appropriate reliability test for aged individual SAC-Bi solder joints under single and varying stress amplitude conditions.

2. Conduct reliability analysis of aged individual SAC-Bi solder joints under single and varying stress amplitude conditions.
3. Reveal and compare the fatigue of aged SAC-Bi solder alloys under single and varying stress amplitude conditions.
4. Study the effect of aging time and varying stress amplitude condition on the fatigue of individual SAC-Bi solder joints.
5. Identify precipitates and IMC layers of aged individual SAC-Bi solder joints and identify failure modes under single and varying stress amplitude conditions.
6. Develop the appropriate model to predict the fatigue life of aged SAC-Bi solder alloys under varying stress amplitude conditions.

1.8 Dissertation Organizations

In this dissertation, there will be 9 chapters. Chapter 1 will give a general introduction about the problem statement and research objectives. Chapter 2 will focus on the background review of electronic packaging, reliability tests, and analysis. Chapter 3 will be the literature review of the outlines of studies by the others including the solder materials' properties and fatigue models. Chapter 4 will describe the detailed experiment design and analysis methods. Chapter 5 will focus on the fatigue analysis of individual SAC-Bi solder joint under single stress amplitude conditions. Chapter 6 will focus on the fatigue of individual SAC-Bi solder joint under varying stress amplitude conditions. Chapter 7 will focus on the effect of aging on fatigue of individual SAC-Bi solder joint under single and varying stress amplitude conditions. Chapter 8 will focus on the fatigue modeling analysis of aged individual SAC-Bi solder joint under varying stress amplitude conditions. Chapter 9 will summarize the work of dissertation and some guideline for future work.

Chapter 2 Electronic Manufacturing and Reliability Analysis

2.1 Electronic Assembly Technology and Components

In electronic industry, many flexible and reliable methods were developed to assembly electronic components on the ICs. Based on the mounting type, there typically exist two popular electronic assembly technologies in the history of the electronic industry. The first one is the THT. And the second one is the SMT. Both are widely used depending on the specific requirements of size, cost, performance, reliability, etc.

2.1.1 THT and Through-Hole Components (THC)

THT was first developed in 1950s, which is defined as the technology where components using leads are inserted into the plated through holes drilled in the ICs. Basically, the components with lead will be inserted into circuit board first, and fluxes will be applied on the back of circuit board. Then a preheat process is applied to active the flux and minimize the thermal shock of circuit board. At last, a wave soldering process is applied to form the solder joints after filling the through holes with solder material and forming fillets on both sides of circuit board (See Figure 2-1).

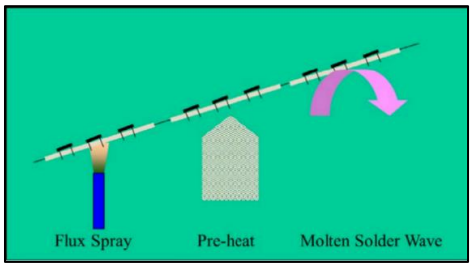

Figure 2-1 Waving Process of THT

Meanwhile, there are two types of THC: axial lead and radial lead components, which are shown in Figure 2-2. The axial components have a lead which run through the whole component and both ends of the component's lead wire are inserted into separate holes in the circuit. Therefore, it allows component to attach closer and flatter on the circuit board surface. Typically, carbon resistors, electrolytic capacitors, fuses, and LEDs are axial lead components as examples. On the other hands, the radial lead components have the leads normally projected from the same side of component, which occupies less surface area and gives the radial a vertical profile and a smaller printed wire footprint. Thus, radial lead components are more popular in high density circuit board. Figure 2-2 shows examples of both axial lead components (Upper left) and radial lead components (Upper right).

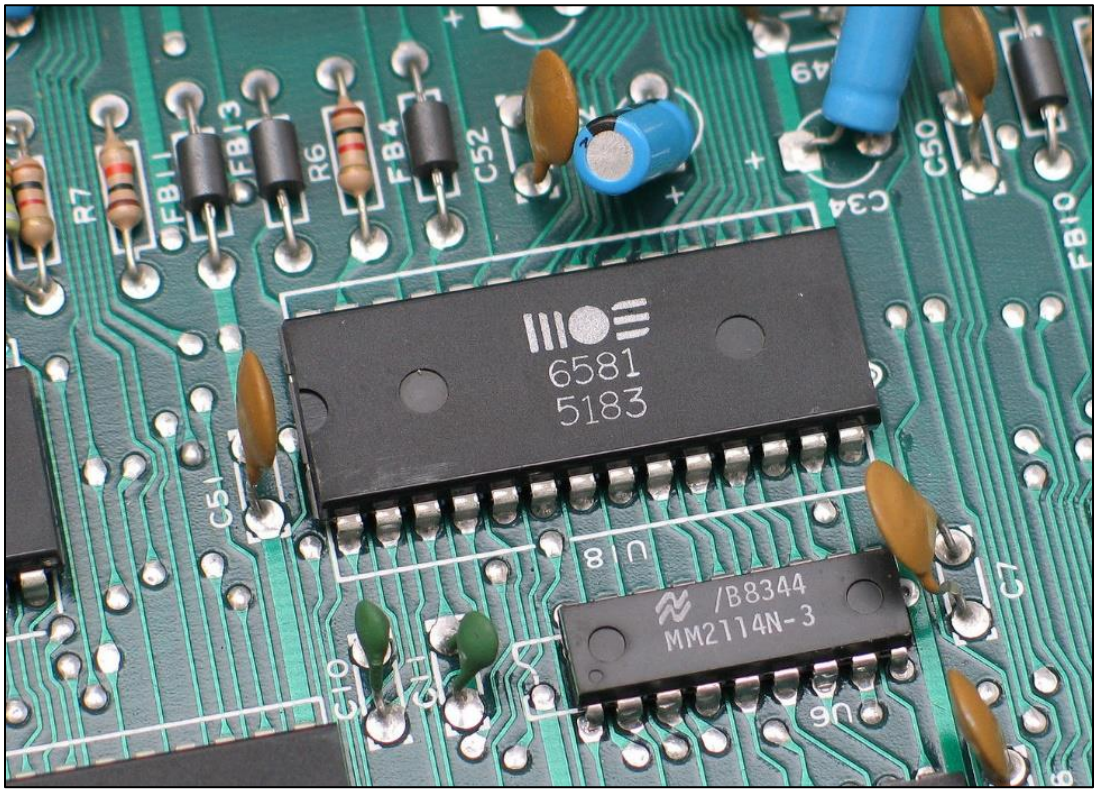

Figure 2-2 Example of Axial (Upper left) and Radial Lead Component (Upper Right)

2.1.2 SMT and Surface-Mounting Components (SMC)

SMT was developed a little later than THT, in the 1960s, and became popular in 1980s, because of the requirements of smaller size and the higher I/O density of electronic products. It made great contributions to changing the bulky and heavy electronic products to portable and light electronic products, with more and more functions. Basically, components are mounted directly on the substrate surface of circuit board using SMT, whereas components are inserted into the circuit board using the THT. As it was said in the 1st chapter, there are various types of surface mounting assemblies, but typical assembly contains three major steps: printing, placing, and reflowing (See Figure 2-3).

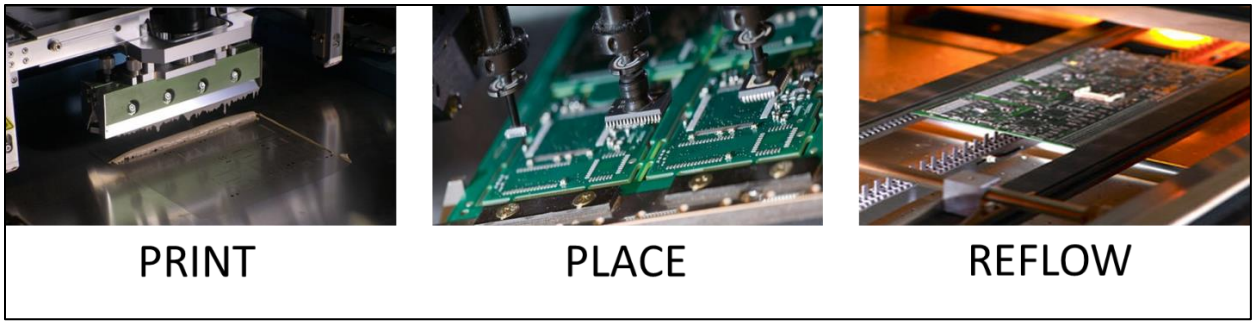

Figure 2-3 Surface Mounting Assembly Steps

Basically, in the printing process, the solder paste is firstly deposited on stencil, where the open hole is the position of solder joints (See Figure 2-4). Then SMCs are placed using picking and placing machines. At last, the PCBs and components will be reflow-soldered to build surface mount assembly. Normally, there will be extra cleaning and testing steps after the reflowing process. In addition, the waving soldering will be also applied at the suitable time, if there are some THCs on the circuit board.

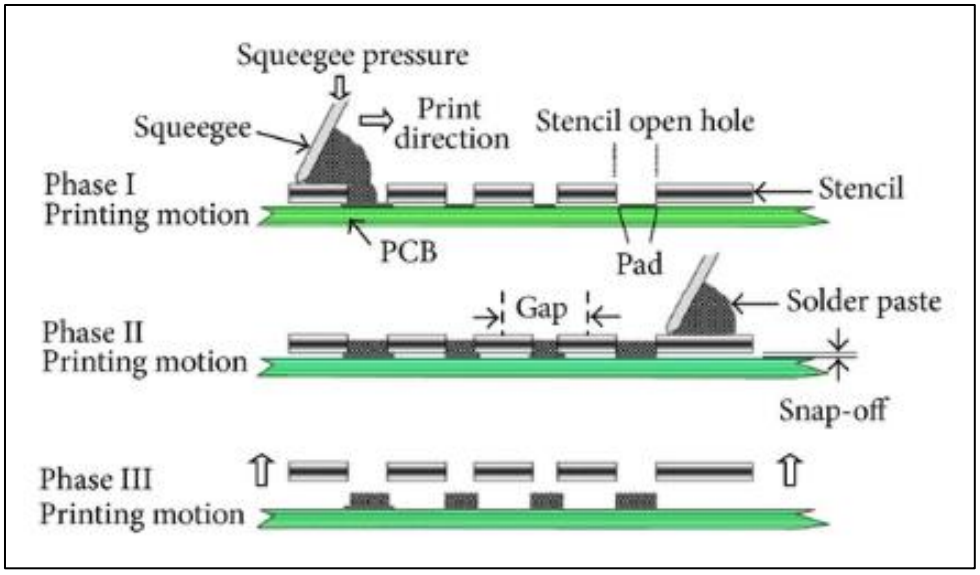

Figure 2-4 Schematic of Printing Process

In Figure 2-5, there are multiple passive components like resistors and capacitors, and active components like Small Outline Transistors (SOTs), Flip Chips (FCs) with different sizes, which apply the SMT on the circuit board. As it is shown, all the components are attached on the surface of the circuit board supported by solder joints and there are no holes drilled in the circuit board.

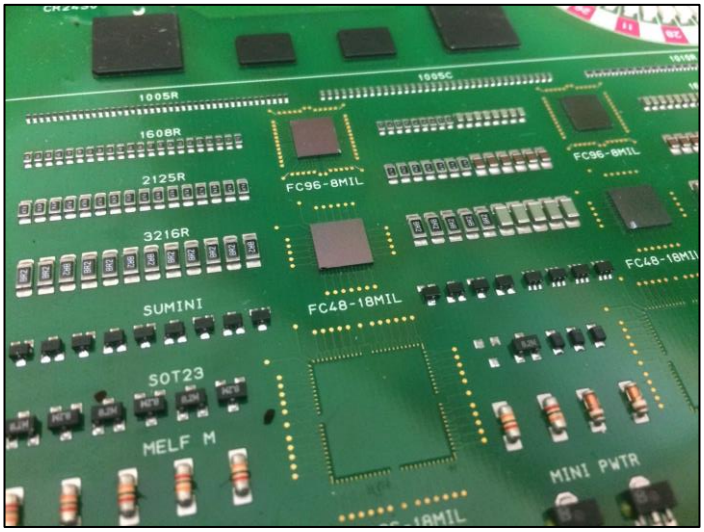

Figure 2-5 Example of Passive Components

2.1.3 THT vs. SMT

Obviously, the main difference between THT and SMT is the way to interconnect components and circuit board. Since the SMT is so popular in current electronic industry, people may misunderstand that the THT is outdated and disappeared in current electronic industry. However, it is still commonly used in industry and a new electrical interconnection between layers by the through holes called “Vias” were developed. In Figure 2-6, there are many conductive through holes which connect different layers and allow a more complex circuit design in the circuit board.

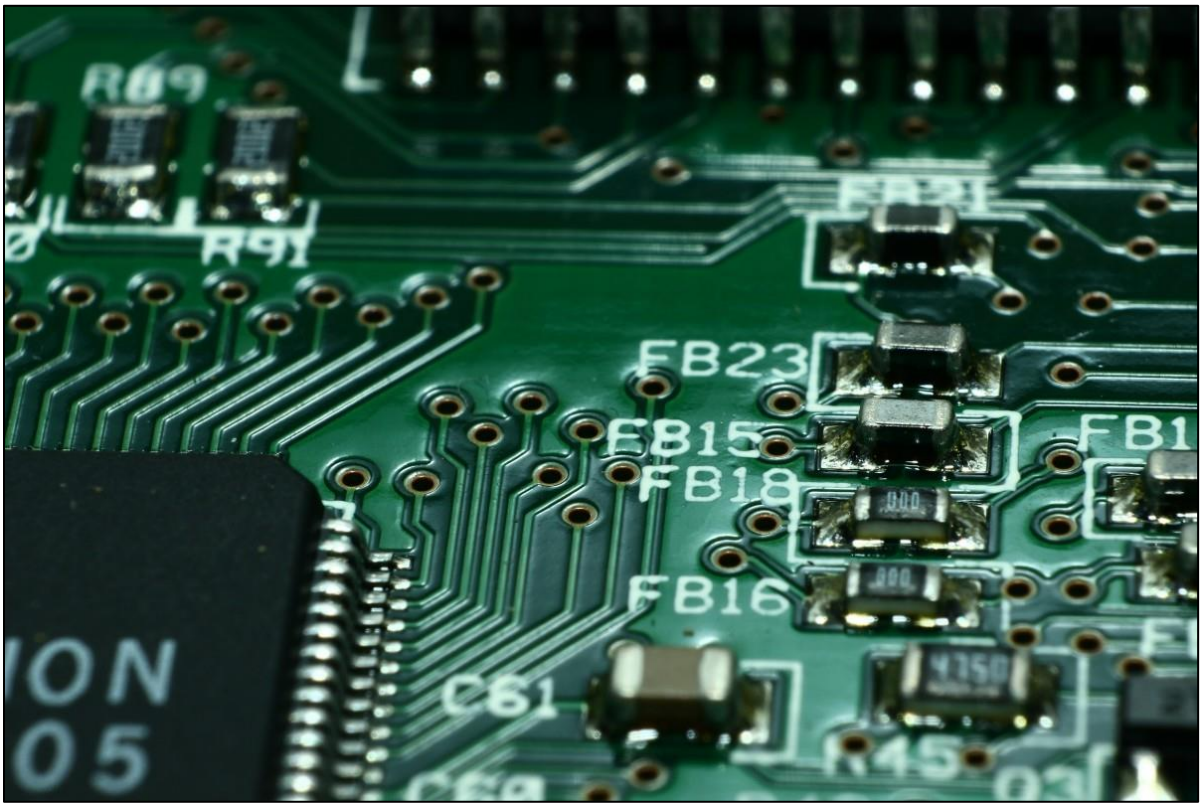

Figure 2-6 Examples of Conductive Through Holes Called “Vias”

Regarding the characteristics of both technologies, people are always thinking about how to apply the two technologies properly in design of electronic packaging. On one hand, the leads in the

THT can provide stronger mechanical connections than SMT. Also, THT is good for testing and prototyping. And some Through-Hole components (THCs) are less expensive. On the other hands, there are few holes in SMT, which will save much time and cost from the drilling process. Besides, SMT is able to allow more I/O and functions per substrate area and it is more repeatable and efficient compared with THT. Meanwhile, THT requires soldering on both sides of circuit boards, but generally SMT only needs soldering on one side of circuit board, which will increase the utilizations of circuit board area.

2.2 The Printed Circuit Board for Electronic Packaging

The PCB is a substrate to provide mechanical support, electrical connections, and heat dissipation for electronic or electrical components. It plays a crucial role in the reliability of electronic assemblies, so many properties must be taken into consideration when selecting the materials of PCB, such as Coefficient of Thermal Expansion (CTE), stiffness, strength, and conductivity. Among these properties, the mismatch of CTE will be the main reason for the fatigue failure under the realistic service conditions. Generally, the CTE of component packages will be different from substrates', which means the size change of component packages will be different from the size change of substrates when working temperature is changing. The size change will induce forces on the solder joints which connect component packages and substrates, and then the solder joints will be strained and fail eventually after thermal cycles, which is shown in Figure 2-7. Therefore, the general solution will be to use substrate materials and components with similar CTE. For an example, ceramic substrates are widely used with ceramic packages together, which avoids mismatch of CTE. Besides, a substrate called constraining core substrates was proven to solve the CTE mismatch problem effectively. The basic idea is to produce a substrate with multiple layers,

where the core has a very low CTE. The constraining core substrates can be either a metal or graphite epoxy.

However, it is not always the case to use same material in substrate and components and use constraining core substrates, because of costs and technology limitations. Therefore, people must improve solder joints' properties to endure the stress and strain because of mismatch of CTE.

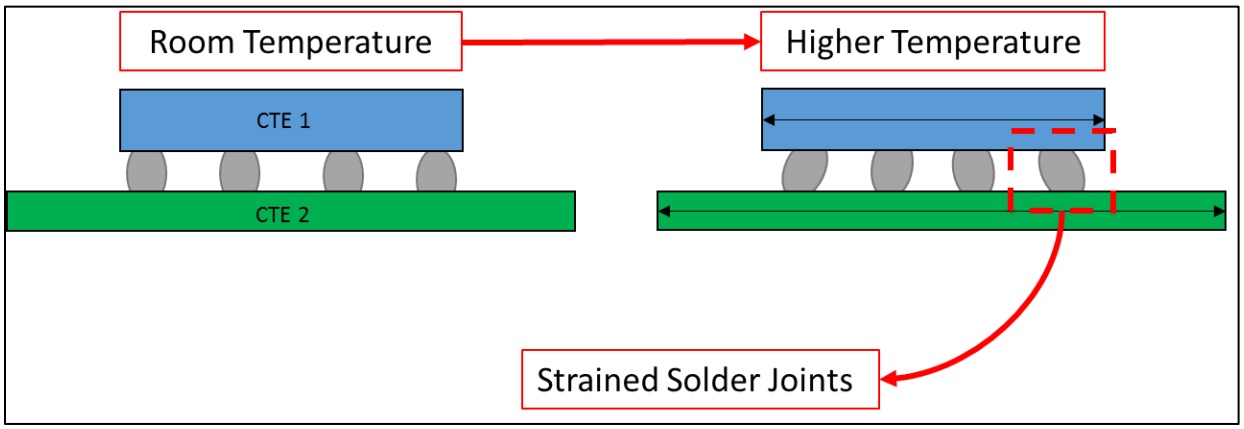

Figure 2-7 Schematic of Fatigue Due to Mismatch of CTE

2.2.1 Substrate

There are various substrates available in the market and they can be classified into categories based on their dielectric material or their fabrication technique. The most common substrates are using an organic dielectric material with copper as the conductive paths. Among them, the FR-4 is one of the most representative substrates, which consists of fiberglass cloth impregnated with an epoxy resin. Its properties are summarized in Table 2-1.

Table 2-1 Properties of FR-4 Substrate

Characteristics	Value

Humidity absorption (%)	<0.1%
Bond strength (kg)	>1,000kg
Temperature Index (℃)	130℃ - 140℃
Glass transition temperature (℃)	Vary from 120℃ to 240℃
High Voltage Arc Resistance (Sec)	300s
Thermal conductivity, through-plane (W/(m·K))	0.29 W/(m·K) [2], 0.343 W/(m·K) [3]
Thermal conductivity, in-plane (W/(m·K))	0.81 W/(m·K) [2],1.059 W/(m·K) [3]

Its price is low, and it is able to provide strong strength, good insulation property, and arc resistance with nearly zero humidity absorption. However, its glass transition temperature is near the temperature range of component soldering, which will cause damage to the substrates without proper temperature control. Besides, it has very bad thermal conductivity and thus makes thermal management much harder.

In addition, another option for substrate is the ceramic substrate, which can make up the cons of the organic boards. However, the cost and weight penalty limit the use of ceramic substrates. Thus, the ceramic substrates are used more in military and avionics [2]. Generally, the ceramic substrates can be classified by the manufacturing method and metallization type [2]: (a) Thick Film (b) Thin Film (c) Co-fired (d) Direct-Bond Copper.

Besides, the other substrates such like porcelainized steel substrates and compliant layer substrates are developed and used as well under different demands.

2.2.2 Solder Mask

Basically, the solder mask is a thin layer of polymer that is applied on the trace to avoid oxidation and prevent solder bridging. The solder mask can be classified to temporary and permanent categories, which is shown in Figure 2-8. Meanwhile, there are two solder mask designs: (a) Solder Mask Defined (SMD) and (b) Non-Solder Mask Defined (NSMD). The schematic in Figure 2-9 shows the difference of the two designs.

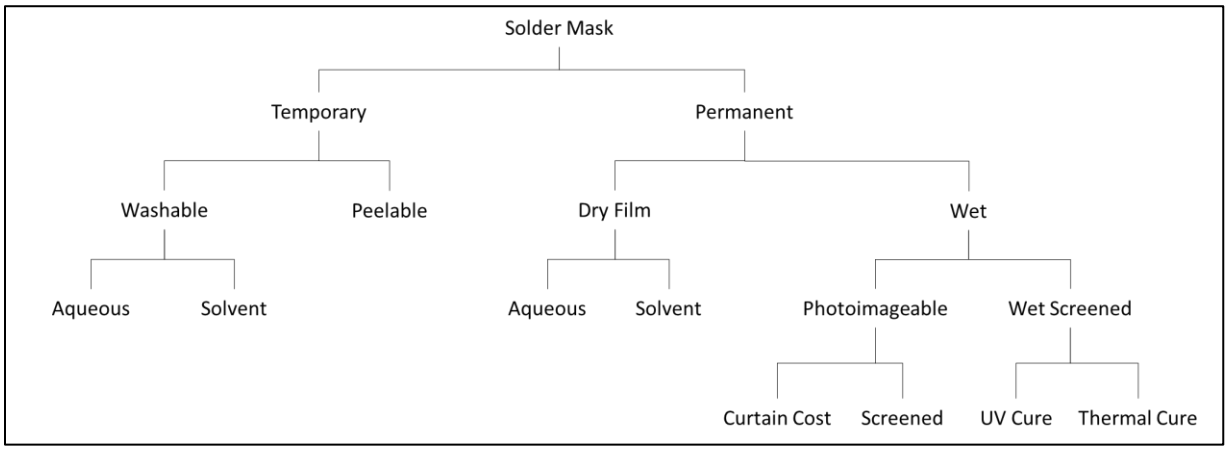

Figure 2-8 Categories of Solder Mask

Basically, the Non-Solder Mask Defined (NSMD) leaves extra space around the copper pads. In the case, there will be more surface areas for connecting solders with the copper pads. Therefore, it is more commonly used because it can provide stronger interconnections and better fatigue resistances.

Furthermore, the Solder Mask Defined (SMD) will cover a portion of the copper pads which reduces the area that the components are soldered on, but it can prevent the copper pad lifting off from the substrate because of thermal-mechanical stresses.

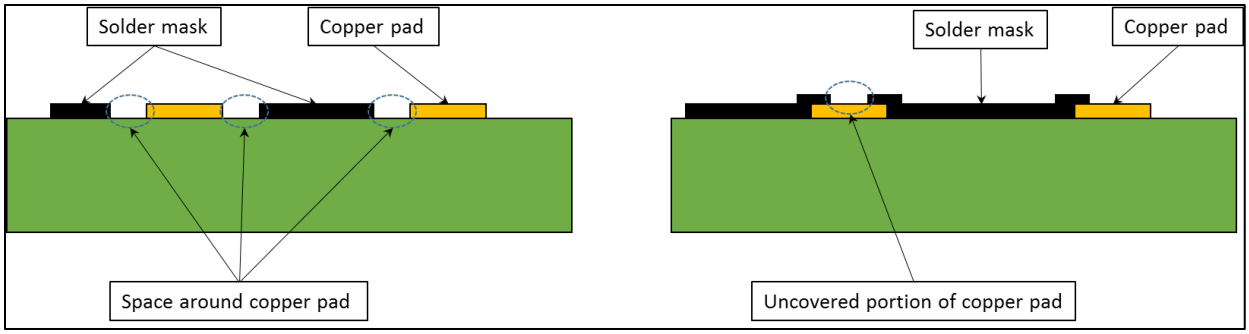

Figure 2-9 Schematic of Solder Mask Design: NSMD (Left) and SMD (Right)

2.2.3 Surface Finish

The surface finish initially aims to protect copper pad from oxidation before soldering any components, since the solder masks normally do not cover copper pad or only cover a portion of copper pad (See Figure 2-10). Furthermore, the surface finish is expected to enhance the assembly process and provide a solderable surface for soldering process. There is no one surface finish which can satisfy all the requirements in industry. People must trade off after considering cost, shelf life, wettability, solderability, thermal-mechanical resistance, fine assembly, lead/lead-free materials, etc. Here I will introduce several commonly used surface finishes.

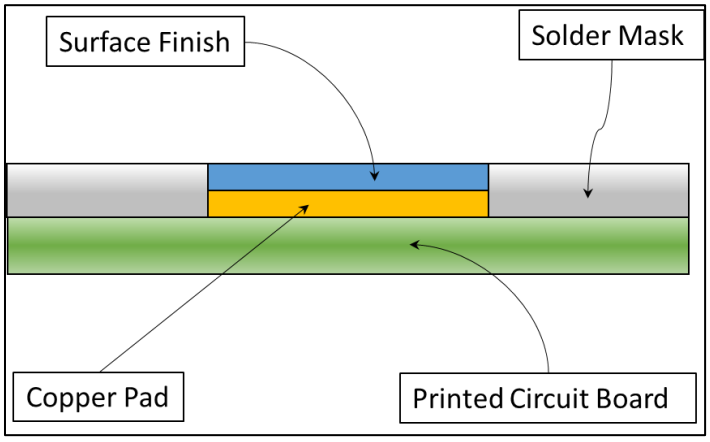

Figure 2-10 Schematic of Surface Finish

The oldest surface finish is to apply a thin Sn/Pb coating through the Hot Air Solder Leveling (HASL) process, which was used since 1980s. In the Hot Air Solder Leveling (HASL) process, the circuit board is immersed into a molten Sn/Pb environment, and the excess Sn/Pb will be blown off by the hot air across the surface of the circuit board. This process will generate uneven surfaces and it is not suitable for fine pitch components. Besides, there will exist extreme thermal shock, which will cause the board warp, delamination, damage to the plated holes, and defects that reduce the reliability of electronic products.

Besides, there are many other surface finishes available in the market. The OSP is one of the surface finishes, which is environment friendly and normally used to cover the bare copper pads. The film of OSP is very thin to allow fluxes dissolving it on the copper in the assembly process, so the film is easy to be scratched. It can provide a flat surface and consistent solderability with simple process and low cost. However, it will degrade in the environment with high temperature and humidity, and it will have short shelf lifetime (about 6-12 months).

Another popular surface finish will be Electroless Nickel Immersion Gold (ENIG), which contains a double layer metallic coating. One of the layers will be nickel as the surface on which the components are soldered. The other layer is coated with gold, which is used to protect the nickel during storage. This surface finish can satisfy the demand of flat surface, good solderability, and wettability. However, it is expensive and causes “Black Pad”.

Meanwhile, the surface finish called Immersion Silver (ImAg) is getting widespread due to silver has good conductivity and the rising lead-free demands. However, the silver is an active metal, so the Immersion Silver (ImAg) needs careful storage and packaged in case of contaminants.

Basically, it is a good candidate for a fine assembly and flat pack with low cost. Meanwhile, it can provide excellent wettability and solderability using simple process.

2.3 Soldering Technology

Soldering, brazing, and welding are the widely used process to join metals together. The basic difference of them is the working temperature. Among them, the working temperature of soldering is lowest (210℃ to 230℃) and mostly used in the electronic industry. In all cases, the metallurgical bond is strongly influenced by the formulation of IMC layers which is a brittle and crystalline structure. It usually contains new compositions of a certain ratio of two or more metallic elements and normally observed near the interface between solder ball and base metal (See Figure 2-11) [6, 7, 8, 9, 10, 11]. Typically, the composition, the thickness and the growth rate of IMC layers play crucial roles in the reliability of solder joints [12, 13, 14, 15]. Before going deep to that, I will start with what is the solder paste and the normally used solder material.

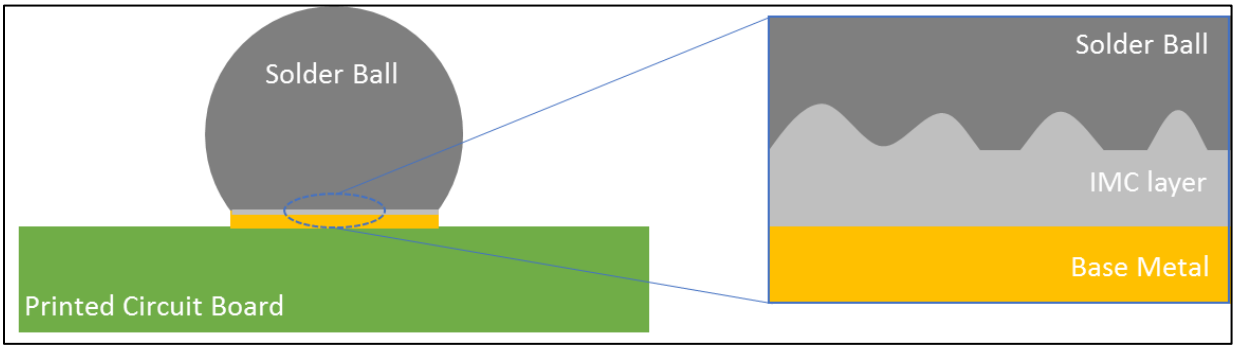

Figure 2-11 Schematic of IMC Layers

2.3.1 Solder paste

Generally, the solder paste is a mixing of solder alloy powders and fluxes with solvents, activators, carriers, rheological modifiers, and other additives. The solder alloy powders will be the main consist of solder joints by weight. Therefore, its shape and size distribution are important factors for the quality of solder paste printing and the final quality of solder joints. With the development of finer pitches, the smaller size of powder is required, because larger particles will clog screens and stencils. However, smaller particles will be more expensive. Based on the IPC standard J-STD 005, solder paste can be classified into "Types" by the particle size [16], which is shown in Table 2-2.

Table 2-2 Classification of the Solder Paste

Type	<0.005% larger	<1% larger	>90% between	>10% smaller
1	180μm	150μm	150-75μm	20μm
2	90μm	75μm	75-45μm	20μm
3	53μm	45μm	45-25μm	20μm
4	45μm	38μm	38-20μm	20μm
5	32μm	25μm	25-15μm	15μm
6	25μm	15μm	15-5μm	5μm

The flux in solder paste aims to ensure cleaning surfaces, enhance the wettability of solder material, and prevent the oxidation of solder powder before soldering process and it will be fugitive and nonfunctional after soldering process [2]. Also, there is a standard, J-STD-004B, which defines a flux identification system based on the flux activity levels (Low, Medium, High) and flux

compositions (Rosin, Resin, Organic, Inorganic) [17]. Generally, the flux can be applied by brush, flux core wire, foaming, spraying and jetting.

2.3.2 Solder Materials

The solder materials vary a lot because many elements are added in solder alloys, such as tin (Sn), lead (Pb), nickel (Ni), copper (Cu), Silver (Ag), aluminum (Al), iron (Fe), bismuth (Bi), zinc (Zn), antimony (Sb), indium (In). The various compositions constitute new binary, ternary, and complex systems of solder alloys. Typically, metallurgical phase diagram is used for a better understanding of intermetallic bonds, leaching and dissolutions. A common binary eutectic Sn-Pb solder system is shown in Figure 2-12 as an example.

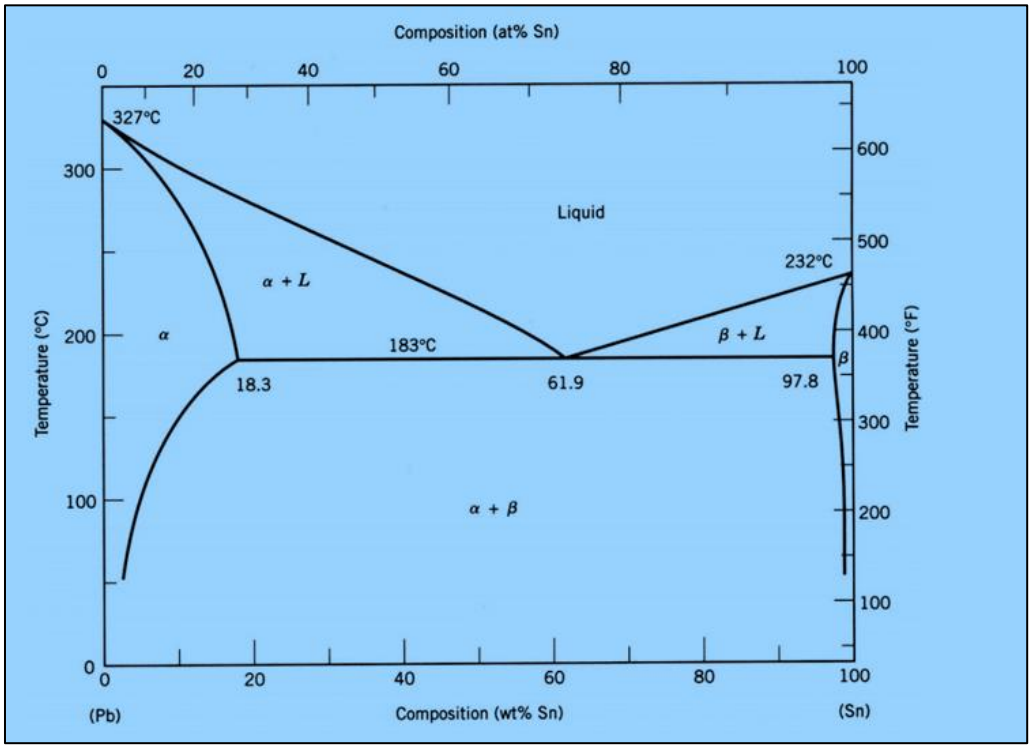

Figure 2-12 Binary Sn-Pb solder Metallurgical Phase Diagram

Though the properties of solder materials vary a lot depending on the compositions and microstructures, the solder materials must be good enough to keep the solder joints maintaining good conductivity and thermal-mechanical reliability. Also, some other properties should be taken into considerations, including cost, melting temperature, solderability, environment and health concerns, compatibility with manufacturing system, etc.

As it is introduced previously, people seldom use single pure metal phase as the solder materials and various elements are applied to strengthen solder alloys. Basically, the reason of strengthening by adding new elements is that these added elements can change the microstructures of solder materials. Once the new element is induced, the atoms of new element will be added into the crystalline lattice of base metal. Normally, the size of impurity atoms is different with the atoms of base metal, which will impose lattice strains and forms stress fields (See Figure 2-13). The stress fields interacting with atom dislocations, imped distort of crystal lattice and result in the rise of yield stress of solder materials. In addition, the second phase particles formed during reflow process will result in alloys strengthening, which is called precipitation hardening. The precipitation particles cause lattice mismatches and create stress fields, which slows down dislocation. In general, there are several hardening methods by precipitations: coherency hardening, modulus hardening, chemical hardening, and order hardening.

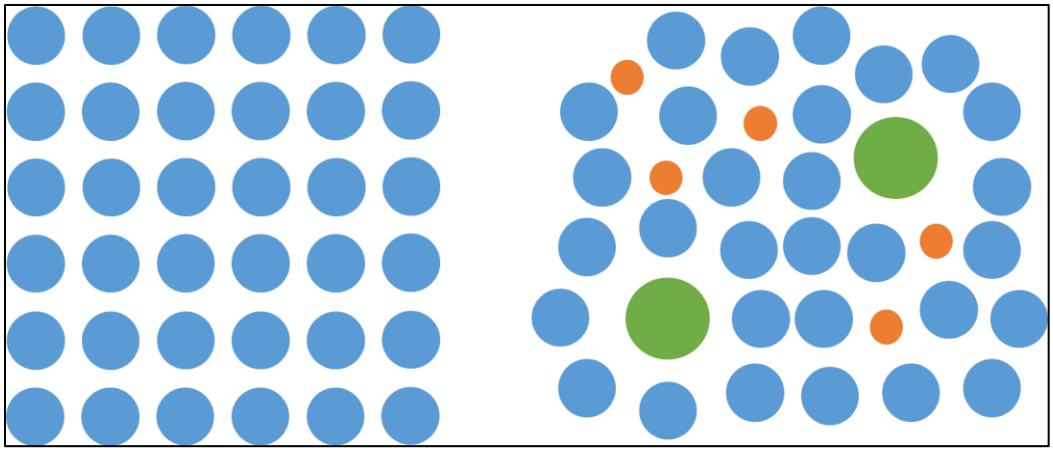

Figure 2-13 Schematic of Pure Metal Phase (Left) and Multiple Elements Phase (Right)

2.3.3 Mechanical Properties of Solder Alloys

The solder joints connect all the electronic component in PCBs. Hence, the mechanical properties of solder joints will be highly related with the reliability of electronic products. Additionally, the solder alloys are the main composition of solder joints. Therefore, the mechanical properties of solder alloys will profoundly influence the reliability of solder joints and finally the reliability of electronic products. Generally, people are concerned about the mechanical properties, such like tensile and ductility properties, creep resistance, fatigue properties, etc.

2.3.3.1 Tensile and Ductility Properties

Basically, the tensile strength or ultimate strength is a point that describes the maximum tensile stress that an objective can endure before failure. And the yield strength is usually defined as the stress that will cause a permanent deformation of 0.2% of the original dimension. Both can be seen from a stress-strain graph, which is shown in Figure 2-14.

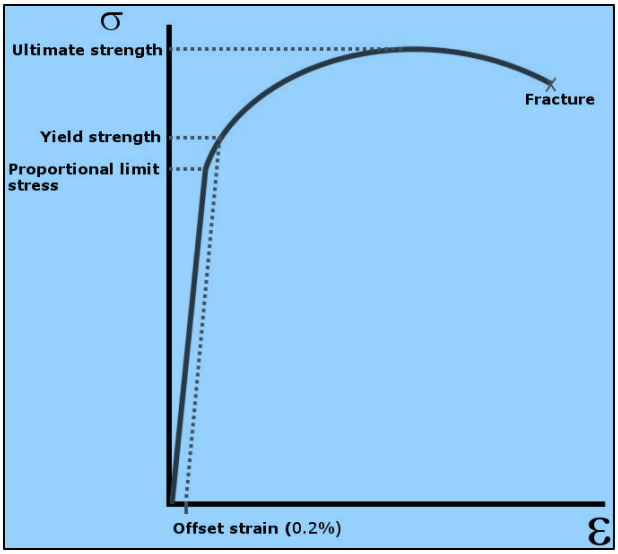

Figure 2-14 Example of Stress-Strain Performance

In the nominal stress-strain curve, there will be a strain hardening stage at first when the stress is applied on the material. Before the yield strength point, the material can return to its original size, which is defined as the elastic deform region. However, the material will plastic deform after the yield point and the nominal stress will reach a peak (the ultimate strength or tensile strength) and then decrease as the strain increase, which indicates that material is broken. Meanwhile, the ductility measures the ability of a material to withstand plastic deformation without broken. Though most solder joints will not work under extreme condition, the ultimate strength, yield strength, and ductility will be good references for understanding the limitations and properties of the solder alloys.

2.3.3.2 Creep resistance

The creep resistance is to describe the tendency of a solid material to deform gradually in a temperature under some stresses which are below the material's yield strength. The precipitations

and grain size of the solder alloys will influence the creep resistance. In general, there exists 3 stages in a creep test (See Figure 2-15) in the Strain-Time graph [21]. In the primary stage, the creep will rise rapidly. Then it will keep constant in the secondary creep range. Finally, it will increase rapidly until fracture in the last stage.

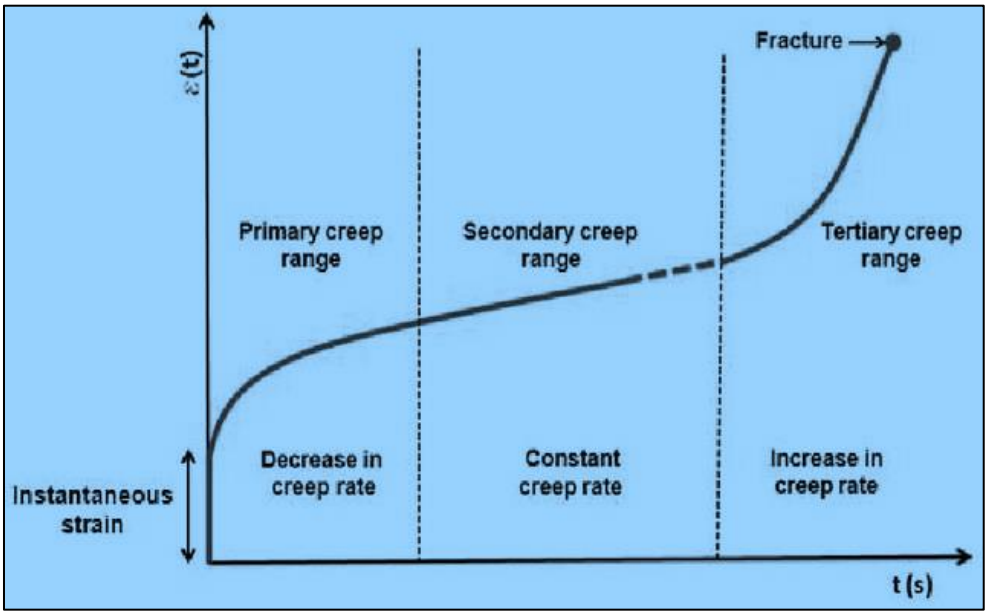

Figure 2-15 Performance of A Typical Creep Test

2.3.3.3 Fatigue properties

The fatigue failure is defined as the failure of materials under applied load which is much less than the strength of the material. In this case, it is one of the most important references for electronic product's life. Usually, the fatigue failure starts with the crack initializations, then crack growth, and propagations until the final break under stress. The applied load mainly results from the mismatch CTE and mechanical vibrations. Though the applied load is much less than the strength of the material, it will gradually damage the material by thousands of cycles. Normally, an S-N

curve is used to describe the fatigue properties of the solder alloys which is shown in Figure 2-16. According to the S-N curve, a number of cycles to failure can be estimated when a stress is given.

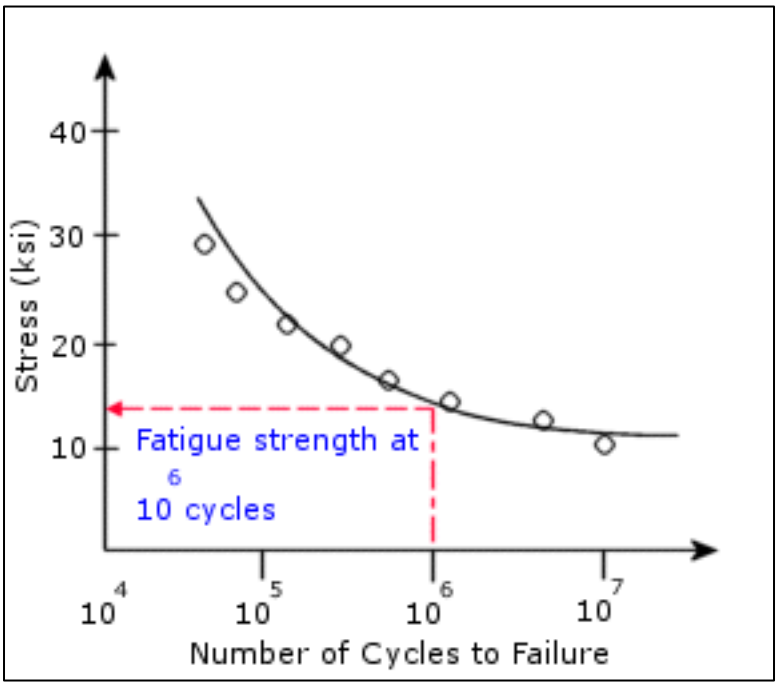

Figure 2-16 Example of S-N Curve

2.3.4 Solder Methodology

In addition to the solder paste and solder materials, the soldering process is important and needs well controlled, which refers to the reflow method. The commercial available reflow process includes conduction, infrared, vapor phase, hot gas, convention, laser, etc. Basically, the reflow process is a dynamic heating process to melt the solder paste and forms the solder joints. Typically, PCBs with solder pastes will go through the preheat zone, thermal soak zone, reflow zone, and cooling zone (See Figure 2-17). According to the flow, the key parameters of the reflow process will be temperature, temperature changing rate, and time in each zone.

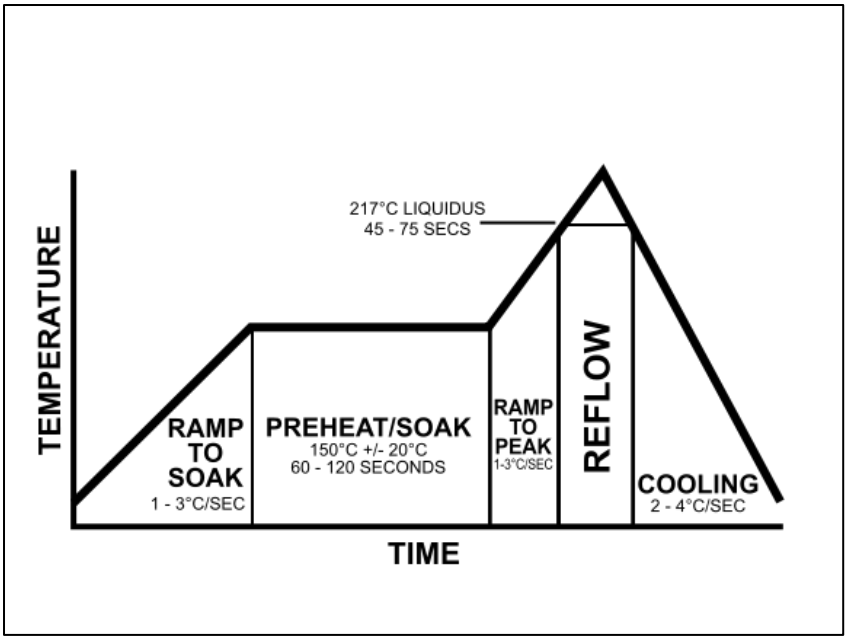

Figure 2-17 Example of Reflow Process

Generally, the entire circuit board need to be heated safely in the preheating zone to a target temperature with consistent rate that is measured in degrees Celsius per second. A high temperature slope rate may result in damage of some sensitive components on the PCBs. Before reflowing, the PCBs will enter the soak zone to activate fluxes and remove the solder paste volatiles. Then the circuit board will go through the reflow zone in which the temperature is above the melting temperature of the solder paste. The reflow temperature and time are the key to successfully form solder joints in this process. Finally, the cooling zone is ready to cool the heated circuit board and solder joints. Similar with the preheating zone, the cooling rate is important, which affect the formation of the IMC layer. A high cooling rate may cause the thermal shock of components on the boards. A cooling rate of 4 ℃/s is commonly recommended.

2.4 Solder Joint Reliability Test

Reliability tests are used to reveal the performance of product under realistic service conditions. As it is introduced, the reliability of electronic products is highly related the reliability of solder joints. Therefore, it is essential to figure out how the solder joints perform in reliability tests. The result of different reliability tests will improve the understanding of solder joints and then improve the understanding of electronic products. Generally, the condition in reliability test will be harsher than the operation condition, which is well known as Accelerated Life Test (ALT). The purpose of Accelerated Life Test (ALT) is to yield sufficient failures in short time, which will save us time and money. Usually, the accelerate factor is needed to relate tested response to its realistic performance under realistic service conditions. Here we will introduce some common tests in the reliability analysis of solder joints.

2.4.1 Thermal Cycling test

The thermal cycling test is one of the most widely used tests in electronic industry, because the electronic components will usually dissipate heat and many electronic products are working under extreme temperature conditions. Additionally, the size of component, PCBs, and solder joints will change a little bit as the temperature is varying. Meanwhile, the expansion and shrinkage rate for various material are not same. So, the stress is introduced once temperature is changing. In short, the basic idea of thermal cycling test is to simulate how well solder joints or electronic products will work under varying temperature conditions. In the thermal cycling test, the objective will normally go through a thermal cycle with high/low temperatures that exceed the actual working temperatures. The common test standard includes JEDEC standard JESD22-A104 Thermal Cycling and IPC 9701 Performance Test Methods. Typically, the temperature profile in a thermal cycle test is shown in Figure 2-18. For example, the temperature will increase up to the max limit,

and hold on for a dwell time. After that, the temperature will drop back to the min temperature limit and hold on for a dwell time. Then the temperature will follow the same profile according to the setup. Clearly, several parameters are important based on different solder materials, including max and min temperature limit, temperature changing rate, and dwell time.

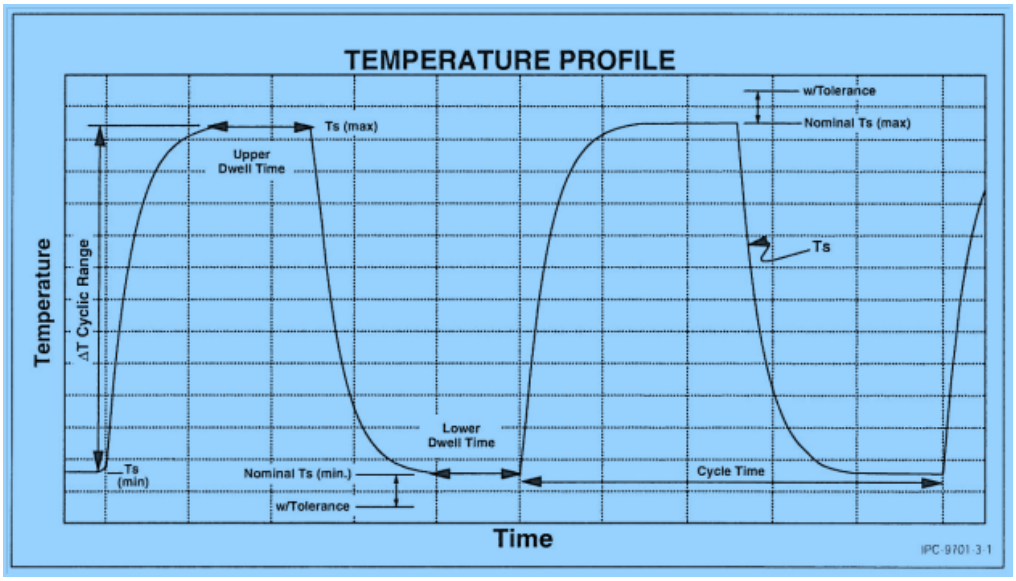

Figure 2-18 Temperature Profile of Thermal Cycling Test

2.4.2 Isothermal Test

Though the changing temperature is a virtual reason for degradation of the electronic product, the electronic product will not stay new forever even if they are not used. In the case of humidity and oxidation, the solder joint will degrade gradually because most of solder alloys are very active and they can absorb moist or react with oxygen, even if they are not working. Thus, the isothermal test is proposed to keep the objective under a constant temperature for a time, which indicates the shelf life of product. It was reported by Sinan [22] that the SAC305 solder joints' characteristic fatigue life significantly drops after room temperature aging for 4 years (See Figure 2-19). It was also

reported that the shear strength and hardness of solder joints will be reduced up to 20% under room temperature [22].

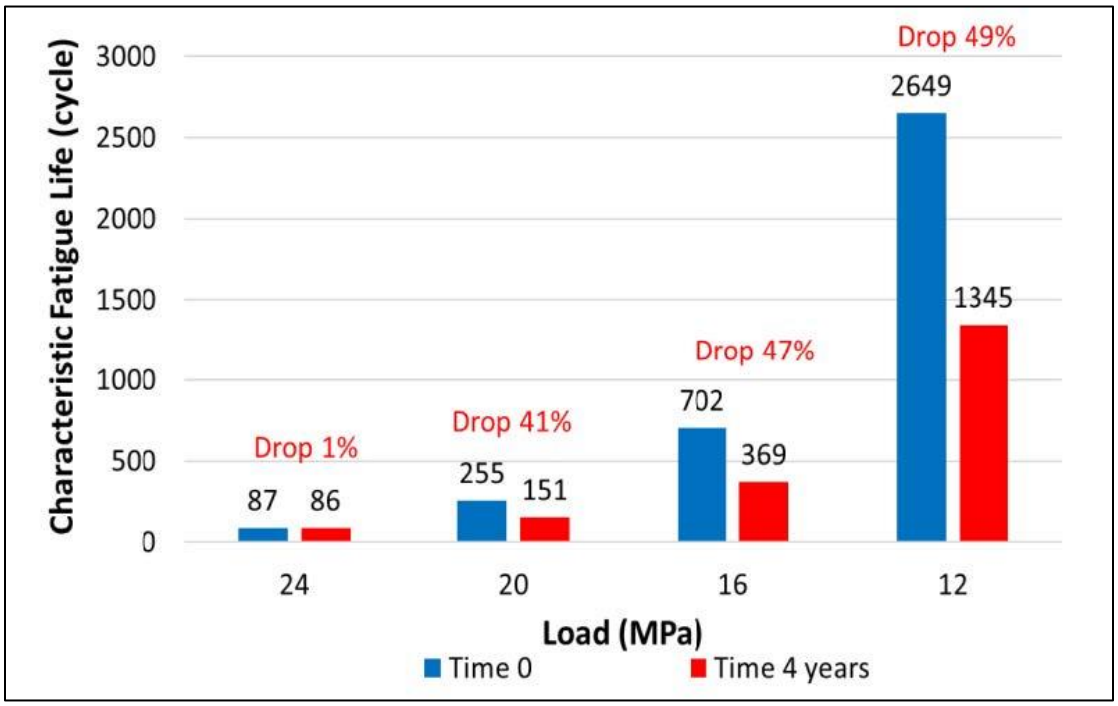

Figure 2-19 Solder Joint Degradations after 4 years Room Temperature Aging

2.4.3 Mechanical Vibration Test

Electronic product works not only under varying temperature conditions, but under varying vibration conditions. For example, the sensor attached on the vehicle engines must go through hard vibrations during its entire service life. Therefore, the solder joint must endure extreme stress and strain from environment, ensuring that electronic product can function very well during its service life. Hence, the mechanical vibration test is widely used to figure out the fatigue properties for solder joints by inducing extra stress and strain until final failure. Based on the setup, it can be divided into Stress-controlled fatigue test and Strain-controlled fatigue test. Based on the

deformation type, it can be divided into Low Cycle Fatigue (LCF) test and High Cycle Fatigue (HCF) test. Whatever test type is, the plastic deformation is considered as the main reason for fatigue failure. In short, the plastic deformation will damage the material permanently even though the damage is not large enough to break down entire material. The Strain-controlled fatigue test is preferred in reality because the strain is easier to be fixed. Also, people may focus more on Low Cycle Fatigue (LCF) test because High Cycle Fatigue (HCF) test sometimes are driven by both elastic and plastic deformation. Whatever type of the fatigue test is, the stress and strain data will always be recorded to form a hysteresis loop in a Stress-Strain graph which is shown in Figure 2-20. The loop area represents the plastic deformation energy in one cycle. σ represents stress, and ε represents plastic strain.

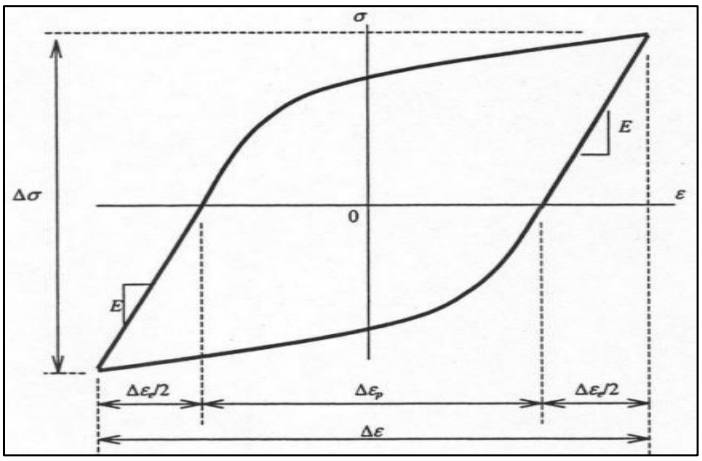

Figure 2-20 Example of Hysteresis Loop

Normally, the amplitude in a fatigue test is simple and constant. However, the loadings are usually varying during the service life of electronic products, which indicates that the loading amplitude on the solder joints are frequently changed as well (See Figure 2-21). And it has been proved [23, 24, 25] that the result of the fatigue test may be misleading without considering the service load

histories. Due to the complex of loading histories, it is hard to count the cycle to compare the effect of varying amplitude load histories to fatigue data and curves obtained with simple constant amplitude load cycles [26]. The most popular one was called “Rainflow counting” [27] and the other count methods include range-pair method, Level-Crossing method, peak counting method and racetrack counting method.

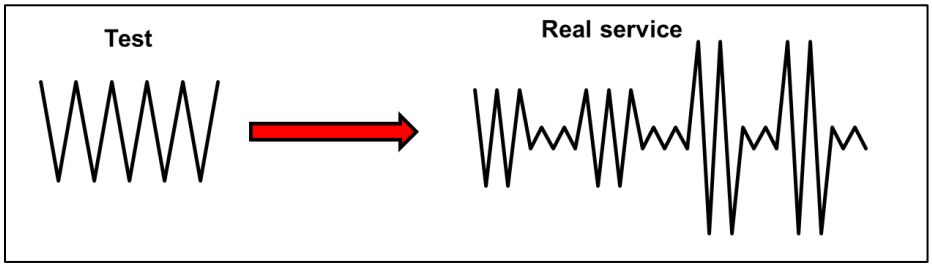

Figure 2-21 Comparison of Loading Amplitude in Fatigue Test and in Real Service Condition

2.5 Statistical Reliability Models and Weibull Distribution

As it was introduced before, the solder joints cannot be entirely identical, so the reliability of every solder joint will be different, though they are made by same material and go through same process. Besides, there exist thousands of solder joints in the electronic packages. Thus, the reliability of electronic system will depend on the reliability of every solder joint. Therefore, we need statistical reliability models to evaluate the reliability performance of a solder joint, electronic package, or system.

Here we are defining the reliability as the statistical probability that a solder joint, electronic package, or system will perform as required without failure under specific conditions for at least a specified time. Generally, the reliability will be defined as a function of the time to failure (T):

$$R(t) = Probablity\{T \geq t\} \tag{2.1}$$

Meanwhile, the probability that a failure occurs is defined as:

$$F(t) = 1 - R(t) = Probablity\{T \leq t\} \tag{2.2}$$

Thus, the probability density function of the failure distribution will be (provided that F is differentiable):

$$f(t) = dF(t)/dt = -dR(t)/dt \tag{2.3}$$

In addition, the hazard function is defined as:

$$\lambda(t) = f(t)/R(t) \tag{2.4}$$

Furthermore, it exhibits a "bathtub shape" as shown in Figure 2-22 [28]. Typically, the hazard rate function will decrease in the burn-in period. Then the hazard rate function will stay constant overtime in the useful period. Finally, the hazard rate function will increase overtime.

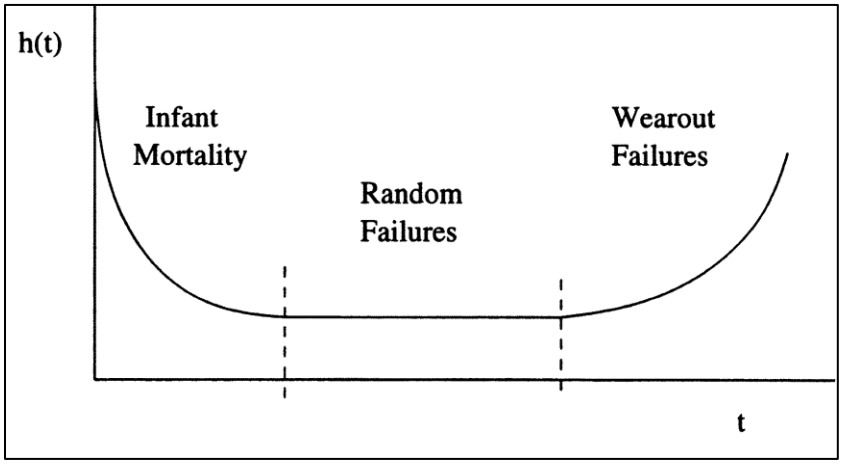

Figure 2-22 Bathtub Curve of Hazard Rate Function

Additionally, the Weibull distribution is one of the most widely used distributions when statistically modeling the failure data. The probability density function of Weibull distribution is defined as:

$$f(t) = \frac{\beta}{\theta}\left(\frac{t}{\theta}\right)^{\beta-1} e^{-(t/\theta)^{\beta}} \tag{2.5}$$

where β is the Weibull shape parameter, and θ is the Weibull scale parameter. The Weibull distribution can fit data in many cases, because β is able to capture on the shape of the distribution. And θ represents the 63.2% of the population are expected to fail, which is considered as the estimate of the fatigue life in the fatigue test. Also, it is well known as the characteristic fatigue life.

Chapter 3 Literature Review

From the previous chapter, we understand the importance of the solder alloys and access to the basic reliability analysis on the solder joints. As more and more solder alloys are being developed, the compositions of the IMC layers are becoming more complicated, with different combinations of the added elements and base material. Thus, much research was studying the properties of solder alloys, IMC layers, and reliability analysis of solder joints for better understanding their performances. In this chapter we will introduce several popular and representative solder alloys and their properties. Besides, some famous fatigue models will be introduced as well.

3.1 Eutectic Sn-Pb solder alloys

In the history of electronic industry, Sn-Pb solder materials have been widely used for very long time due to its proper melting temperature, low cost, good solderability and strong mechanical properties [18, 19, 20, 29]. Basically, the tin enhanced the solder's tensile and shear strength, and lead improve the ductility of the solder. Typically, most of alloys will have pasty range, where the alloy is partially solid and liquid. This property makes these alloys unpredictable and hard to work with, because the compositions in the solid and liquid alloy are different. However, the 63%Sn-37%Pb can be entirely melted to liquid and entirely solidified to solid at 183℃ which is compatible with the manufacturing process and the other components in assembly. Furthermore, it can satisfy the electronic packaging's mechanical, electrical, and thermal demand. That is the reason that Sn-37%Pb was popular in the market. In addition, studies [30, 31]proved that the lead will not form any IMC layers with tin (Sn), the pad material copper (Cu) and nickel (Ni). However, people found

two IMC layers with copper pads: Cu_6Sn_5 and Cu_3Sn; and one IMC layers with nickel pads: Ni_3Sn_4, which are shown in Figure 3-1 [31].

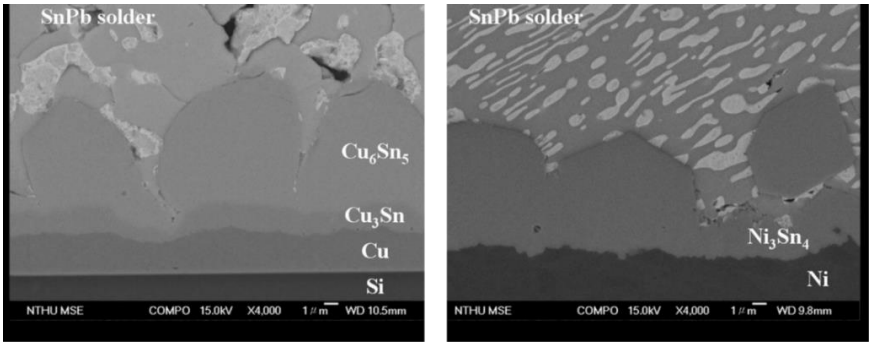

Figure 3-1 Composition of IMC Layers in SnPb Solder with Copper Pads and Nickel Pads

However, with the development of electronic industry, the replacing rate of the electronic products rise dramatically, whereas the recycling of computer product was few in 1998 [32]. Thus, the toxic lead from electronic products will leach out into the soil after the products are buried in the landfill and finally becomes a hazard for environment and human beings' health. The government, market, Industry Institute of European, Japan, and United States were restricting the use of lead product and pushing the electronic industry into a lead-free direction [33, 34, 35]. Thus, the current popular topic is to look for potential candidate elements to replace the toxic lead.

3.2 Binary Lead-free solder alloys

In the selection of substitutes, people must consider the cost, availability, solderability, thermal-mechanical properties, and compatibility with manufacturing process. Initially, people were trying to replace the lead with the other elements to build the new binary Pb-free eutectic alloys. However, none of them can satisfy all the demands above at the same time. Here I will introduce several representative binary Pb-free eutectic alloys.

3.2.1 Sn-Cu

The common composition is Sn-0.7%Cu and its melting temperature is high at 227℃. It is low cost because copper is a common element. However, the tin is prone to whisker growth, which may cause electrical shorts [36]. Also, the strength is low, and ductility is high due to the large amount of Sn. The composition of IMC layers with copper and nickel substrate are similar with Sn-Pb. But the concentration of Cu will influence the formation of IMC layers with the copper and nickel substrates during reflow process.

3.2.2 Sn-Ag

Ag is able to provide good mechanical property and excellent wettability on Cu substrates. The eutectic temperature of Sn-3.5%Ag is 221℃. The microstructure of the bulk material is full of β-Sn and a eutectic dispersion of Ag_3Sn [37]. And the cooling rate will affect mechanical properties by affecting the size and morphology of Ag_3Sn, which is shown in Figure 3-2 [38].

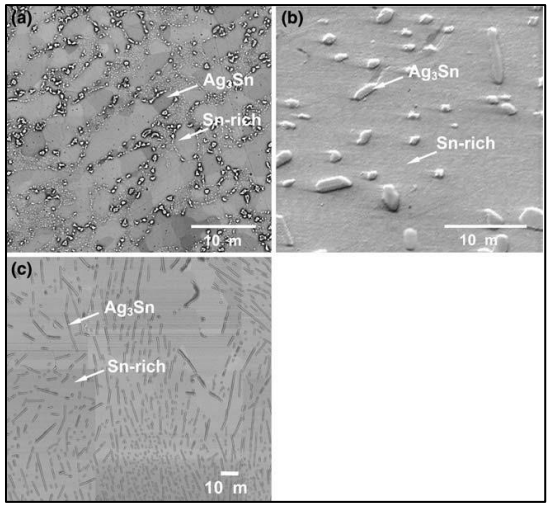

Figure 3-2 Micrographs of the (a) Water-Cooled, (b) Water-Cooled Aged, and (c) Furnace-Cooled Sn-3.5Ag Solder Microstructures Highlighting the Varying Size and Morphology of the Ag3Sn Intermetallic

Basically, a high cooling rate will result in fine dispersions of Ag_3Sn, while a low cooling rate will result in needle-like Ag_3Sn. And it was suggested to use lower soldering temperature, fast cooling rate and short reflow time to producing eutectic Sn-Ag/Cu solder joints with better shear strength, ductility and creep resistance [15].

3.2.3 Sn-Zn

The amazing advantage of Sn-Zn is that its melting temperature (i.e., 198℃ for Sn-9%Zn) is similar to Sn-Pb alloy (183℃) and it also has excellent mechanical properties [39, 40]. Figure 3-3 shows the microstructure of a Sn9%Zn solder alloy with the fine Zn-rich phases being dispersed in the Sn-rich matrix [41]. However, its wettability is pretty bad [42, 43]and it needs special fluxes to avoid oxidation and improve wettability [29]. Also, the addition of amounts of alloying elements is an effective way to improve the mechanical property and wettability. For example, Bi is able to reduce the surface tension and lower the melting temperature of Sn-Zn alloy [44]. Also, the addition of Ag can improve the wettability and ductility of Sn-Zn [45, 46]and In can effectively reduce the melting point as well [29]. Al and Cr can improve the oxidation resistance of Sn-Zn alloy [41].

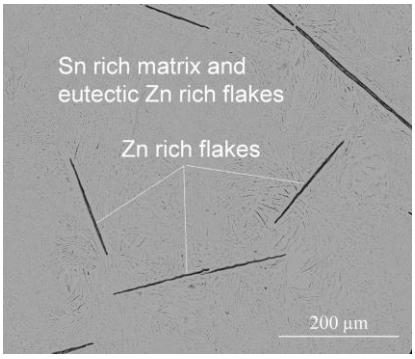

Figure 3-3 Microstructure of a Sn9%Zn Solder Alloy

3.2.4 Sn-Bi

The Sn–Bi alloy has a eutectic composition of 42Sn–58Bi and a relatively low eutectic temperature of 139°C [47]. The surface tension of eutectic Sn-Bi is lower than the surface tension of eutectic Sn-Pb [48]. The microstructure of Sn-Bi is lamellar, as the black phase is Sn and the white phase is Bi, which is shown in Figure 3-4 [49]. The study shows that the growth rate of IMC layers for Sn-Bi/Cu substrate is less than the Sn-Pb/Cu substrate [50]. And Bi was found to segregate to the interface, between Cu-Sn IMC and solder alloy, on the anode side [51]. While eutectic Sn-Bi does have a high strain rate sensitivity that results in low elongations at high strain rates, it has good ductility at low strain rates [52]. And it is reported that the increase of Bi content in Sn-Bi deteriorated the shear strength of solder joints. The addition of Bi into Sn solder was also inclined to produce brittle morphology with interfacial fracture, which suggests that the addition of Bi increased the shear resistance strength of Sn-Bi solder [53].

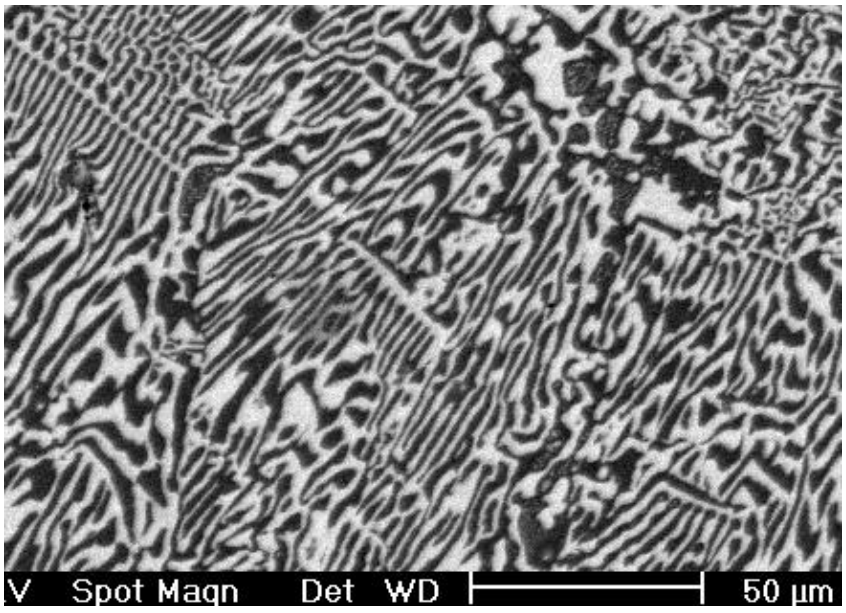

Figure 3-4 Microstructure of Sn-Bi

3.3 Near-Eutectic Sn-Ag-Cu solder alloys

Sn-Ag-Cu Solder alloys are popular candidates and most widely used commercial alloys for replacing the lead-based alloys. The phase diagram of Sn-Ag-Cu is shown in Figure 3-5 [54]. The commonly used alloys SAC305 has a melting temperature as low as 217℃.

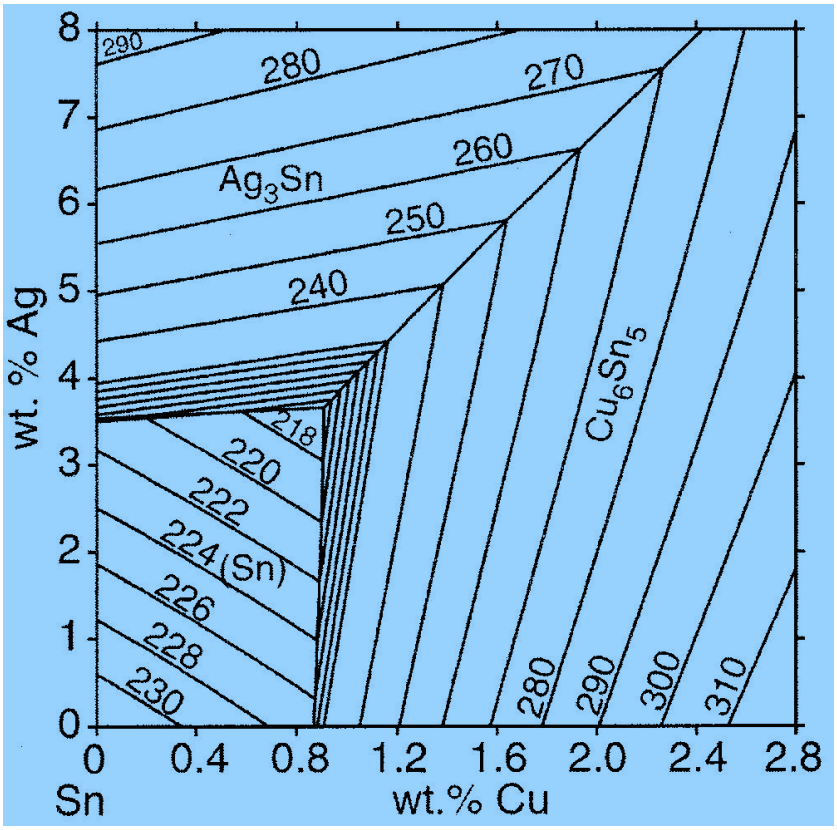

Figure 3-5 Phase Diagram of Sn-Ag-Cu

And the fraction of Ag will dramatically impact the mechanical performance of Sn-Ag-Cu alloys. It has been proved that the solder joints which contain the high-Ag content alloys are prone to drop-shock and creep failure due to the large amount of Ag_3Sn will make the solder joints more brittle [29, 30, 31]. Decreasing the volume fraction of Ag which reduce the fraction of Ag_3Sn is a straightforward solution, but the thermal cycling performance and the modulus and yield strength

are reduced as the volume fraction of Ag is reducing [30, 32, 33, 34]. Therefore, the second solution is to add some alloying elements into Sn-Ag-Cu solders, such like Ni [30], Fe [35, 40], Ce [54], Al [36, 37], Zn [29, 43], Bi [15, 39], Sb [42], etc., to refine the microstructure, promote IMC segregation and finally to improve the mechanical and thermal properties.

It is interesting to highlight the effect of Bi on the solder alloys. It was reported that Bi can enhance the tensile strength of the solders but decrease their elongations [29, 44] and improve the wettability of SAC alloy [45]. Meanwhile, J. Zhao et.al [46] found that Sn-3Ag-0.5Cu-1Bi and Sn-3Ag-0.5Cu-3Bi have higher resistance to the crack growth, resulting from the strengthening effect of Bi constituent, but it will be harmful to the mechanical properties if Bi exceeds a certain concentration. And M.J. Rizvi [55] found that a small amount (like 1 wt%) of Bi in SAC solder can reduce the solder's melting temperature, growth rate of intermetallic and consumption of Cu. In addition, M.J. Esfandyarpour et.al [41] found that Bi can reduce β-Sn size in Sn-Cu-Ni-Ge solders which is consistence with the result found by KARIYA and OTSUKA [47]. Also, it was reported that the fatigue life with addition of Bi was significantly reduced in the strain-controlled test by Kanchanomai C et.al [48]. Several reports have shown that the addition of Bi is able to delay the propagation of IMC layers [50] and change the microstructure of SAC157 from β-Sn grains to small needle-like Ag_3Sn and dark grey Cu_6Sn_5 particles [51].

3.4 Fatigue Model of the Doped Solder Joints

3.4.1 Coffin-Manson Fatigue model

The Plastic deformation is considered as the main reason for fatigue failure and thus the plastic strain is very important for the reliability and fatigue performance of solder joints. Therefore, one

of the most popular plastic strain based fatigue model was stated, called Coffin-Manson Fatigue model [52], which predicts the low cycle fatigue life based on the plastic strain range:

$$\mathrm{N} = \theta^{\frac{1}{\alpha}} * \varepsilon^{-\frac{1}{\alpha}} \tag{3.1}$$

where N represents the fatigue characteristic life, ε represents plastic strain, θ and α are the fatigue ductility coefficient and fatigue exponent, respectively.

3.4.2 Morrow Energy Model

Morrow energy model is a widely used model to estimate the fatigue life based on the inelastic work per cycle at steady states [56], which is listed below:

$$\mathrm{N} = \mathrm{C}^{\frac{1}{m}} * W^{-\frac{1}{m}} \tag{3.2}$$

where N represents the fatigue characteristic life, W represents the inelastic work per cycle at steady states. C and m are the fatigue ductility and fatigue exponent, respectively. Some studies show that this model fails to estimate the fatigue life at different frequencies and temperatures [53, 57].

3.4.3 Corton-Dolan theory

For better understanding the varying stress case, the Corton-Dolan theory was proposed, which assumes the damage accumulation is nonlinear. And the Corton-Dolan model can be expressed by [58]:

$$\sum_i \left(\frac{n_i}{N_1}\right)\left(\frac{\sigma_i}{\sigma_1}\right)^d = 1 \tag{3.3}$$

where N_1 is the fatigue life at the maximum stress σ_1, n_i is the number of cycles at stress σ_i, and d is the Corton-Dolan exponent which is originally defined as material constant. However, the recent studies showed that it also depends on the load spectrum and thus explained how to determine the exponent d [23, 58].

3.4.4 The Miner's rule

Another commonly used theory to predict the fatigue life is the Miner's rule [24] of linear damage accumulation, which defines an index:

$$\text{CDI} = \sum \frac{n_i}{N_i} \tag{3.4}$$

where n_i is the number of cycles at a particular stress amplitude, and N_i is the fatigue life amplitude i. According to the Miner's rule, the material will fail when the index equals to 1. However, the Miner's rule breaks down when it comes to varying amplitude case. The Figure 3-6 shows the CDI result of a varying amplitude test, in which SAC305 solder joints were alternated between 25 cycles at 18MPa and 3 cycles at 27.6MPa until total failure. Based on the Miner's rule, all the samples are estimated to be damaged from 40% to 80%, average about 57%. However, all the samples have already failed in the test, which indicates that the CDI supposed to be 1. Therefore, Miner's rule overestimates the fatigue life of SAC 305 in this varying amplitude test.

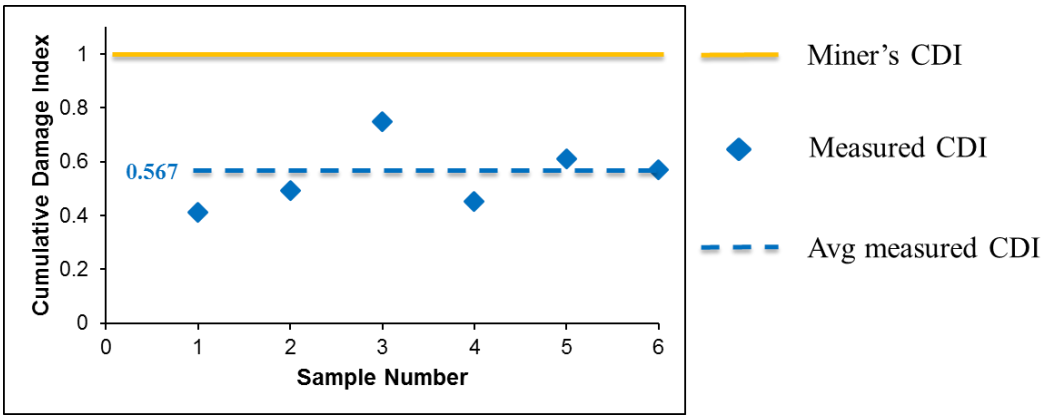

Figure 3-6 Breakdown of Miner's rule

Additionally, it is reported in some preliminary studies that Miner's rule does not work well in varying amplitude case [19, 21, 25, 26, 59, 60], and a modified Miner's model is achieved as below, which defines the amplification factor $f(i)$ [19, 26]:

$$1 = \sum_{i}^{s} f(i) \frac{n_{mi}}{N_m} + \frac{n_{hi}}{N_h} \tag{3.5}$$

where n_{mi} is the number of cycles at low amplitude, N_m is the life at low amplitude, n_{hi} is the number of cycles at high amplitude, N_h is the life at high amplitude. Basically, the amplification factor can be considered as the effect of the high stress cycles on the work per cycle in the following low stress cycles [19]. Meanwhile, the further study divided the amplification factor into the Initial Amplification and the Steady Amplification, and a refinement of the modified Miner's model is achieved as [19]:

$$1 = \sum_{i}^{s} \left\{ f(i)_{in} \frac{n_{in}}{N_m} + f(i)_{st} \frac{n_{mi} - n_{in}}{N_m} + \frac{n_{hi}}{N_h} \right\} \tag{3.6}$$

with

$$f(i)_{in} = \alpha i + b_{in} \tag{3.7}$$

and

$$f(i)_{st} = \alpha i + 1 \tag{3.8}$$

where $f(i)_{in}$ is the amplification function in the initial state, $f(i)_{st}$ is the amplification function in the steady state, α is the slope of amplification function, b_{in} is the amplification constant in the initial state, n_{in} is the number of cycles in the initial states, n_{mi} is the number of cycles at low amplitude, N_m is the life at low amplitude, n_{hi} is the number of cycles at high amplitude, N_h is the life at high amplitude, *i* is the number of intervals. Basically, it was reported that a higher value of high amplitude causes a steeper slope of amplification for the SAC305 alloy [19]. And the slope of amplification in SAC305 increases with number of high amplitude cycles in each set, but it soon levels off [61]. Besides, the value of work amplification at the lower amplitude depends on the sequence of higher amplitudes immediately before it [62].

3.4.5 Other Models

Grover [63] provided a two-level fatigue damage model, which counts damage evolution as the combination of crack initiation and crack propagation:

$$Crack\ Initiation: \sum \frac{n_i}{\alpha N_i} = 1 \tag{3.9}$$

$$Crack\ Propagation: \sum \frac{n_i}{(1-\alpha) N_i} = 1 \tag{3.10}$$

where n_i is the number of cycles at a particular stress amplitude, N_i is the fatigue life amplitude *i*, and α is percentage of life when a significant crack is developed.

Tong Yan Tee et al. [64] proposed a Weibull equation with the availability of two Weibull parameters, β and η, by

$$N = \eta[-\ln(1-F)]^{\frac{1}{\beta}} \tag{3.11}$$

where N is the solder ball fatigue life at corresponding failure rate (F), β is the slope of Weibull plot, and η is the characteristic life at 63.2% failure rate, which can be correlated directly with FEA predicted fatigue life.

Zhu et al. [58] present a new method for determining Corten–Dolan's exponent d and predict fatigue life by accounting for loading interaction effects, where d is defined as a function that decreases with the increasing loading stress amplitude:

$$d(\sigma_i) = \mu \frac{\sigma_i^{\lambda} \delta_f^{1-\lambda}}{\sigma_i} \tag{3.12}$$

where μ is a material constant, σ_i is the *i* th level stress amplitude, δ_f *is* initial static strength, and λ is a load-interaction factor. Therefore, a modified Corten–Dolan model was derived as:

$$N_g = \frac{N_1}{\sum_{i=1}^{k} \alpha_i (\sigma_i/\sigma_1)^{d(\sigma_i)}} \tag{3.13}$$

where $N_g$is total number of cycles to failure and N_1 is number of cycles to failure at σ_1.

Chapter 4 Experiment Design and Method

Typically, all the tests were done with individual solder joints which are mounted on customized PCBs with the Organic Solderability Preservative (OSP) surface finish. As it was discussed, bulk material sample has different fatigue performance with individual solder joints. Therefore, the test with individual solder joint is expected to be a more realistic simulation of solder joints' performance. It is possible to analyze the IMC layer which is well known as the key of solder joints' fatigue performance.

4.1 Solder Joints and Cross-Section Sample Preparation

4.1.1 Materials and PCBs Design

Four types of solder alloys were tested in this research. The table below includes their names and compositions, respectively. Generally, we consider SAC305 (No Bi) as the baseline. The contents of Bi in SAC-I, SAC-Q, and SAC-R are slightly different, as it is shown in Table 4-1.

Table 4-1 Composition of the Solder Materials

Alloy	Composition
SAC305	96.5%Sn, 3% Ag, 0.5% Cu
SAC-I	91.8%Sn, 3.5% Ag, 0.7% Cu, 3%Bi, 1.5%Sb, 0.125% Ni
SAC-Q	92.77%Sn, 3.41% Ag, 0.52% Cu, 3.3% Bi
SAC-R	96.62%Sn, 0.92% Cu,2.46%Bi

The schematic of test vehicle is shown in Figure 4-1. There are 9 solder joints (30 mil diameters) on the FR-4 PCBs (10mm×10mm, 9 Inputs/Outputs (I/Os), 3mm pitch) and its surface finish is the

Organic Solderability Preservative (OSP). Ideally, IMC layers will form between every individual solder joint and the base after reflowing process.

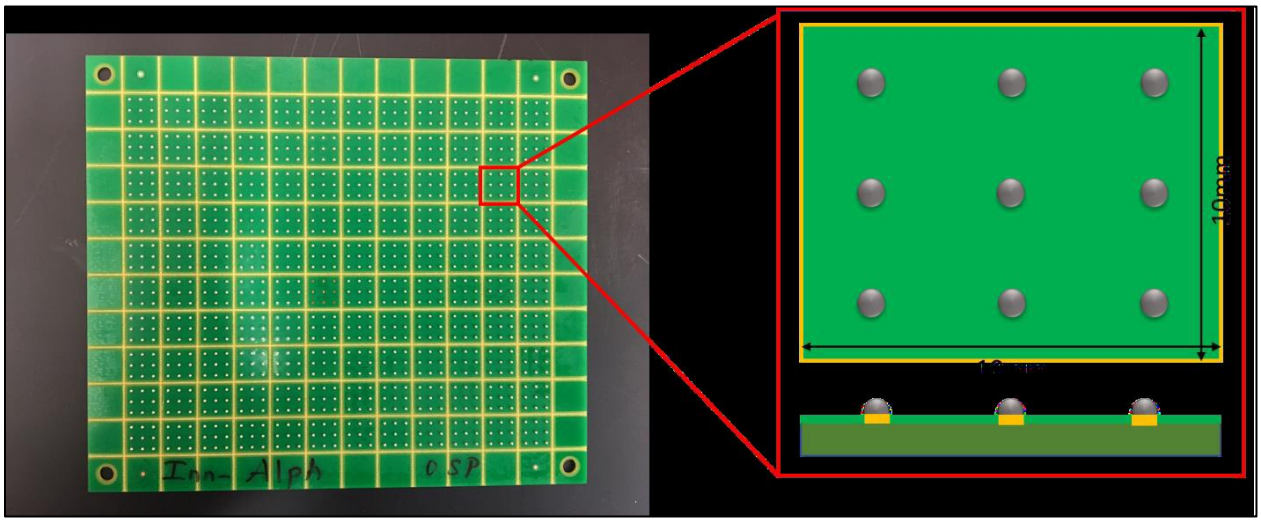

Figure 4-1 Test Vehicle and Individual Solder Joint

4.1.2 Assembly

After the design of PCBs and material of doped solder joints are determined, the machine DEK Galaxy was used for stencil printing which is shown in Figure 4-2. At first, the flux was first applied to prevent the oxides from surfaces and inspected by a microscope to see whether fluxes were applied properly. After that, the solder pastes were applied to PCBs. Also, it was inspected to check the solder paste's volume, area, and positions. Then the solder paste with the PCB would be reflowed by an 8 zones Pyramax 100N reflow oven (see Figure 4-3) within a nitrogen gas environment. The nitrogen was used for protecting the solder joints from oxidation and forming bulbs. And the reflow process would be inspected to check the quality of solder joints in the assemblies.

Figure 4-2 Machine DEK Galaxy for Stencil Printing

Figure 4-3 Pyramax 100N Reflow Oven

4.1.3 Cross-Section Sample Preparation

For studying the microstructure of solder ball, the cross-section process was done before the optical microscope and SEM examination. The cross-section process could be simply divided into three steps: mounting, grinding, and polishing. Basically, the samples were cut into 10mm*20mm pieces and they would be cold mounted the epoxy resin and hardener (Proportion is 6:1). Waiting above 24 hours, the samples with hardened resin would be grinded on a Pace Technologies NANO 1000T grinder-polisher machine (see Figure 4-4). The sandpapers with 240, 320, 400, 600, 800, 1200 Grits (Maily SiC) were used by sequence to reach the solder joints and a plane slicing the solder joints was created. After that, the 3μm polycrystalline and 0.03 diamond suspension were used by sequence to eliminate the scratch on final surface. For the best surface finish quality, the optical microscope would be used for inspections.

Figure 4-4 Pace Technologies NANO 1000T Grinder-Polisher Machine

4.2 Test Machine and Setup

The cyclic fatigue test was conducted under room temperature (25℃) with an Instron 5948 MicroTester which has force range from 2mN (0.2g, 0.0004lbf) to 2kN (200kgf, 450lbf) and high position resolution for 20nm, allowing to record the number of cycles, the stress-strain data, the stiffness, etc., which is shown in Figure 4-5. Meanwhile, a fixture was designed to hold the test tip for fatigue test, and the cut PCBs with solder joints would be attached with glue on the heavy sample holder.

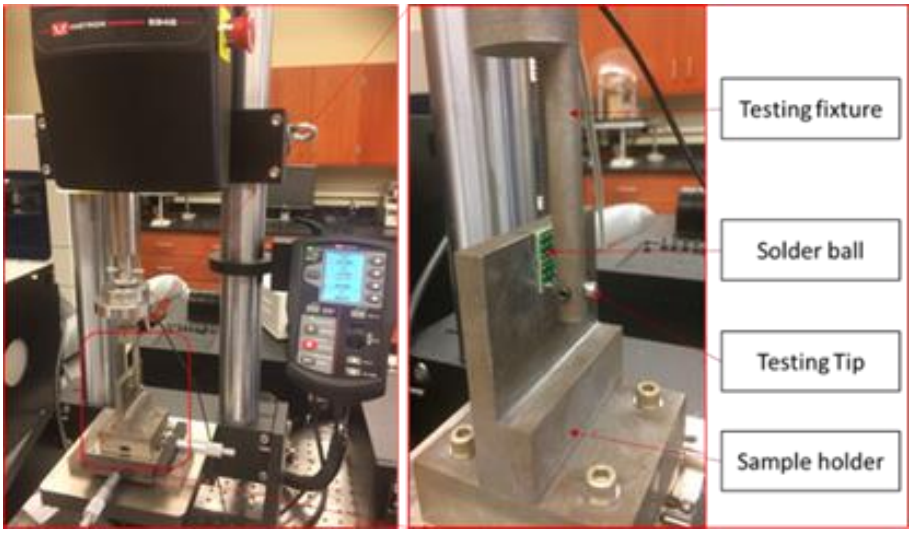

Figure 4-5 Instron 5948 MicroTester

Figure 4-6 below shows the side view of the fixture and how the individual solder joint contacts with the up and down side of the tip used in the test. The inner diameter of the tip is 40mils and the tip is set up 0.05mm off from the surface finish. Typically, the individual solder joint would be fixed on the sample holder and the Testing fixture would cyclically move up and down until the set-up stresses was reached. In the case that the cyclic fatigue test is stress-controlled based,

the failure is defined as moving distance of Testing Tip exceeds 0.6mm (Solder joint is totally separated from the PCB).

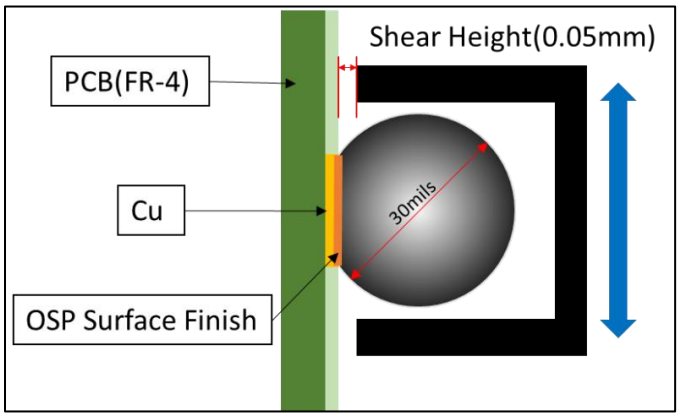

Figure 4-6 Schematic of Cycling Individual Solder Joint in the Fatigue Test

Besides, the ZEISS Axio Imager.M2m Optical Microscope with an Axiocam 503 color microscope camera (See Figure 4-7) was used to analyze the microstructure after solder ball is cross-sectioned. The optical microscope provides 5 objective magnifications (50, 100, 200, 500, and 1000x). Meanwhile, the Axiocam 503 color microscope camera is able to provide the resolution of fine structures as high as 4.54μm. Also, it is able to take 38 at most images per second at full resolution and features a dynamic range of 1:2500 for precise reproduction.

Figure 4-7 ZEISS Axio Imager.M2m Optical Microscope

In this research, the Hitachi S-2460N Scanning Electron Microscope (See Figure 4-8) was also used to specify microstructures and compositions of solder joints. Basically, the machine works under high vacuum environment and its instrument has an accelerate voltage range from 0.5-25kV.

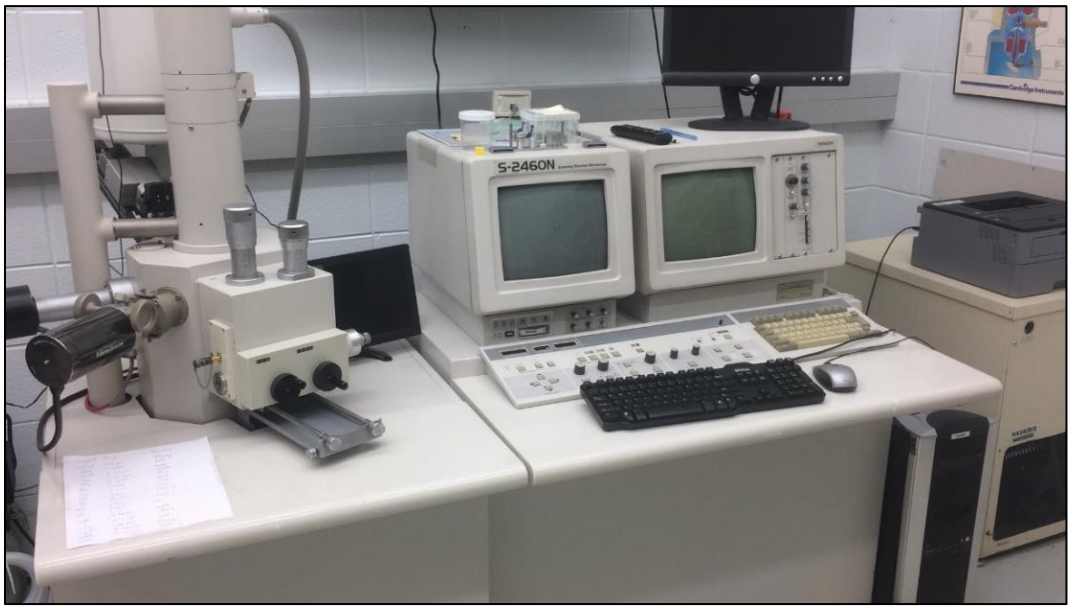

Figure 4-8 Hitachi S-2460N Scanning Electron Microscope

4.3 Proposed Test Plan

4.3.1 Study 1

The objective of study 1 is to investigate the fatigue performance of the solder alloys adding Bi under single stress amplitude conditions. Basically, four types of solder alloys (SAC305, SAC-R, SAC-Q, and SAC-I) were tested under room temperature (25℃). Shear fatigue tests were conducted to record the fatigue life, strain, stress information etc., according to the method mentioned in the previous section. Each type of solder alloy was tested under at least 4 stress levels and replicated at least 7 times under each stress level. The range of stress levels for each kind of

solder alloy is selected based on the solder alloy's characteristic fatigue life which is between 100 and 10,000 cycles. The test plan is specified in Table 4-2, which is shown below.

Table 4-2 Test Plan of Study 1

Solder Alloy	Stress level	Replicate	Solder Alloy	Stress level	Replicate
SAC305	16MPa	7	SAC-Q	24MPa	7
	20MPa	7		28MPa	7
	24MPa	7		32MPa	7
	28MPa	7		36MPa	7
SAC-R	16MPa	7	SAC-I	20MPa	7
	20MPa	7		24MPa	7
	24MPa	7		28MPa	7
	28MPa	7		32MPa	7

4.3.2 Study 2

The objective of study 2 is to investigate the effect of varying amplitude cycling on individual SAC-Bi solder joints fatigue. Basically, three types of solder alloys (SAC305, SAC-R, and SAC-Q) were tested under room temperature(25℃). Cyclic fatigue tests will be conducted to record fatigue life, strain, stress information etc., according to the method mentioned in the previous section. However, the individual solder joints were cycled under varying stress levels (mild and harsh) and Figure 4-9 shows a schematic of varying stress amplitude test of SAC305. Basically, the individual SAC305 solder joint was cycled 25 times under 18MPa and then 3 times under 27.6MPa. And the stress amplitude would be cyclically alternated between 18MPa and 27.6MPa

until total failure. The mild stress (18MPa) and harsh stress (27.6MPa) were estimated based on the single stress amplitude test from Study 1 and a pre-test was done to verify the mild and harsh stress level associated with characteristic fatigue life of 2500 cycles and 300 cycles, which is shown in Figure 4-10.

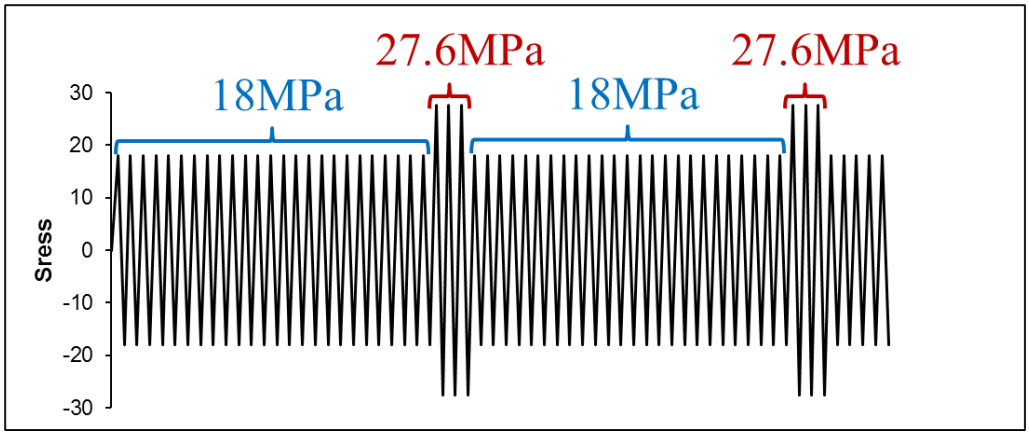

Figure 4-9 Schematic of Individual SAC305 Solder Joint under Varying Stress Amplitude Test

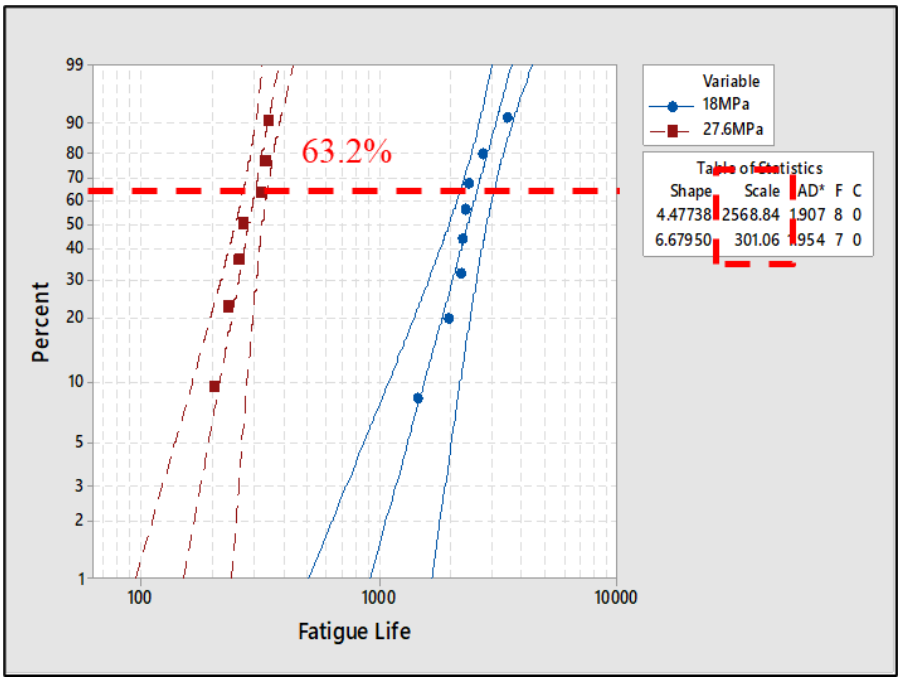

Figure 4-10 Characteristic Life of SAC305 under 18MPa and 27.6MPa

In the varying amplitude test, solder joints were cycled alternating the mild and harsh stress verified from the single stress amplitude test. For each kind of solder alloy, at least 7 replicates were done by alternating 25 mild stress cycles and 3 harsh stress cycles until total failure in Table 4-3. The design of experiment is based on the damage accumulation concept. Basically, the accumulated damage under different stress amplitudes were expected to be same, since these different stress amplitudes were all associated with same 2500 and 300 characteristic life (cycles). Generally, one alternate from 25 mild stress amplitude cycles to 3 harsh stress amplitude cycles were expected to accumulate 2% damage (25/2500+3/300=2%). Therefore, we were expected to have 50 alternates in the varying stress amplitude tests. However, all the solder joints failed much earlier than the expectation, which will be shown later.

Table 4-3 Test plan of Study 2

Alloy	Test Matrix	
	Test method	Replicate
SAC305	25 Mild stress cycles+3 Harsh stress cycles	7
SAC-Q	25 Mild stress cycles+3 Harsh stress cycles	7
SAC-R	25 Mild stress cycles+3 Harsh stress cycles	7

4.3.3 Study 3

The objective of study 3 is to investigate the aging effect on Bi-doped solder joints fatigue in the varying amplitude case. Basically, three types of solder alloys (SAC305, SAC-R, and SAC-Q) would be tested, and individual solder joint would be aged at 125℃ for 10 hours and 1000 hours respectively before the cyclic fatigue test.

After that, each kind of solder alloy was tested under at least 4 stress levels and replicated at least 7 times for each stress level according to Table 4-4. The stress level range for each kind of solder alloy was selected based on the solder alloy's characteristic fatigue life which is between 100 and 10,000. This part is similar with the test plan of Study 1.

Table 4-4 Single Stress Amplitude Test Plan of Aged Solder Alloys

Solder Alloy	Stress level	Replicate	Solder Alloy	Stress level	Replicate
10hour/1000hour SAC305	16MPa	7	10hour/1000hour SAC-Q	24MPa	7
	20MPa	7		28MPa	7
	24MPa	7		32MPa	7
	28MPa	7		36MPa	7
10hour/1000hour SAC-R	16MPa	7			
	20MPa	7			
	24MPa	7			
	28MPa	7			

Additionally, a pre-test of each combination of solder alloy and aging condition was done to verify the mild and harsh stress level associated with characteristic fatigue life of 2500 cycles and 300 cycles. Then a varying amplitude test for each case was conducted according to Table 4-5, which will be similar with Study 2.

Table 4-5 Varying Amplitude Test Plan of Aged Solder Alloys

Alloy	Aging Time	Test Matrix	
		Test method	Replicate
SAC305	0h	25 Mild stress cycles+3Harsh stress cycles	7
	10h	25 Mild stress cycles+3Harsh stress cycles	7

	1000h	25 Mild stress cycles+3Harsh stress cycles	7
SAC-Q	0h	25 Mild stress cycles+3Harsh stress cycles	7
	10h	25 Mild stress cycles+3Harsh stress cycles	7
	1000h	25 Mild stress cycles+3Harsh stress cycles	7
SAC-R	0h	25 Mild stress cycles+3Harsh stress cycles	7
	10h	25 Mild stress cycles+3Harsh stress cycles	7
	1000h	25 Mild stress cycles+3Harsh stress cycles	7

4.4 Fatigue Analysis Method

4.4.1 Characteristic Fatigue Life Analysis

We would fit the Weibull distribution with the fatigue life of the solder joints under each stress level according to equation 2.1. Basically, the probability density function of Weibull distribution would be plotted in a log-log graph as shown in Figure 4-11. Here the scale parameter represents the characteristic fatigue life (cycles) which is the time (cycles) when 63.2% of the solder joints will be expected to fail under specific stress level. For example, the fatigue life (cycles) of 7 individual SAC305 solder joints were collected under 16MPa, 20MPa, 24MPa, and 28MPa, respectively. And each point represents the failure time (cycles) of one individual SAC305 solder joint in Figure 4-11. Also, the characteristic life (cycles) of individual SAC305 solder joints under 4 single stress amplitudes test were specified by the scale parameter in the Table of Statistics in Figure 4-11.

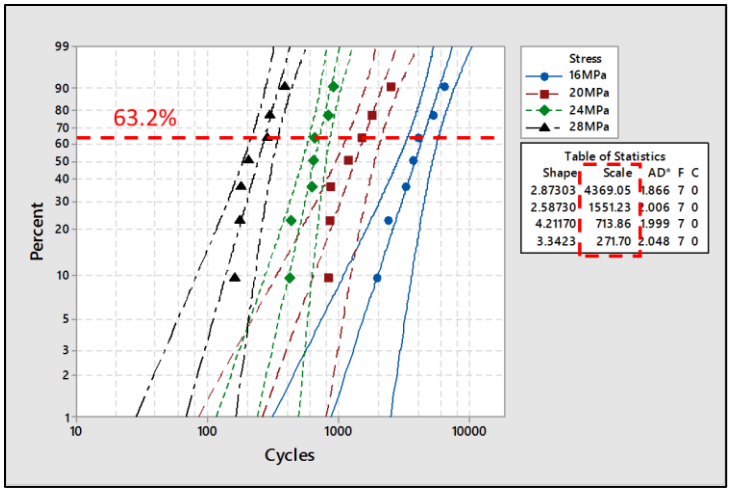

Figure 4-11 Fitted Weibull Distribution and the Characteristic Fatigue Life (Cycles) of SAC305 under Single Stress Amplitude Test

After that, we could fit a function of the characteristic life (cycles) and the stress in a log-log scale graph for each kind of the solder alloy in Figure 4-12. It is possible to estimate the stress levels of associated characteristic life (cycles) of each kind of solder alloy. For example, according to the fitted function in Figure 4-12, we could find the stress 18MPa associated with characteristic life 2500 cycles and the stress 27.6MPa associated with characteristic life 300 cycles. It gives us a reference to find the stress level associated with any specific characteristic life (cycles).

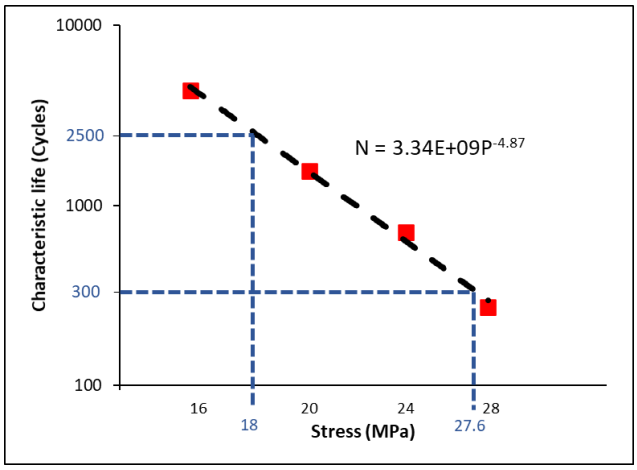

Figure 4-12 Fitted Power Equation of Characteristic Fatigue Life (Cycles) with Stress Amplitude

4.4.2 Plastic Damage Analysis

With the up & down movement of the solder joint in the tip, the change of the stress and strain would be recorded, and every fatigue cycle would form a hysteresis loop in a stress-strain graph. Typically, an example of one cycle's stress-strain of SAC305 under 28MPa was plotted in Figure 4-13, and here we would mainly explain the concept of inelastic work, plastic strain, and loading slope. As it is shown, the inelastic work is defined as the area within the hysteresis loop, and the plastic strain is the width of the loop. Basically, both are able to describe the "damage" accumulated by one cycle, since the cyclic plastic deformation is the main reason for the fatigue damage. Additionally, the initial slope of the hysteresis loop is an empirical measure of the effective stiffness of solder joint in the plane of loading and it represents the softness of material. The smaller loading slope indicates softer material.

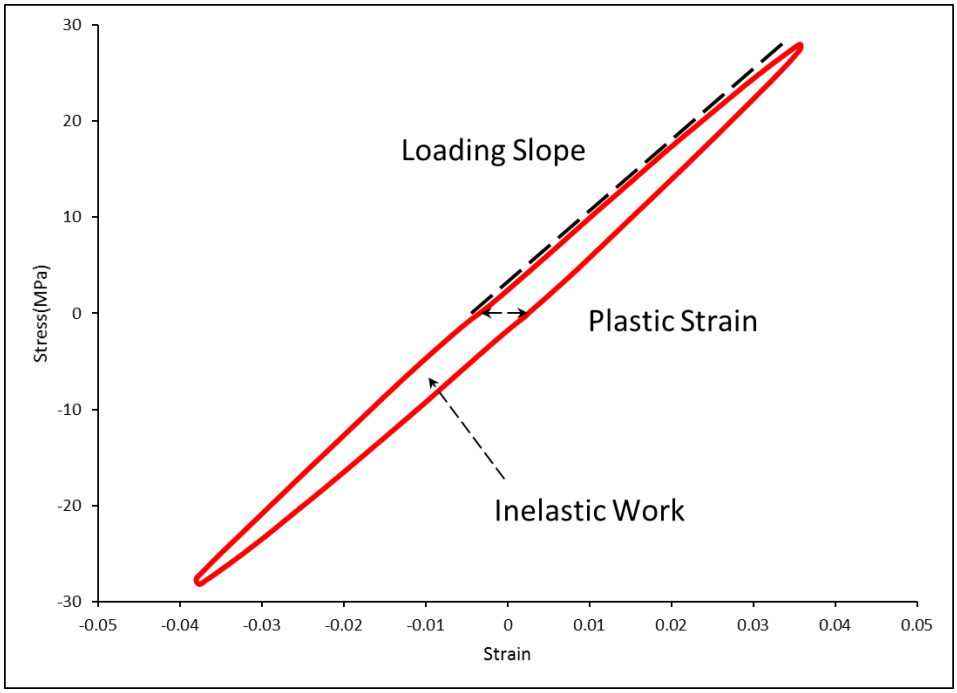

Figure 4-13 Example of a Hysteresis Loop of SAC305 in the Steady State

Then two famous fatigue models are used to evaluate the plastic damage for the 4 solder alloys: Morrow Energy model and Coffin-Manson model. In the Morrow Energy model, the characteristic life (cycles) of SAC305 was plotted as a function of inelastic work per cycle in a log-log scale graph, which is shown in Figure 4-14. As it is shown, more average inelastic work would contribute to less characteristic life (cycles) since average inelastic work indicates the "damage" accumulated for each cycle. And the fitted equation of Morrow Energy Model would be compared for each kind of solder alloy.

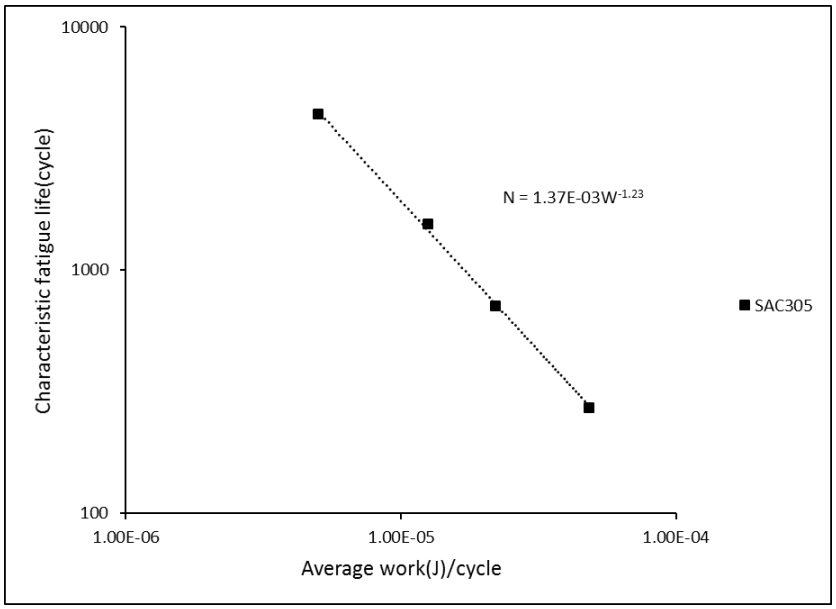

Figure 4-14 Morrow Energy Model of SAC305

In the Coffin-Manson model, the characteristic life (cycles) of SAC305 was plotted as a function of plastic strain in a log-log scale graph, which is shown in Figure 4-15. Same as the inelastic work, plastic strain has a negative relationship with characteristic life (cycles). And the fitted equation of Coffin-Manson Model would be compared for each kind of solder alloy.

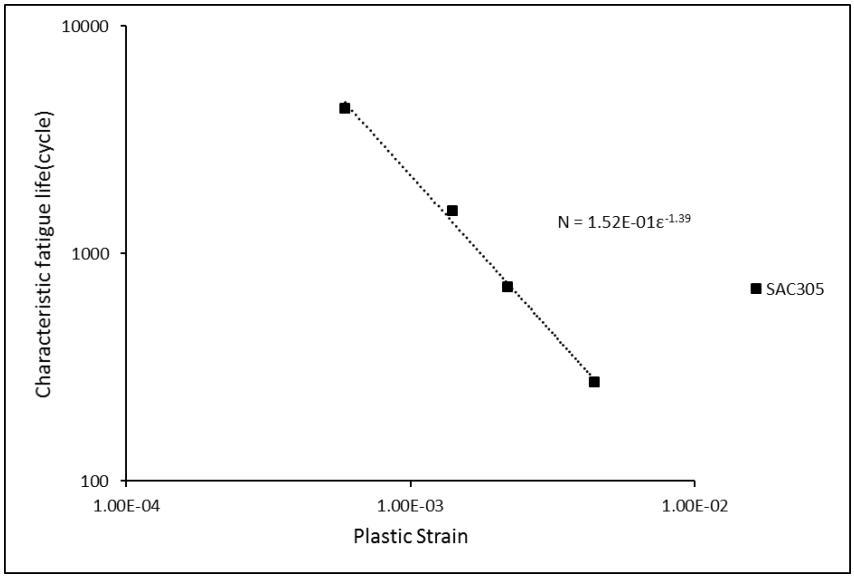

Figure 4-15 Coffin-Manson Model of SAC305

4.4.3 Varying Stress Amplitude Analysis

As the literature review showed, the common damage accumulation model failed to estimate the fatigue life of solder joints under varying stress amplitude conditions. Thus, the reliability analysis of solder joints under varying stress amplitudes would mainly depend on the modified damage accumulation model. And the original common damage accumulation model would be considered as a comparison of estimating individual solder joints' fatigue life.

Figure 4-16 showed an example of inelastic work of SAC305 under single stress amplitude 18MPa. In the single stress amplitude test, the inelastic work would drop in several cycles because of initial hardening and surface flattening. Then it would keep steady for a while, which indicates that the damage would be accumulated almost constantly, when same stress amplitude is applied. In the last 10% of fatigue life (cycles), the inelastic work per cycle would dramatically increase until total failure due to damage accumulations.

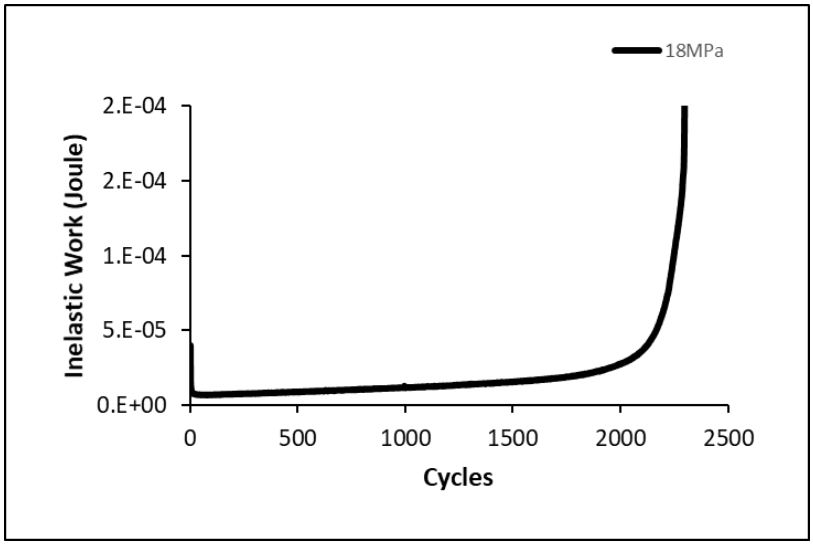

Figure 4-16 Example of Inelastic Work Per Cycle in Single stress Amplitude Test of SAC305

However, in varying stress amplitude test (18MPa-27.6MPa) shown in Figure 4-17, the inelastic work would have a "Step-up" phenomenon after every switch between mild stress amplitude (18MPa) and harsh stress amplitude (27.6MPa). Basically, the inelastic work of the first 25 mild stress amplitude cycles (18MPa) was similar with what we observed in single stress amplitude test. However, after switching to harsh stress amplitude (27.6MPa), the average inelastic work of the mild stress amplitude cycles (cycle 29-53) was slightly increased, though same stress amplitude 18MPa is applied. And after next switch to harsh stress amplitude (27.6MPa), the average inelastic work of the mild stress amplitude cycles (cycle 57-81) was slightly increased again. It indicates that more damage was accumulated per cycle than expected, after every switch from harsh stress to mild stress amplitude cycles, though the same stress amplitude (18MPa) was applied in varying stress amplitude test.

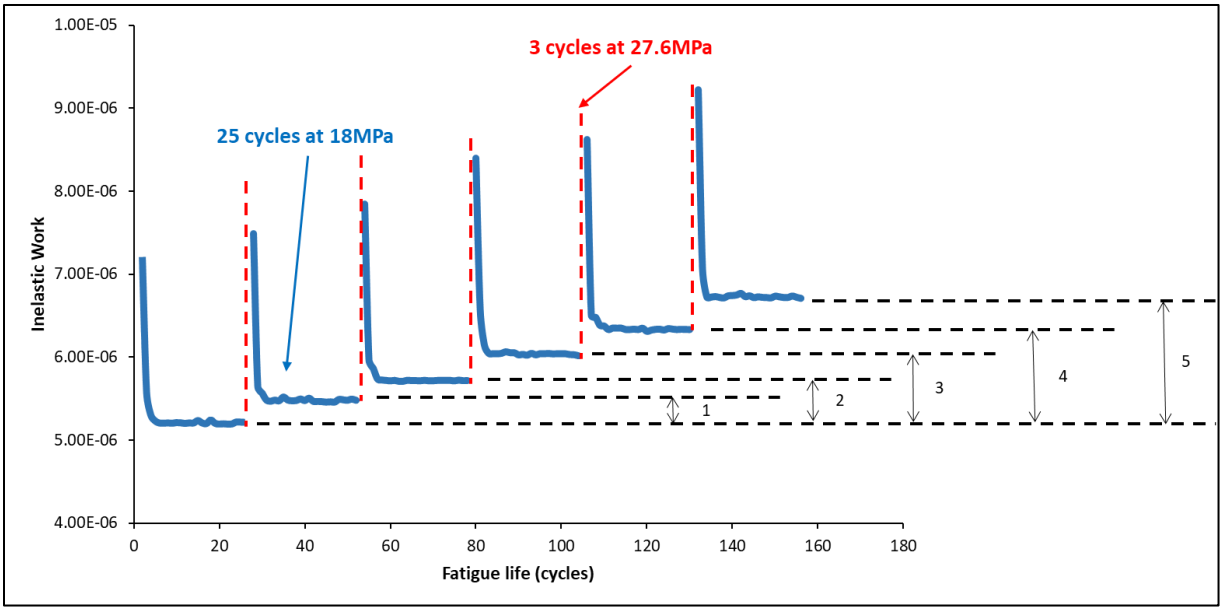

Figure 4-17 Example of Inelastic Work Per Cycle in Varying stress Amplitude Test of SAC305

Therefore, it is essential to quantify how much more damage is accumulated after each switching. And a new factor called amplification factor is proposed. In short, amplification factor would be defined as the ratio of average inelastic work after mild-harsh amplitude switch to average inelastic work before mild-harsh amplitude switch. Therefore, we recorded the average inelastic work of the steady state after every switch in Figure 4-18. For example, the amplification factor of switch 1 would be the average inelastic work after 1st switch over the average inelastic work before 1st switch. According to this method, the amplification factor would be fitted with a linear equation in the early stage, which is shown in Figure 4-19. With crack propagation, the amplification factor would increase dramatically. And we would compare the CDI estimation of individual SAC-Bi solder joints under varying amplitude conditions based on the modified damage accumulation model.

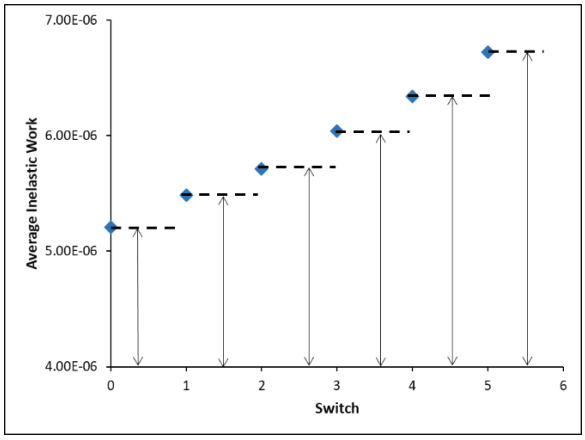

Figure 4-18 SAC305's Average Inelastic Work of Mild Stress Cycles

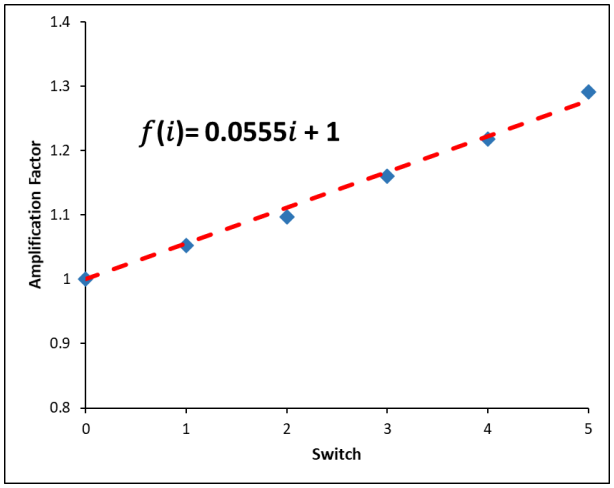

Figure 4-19 Example of One SAC305 Solder Joint's Amplification Function under Varying Stress Amplitude Condition

4.4.4 Aging Effect Analysis

The effect of aging on solder alloys would be discussed under single stress amplitude condition, in the case that we had the test result of solder alloys without aging (Result from Study 1). Figure 4-20 shows the characteristic life comparisons of SAC305 under non aged, 10hour aged, and 1000hour aged conditions. As it is shown, the characteristic life of 10hours aged SAC305 drops about 40%-50% of 0hour aged SAC305 under same stress amplitude condition. And the drop ratios

reach to 60% to 70% after aged for 1000hours. It indicates that the aging time plays a critical role on the fatigue of SAC305. Later, there would be more comparisons about the other solder alloys.

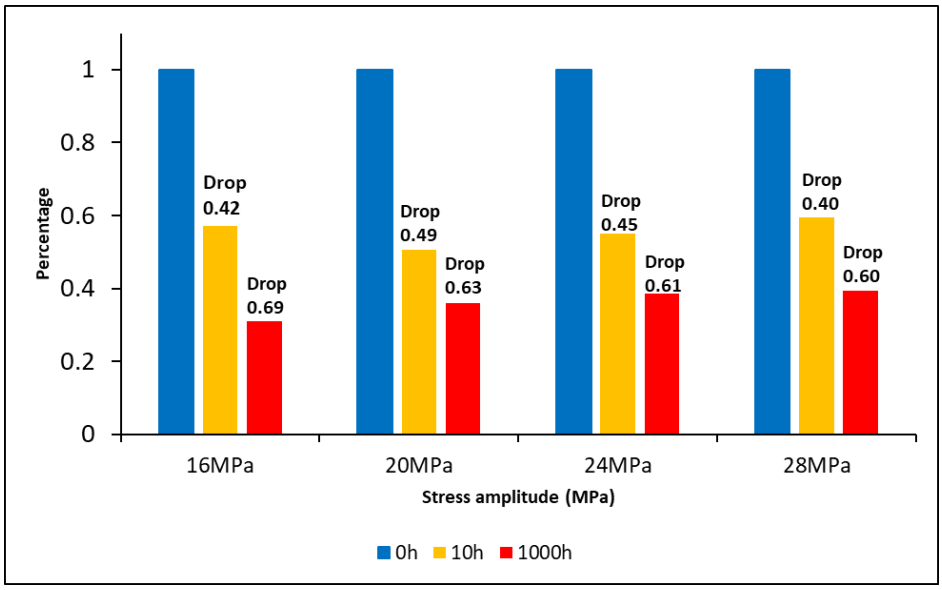

Figure 4-20 Characteristic Life (Cycles) of 0hour, 10hours, and 1000hours Aged SAC305 Solder Joints

Additionally, we would try to figure out how the aging time influences the solder alloys' fatigue under varying amplitude conditions. Therefore, we would use the modified damage accumulation model to estimate the fatigue life of solder alloys. And then compare the amplification functions of different aging cases under varying amplitude conditions (Result from Study 2 and Study 3).

4.4.5 Microstructure and Failure-mode Analysis

The microstructure and failure mode of solder alloys would be analyzed using optical microscope and SEM. Figure 4-21 is a typical example of SAC305 solder joint. SAC305 involves 3% Ag and 0.5% Cu. Ag and Cu interact with Sn to form intermetallic compound particles. These particles enhance the strength and fatigue resistant of solder joints by precipitate hardening. After doing

EDS, it can be seen that the SAC305 solder joint is full of Ag-Sn rich phase and Sn rich phase inf Figure 4-22.

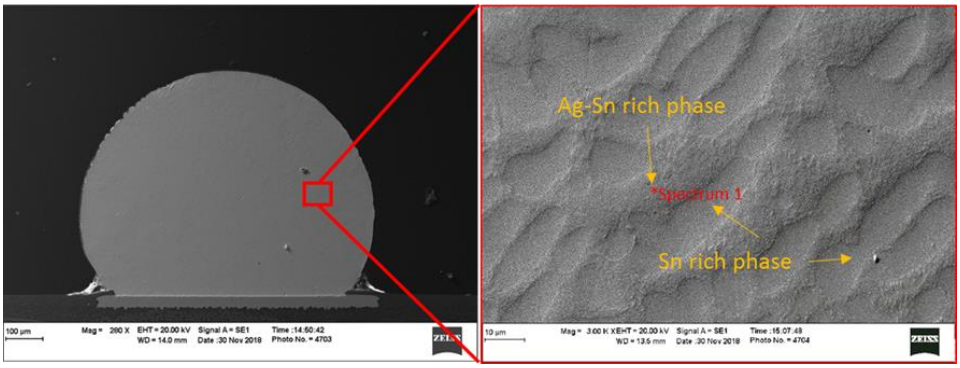

Figure 4-21 Morphology and Microstructure of SAC305 Using SEM

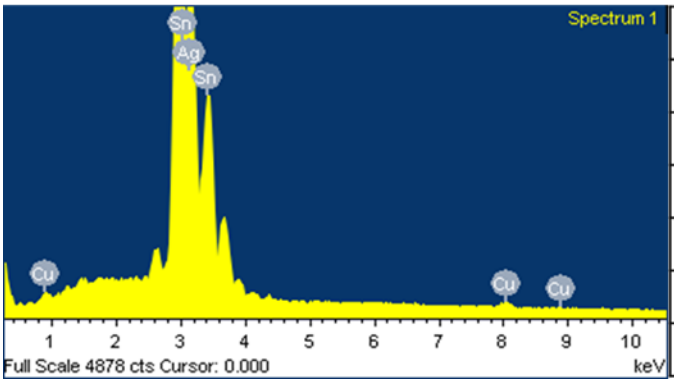

Element	Weight%	Atomic%
Cu K	1.01	1.74
Ag L	74.40	75.57
Sn L	24.59	22.70
Totals	100.00	

Figure 4-22 EDS Spectrum Analysis of SAC305 (Spectrum 1 Location)

Figure 4-23 shows an optical micrograph of SAC305's interface area between solder alloy and Cu substrate. It can be seen that an evenly distributed IMC layer (about 2-3 micrometers) was formed at the interface location. And the failure mode was also analyzed from cross-section view and top view using the optical microscope and SEM. Basically, two failure modes were frequently observed in this study. In Figure 4-24 and Figure 4-25, a typical cross-section view and top view of the fracture of SAC305 are shown. Portions of solder alloy were left on Cu substrate as the

majority of solder alloy separated due to shear fatigue. The crack propagation occurred within the bulk alloy. This failure mode was also frequently observed for SAC-R.

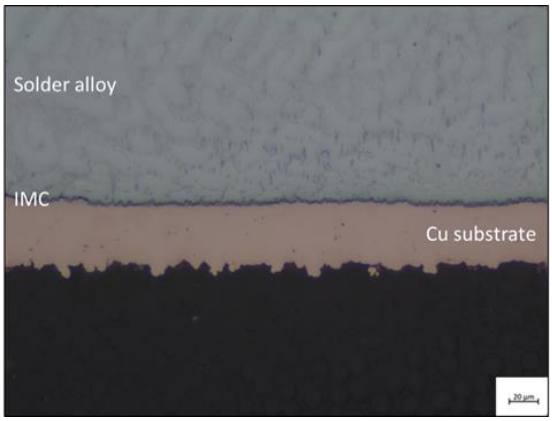

Figure 4-23 Optical Micrograph of SAC305's Interface Area

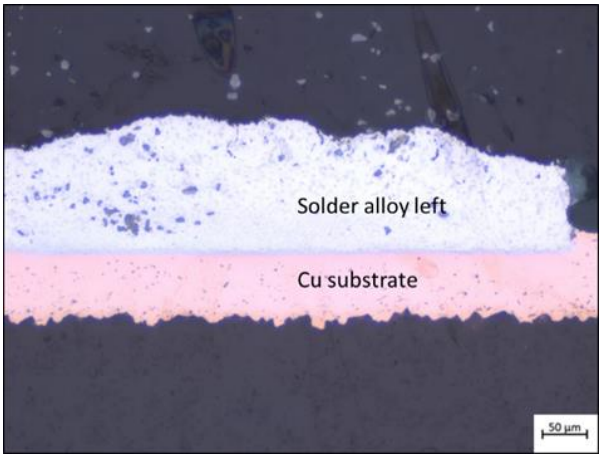

Figure 4-24 Cross-Section View of a Failed SAC305

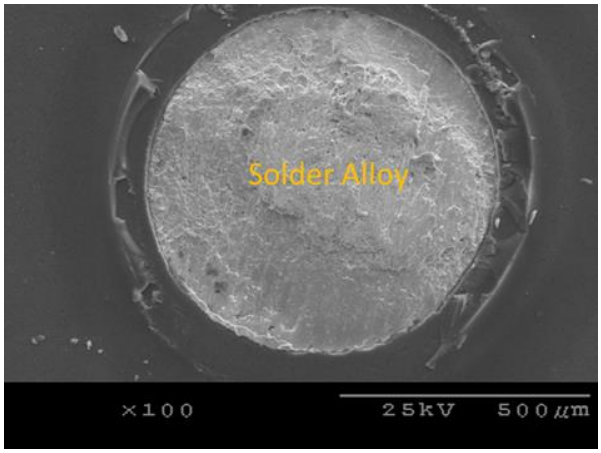

Figure 4-25 Top View of a Failed SAC305

Figure 4-26 and Figure 4-27 show typical cross-section view and top view of the fracture of SAC-I. Almost all the solder alloys were separated, leaving some portions of IMC on Cu substrate. This failure mode was also observed for SAC-Q. SAC-Q and SAC-I alloys have high strength and fatigue resistance due to the combined Ag and Bi content, thus the IMC layer becomes the "bottleneck" of solder joint's strength. Therefore, the crack propagation occurred along the IMC layer.

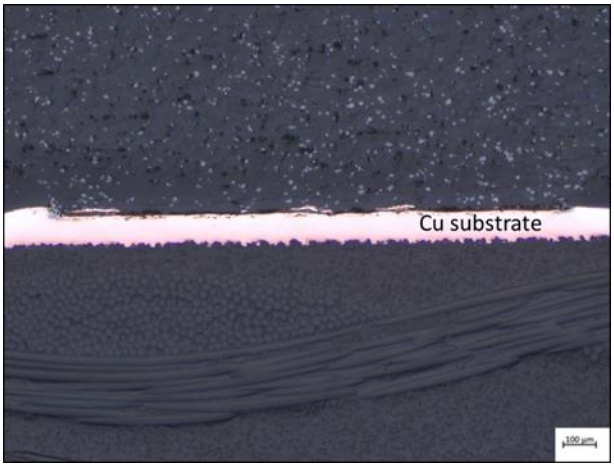

Figure 4-26 Cross-Section View of a Failed SAC-I

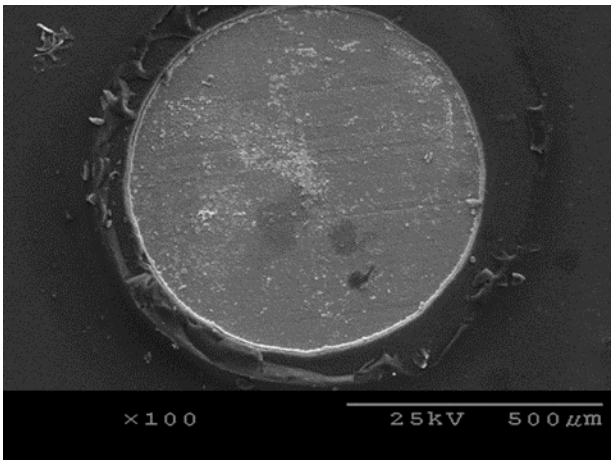

Figure 4-27 Top View Of a Failed SAC-I

Chapter 5 Fatigue Analysis of Individual Solder Joint Under Single Stress Cycling

5.1 Introduction

The reliability of solder joints plays a critical role in electronic assemblies. SnAgCu solder alloys with doped elements such as Bi and Sb is one of the candidates for high reliability applications. However, the mechanical and fatigue properties of the actual solder joint structure have not been studied for these new alloys. There is a great need for understandings of the performance of Sn-Ag-Cu (SAC) alloys with bismuth-doped in realistic settings. Therefore, this part focuses on investigating the fatigue performance of actual realistic solder joints with three solder alloys, named SAC-Q (SnAgCu-Bi), SAC-I (SnAgCu-BiSb), and SAC-R (SnCu-Bi), compared with the SAC305 (SnAgCu) as the baseline. Also, the morphology and microstructure of the solder joints will be discussed.

5.2 Fatigue Life Analysis

As said, the Sn-Ag-Cu type alloys vary from one joint to joint. A major reason can be attributed to the orientation of the anisotropic Sn grains relative to the loading direction and variations in the secondary precipitate distributions. Thus, it requires the extrapolation of experimental failure distributions based on the solder joint fatigue test result. The most commonly used statistical distribution is Weibull distribution. Typically, the fatigue life of individual solder joints for each material under given stress levels was fitted into a two-parameter Weibull distribution. Figure 5-1 shows the fitted Weibull distribution of SAC-Q fatigue life under 20MPa, 24MPa, 28MPa and 32MPa. It can be seen that all the points fall into a 95% confidence bands of Weibull distribution.

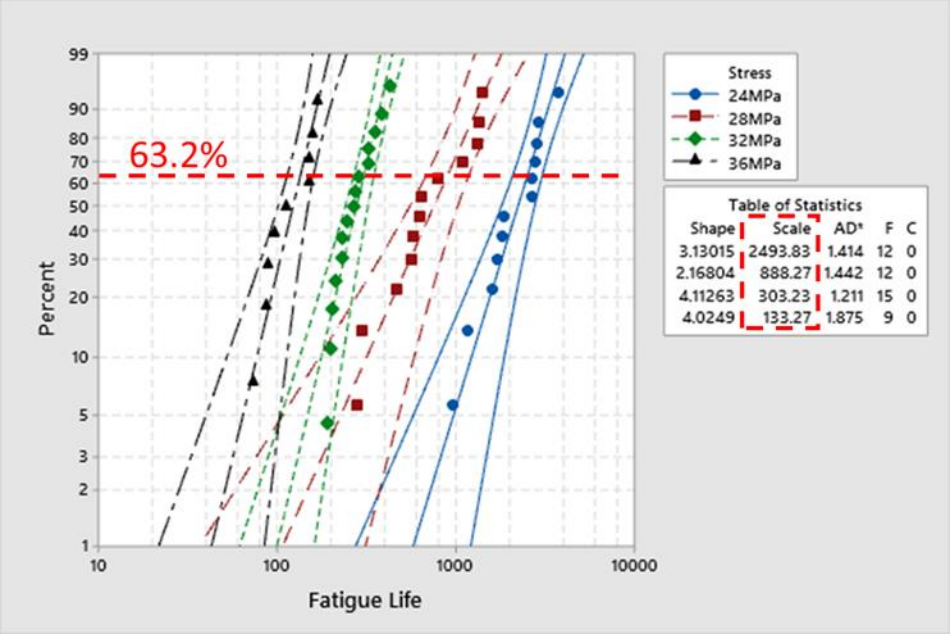

Figure 5-1 Fitted Weibull Distribution and the Characteristic Fatigue Life of SAC-Q under Single Stress Amplitude Test

The shape parameter represents the slope of the fitted Weibull curve, and the scale parameter represents the characteristic fatigue life when 63.2% of the total population fails. Figure 5-2 and Figure 5-3 are showing the fitted Weibull distribution and characteristic life of SAC-I and SAC-R under single stress amplitude test. The characteristic life is not decreasing evenly while the stress level is linearly increasing every 4MPa.

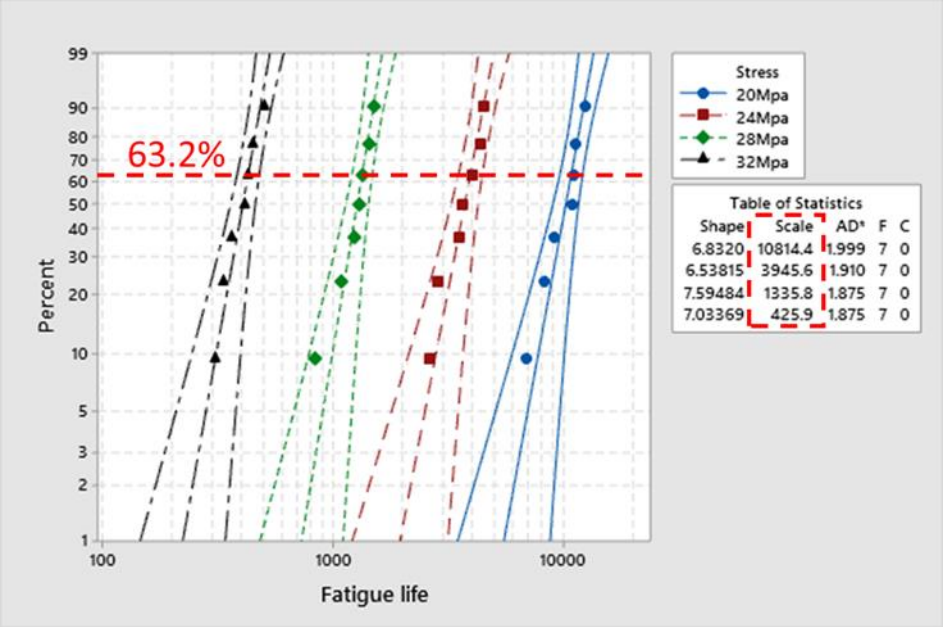

Figure 5-2 Fitted Weibull Distribution and the Characteristic Fatigue Life of SAC-I under Single Stress Amplitude Test

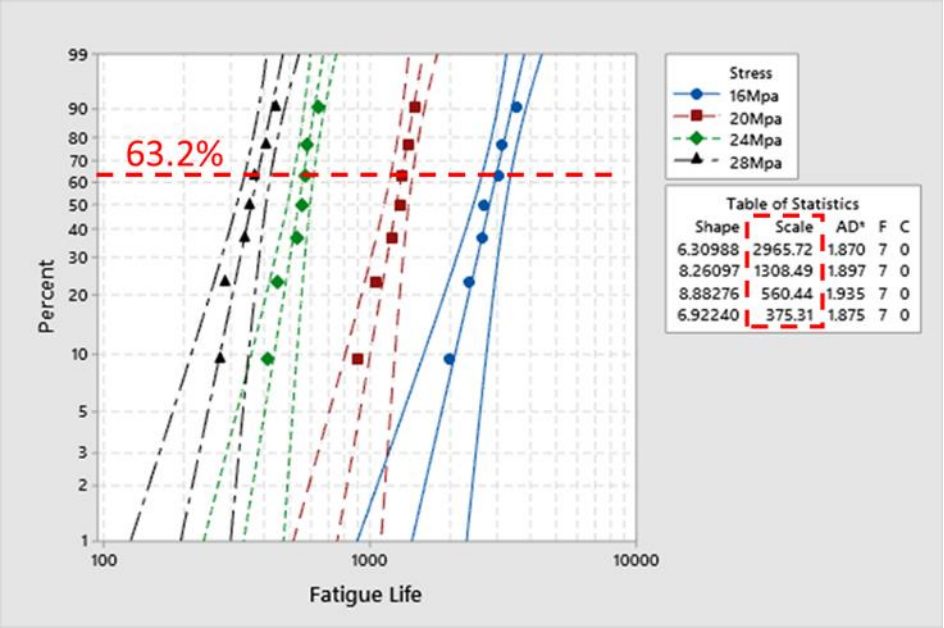

Figure 5-3 Fitted Weibull Distribution and the Characteristic Fatigue Life of SAC-R under Single Stress Amplitude Test

Figure 5-4 shows the relations between the characteristic fatigue life and the stress amplitude of SAC305, SAC-I, SAC-Q, and SAC-R on a log-log scale. And a power equation was fitted.

Generally, the characteristic life of SAC-Q and SAC-I is much higher than SAC305 and SAC-R at any stress amplitude. This is mainly due to the effect of Bismuth (solid solution hardening) and Silver (precipitates hardening) in SAC-Q and SAC-I. However, there is no Bismuth in SAC305 and no Silver in SAC-R, respectively.

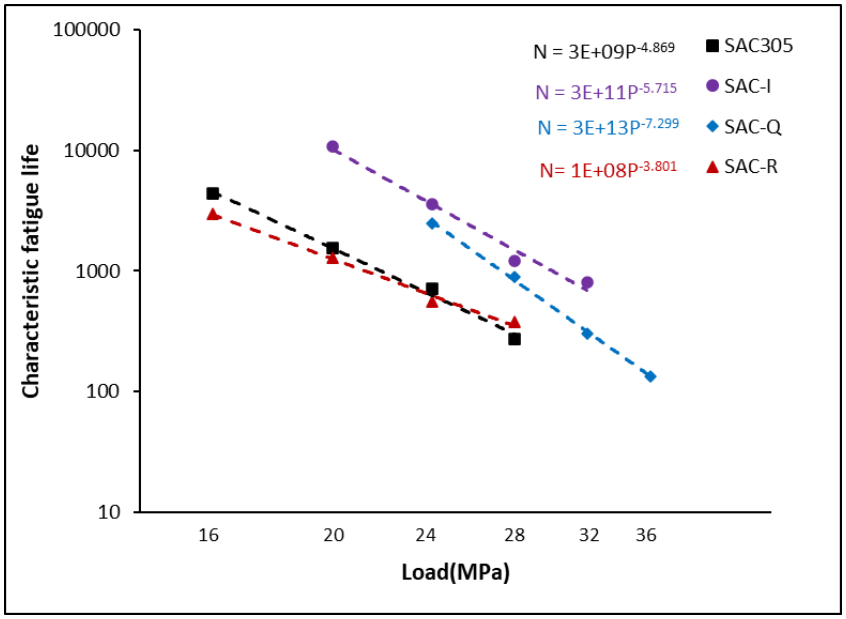

Figure 5-4 Characteristic Fatigue Life of SAC305, SAC-I, SAC-Q, and SAC-R as a Function of Stress Amplitude

Based on the fitted equations, it is possible to estimate the characteristic life of the four solder alloys under lower stress conditions. SAC-Q's performance is superior to the other three alloys under 5MPa and 10MPa, according to the estimations shown in Table 5-1. Also, the fitted equations can provide us a reference to look for our mild and harsh stress amplitude, which will be discussed later.

Table 5-1 Estimation of Characteristic Fatigue Life under 10MPa and 5MPa

Alloy	Characteristic life at 10MPa (cycles)	Characteristic life at 5MPa (cycles)
SAC305	40,000	1,200,000
SAC-I	600,000	30,000,000
SAC-Q	1,500,000	230,000,000
SAC-R	15,000	220,000

5.3 Hysteresis Loop Analysis

The evolution of inelastic work involves 3 stages according to the examples showed in Figure 5-5. Figure 5-5 shows typical SAC305's inelastic work of each cycle under 16MPa, 20MPa, 24MPa, and 28MPa. Basically, the inelastic work per cycle rapidly drops because of the solder joint hardening. Then the inelastic work per cycle will keep steady. And at last, the inelastic work per cycle exponentially increases until complete failure due to the major crack initiations and propagations. In Figure 5-5, we can observe a similar trend for all the cases. And the inelastic work per cycle of the steady region is higher under higher stress amplitudes, which indicates that the higher stress creates more damage in each cycle.

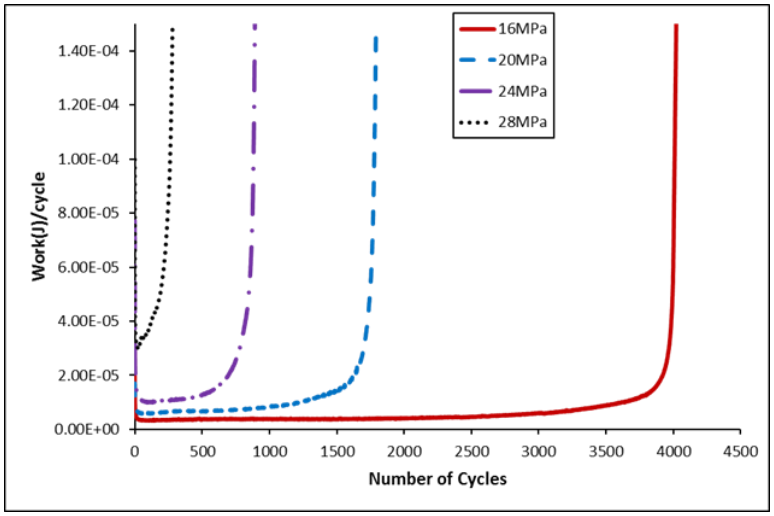

Figure 5-5 Inelastic Work of SAC305 Cycled under 16MPa, 20MPa, 24MPa, and 28MPa

Figure 5-6 shows typical hysteresis loop comparisons of SAC305 cycled at 16MPa, 20MPa, 24MPa, and 28MPa. The hysteresis loop area of 28MPa is significantly larger than the hysteresis loop at 16MPa, which indicates that more "damage" is accumulated in 28MPa cycles. And the width of 28MPa hysteresis loop, which means the plastic strain, is significantly wider than that of 16MPa.

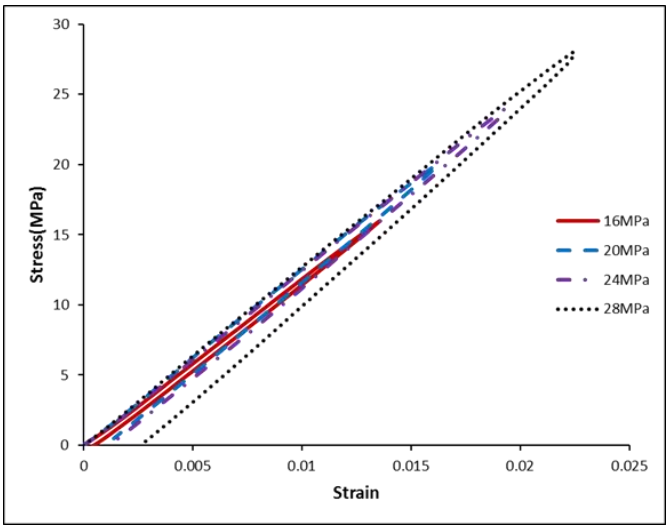

Figure 5-6 Hysteresis Loops in the Steady Region of SAC305 Cycled under 16MPa, 20MPa, 24MPa, and 28MPa

Figure 5-7 shows comparisons of inelastic work per cycle in the steady region of all solder alloys cycled at fixed stress amplitude of 28MPa. Initially, the inelastic work of all the cases will drop after several cycles. However, the inelastic work will stabilize at different levels. SAC-Q and SAC-I have the lowest work per cycle in the steady region, which indicates that SAC-Q and SAC-I are least damaged for each cycle. And the work dissipation per cycle for SAC305 is higher than that for SAC-R.

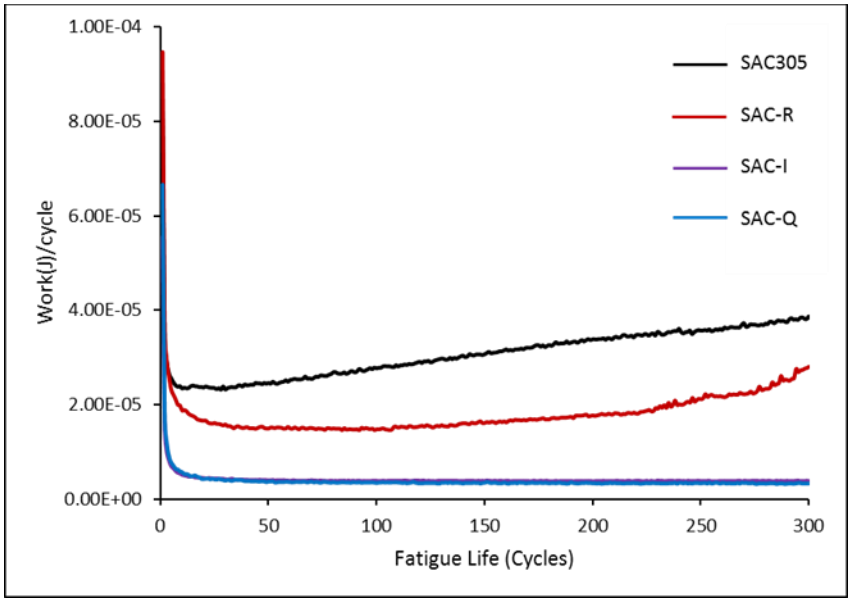

Figure 5-7 Inelastic Work of SAC305, SAC-R, SAC-I, SAC-Q under 28MPa

Figure 5-8 shows typical hysteresis loops at the steady region of SAC305, SAC-R, SAC-I, SAC-Q cycled at 24MPa. Consistent result is observed. Under the same 24MPa, SAC305 has the largest hysteresis loop, which indicates SAC305 stabilize at highest level of inelastic work, since the inelastic work is defined as the area of hysteresis loop. And then it is followed by SAC-R, then SAC-Q, and SAC-I. Generally, a larger hysteresis loop indicates more damage per cycle and thus a smaller number of cycles to failure. Also, SAC305's plastic strain (width of Hysteresis loop) is

largest under 24MPa. It indicates that SAC305 has most strain under the same stress 24MPa, when comparing with the other solder alloys.

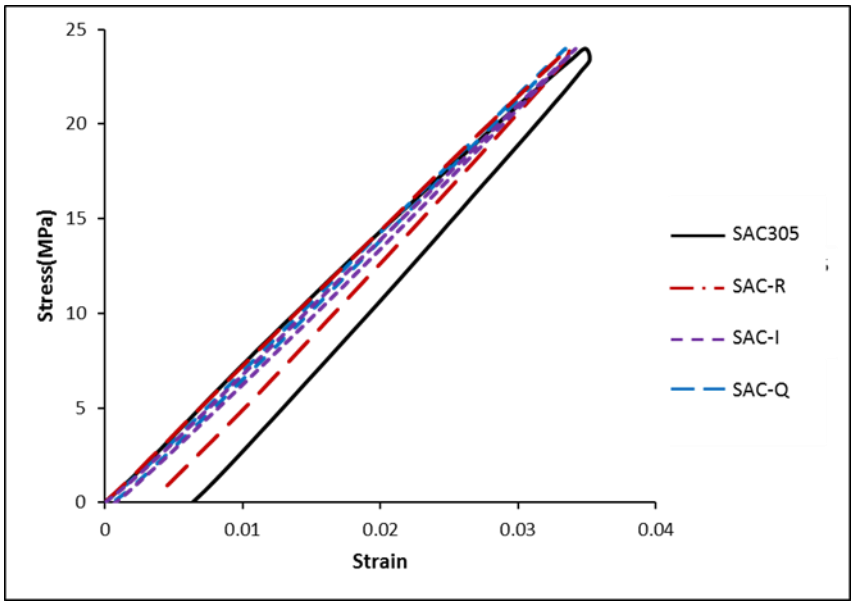

Figure 5-8 Comparison of Hysteresis Loops of SAC305, SAC-R, SAC-I, SAC-Q under 24MPa

Figure 5-9 shows the characteristic life (cycles) versus the average steady work per cycle for all alloys on a log-log scale. The Morrow equation is fitted into each curve, and Morrow parameters are calculated. Table 5-2 shows the detail information of fatigue ductility, C, and fatigue exponent, n, for each solder alloy. Predicting fatigue life based on the Morrow model requires an estimation of the work dissipation per cycle. Generally, the characteristic life (cycles) is shorter when the average inelastic work is larger. In this study, the work per cycle was measured for individual solder joints. SAC305 and SAC-R has close fatigue exponent, and SAC-Q and SAC-I has close fatigue exponent. That is why their fitted Morrow equation lines are almost in parallel in the log-log graph. Additionally, the fatigue ductility of SAC305 is significantly different from the other solder alloys. The possible reason is the exist of Bi in SAC-Q, SAC-I, and SAC-R.

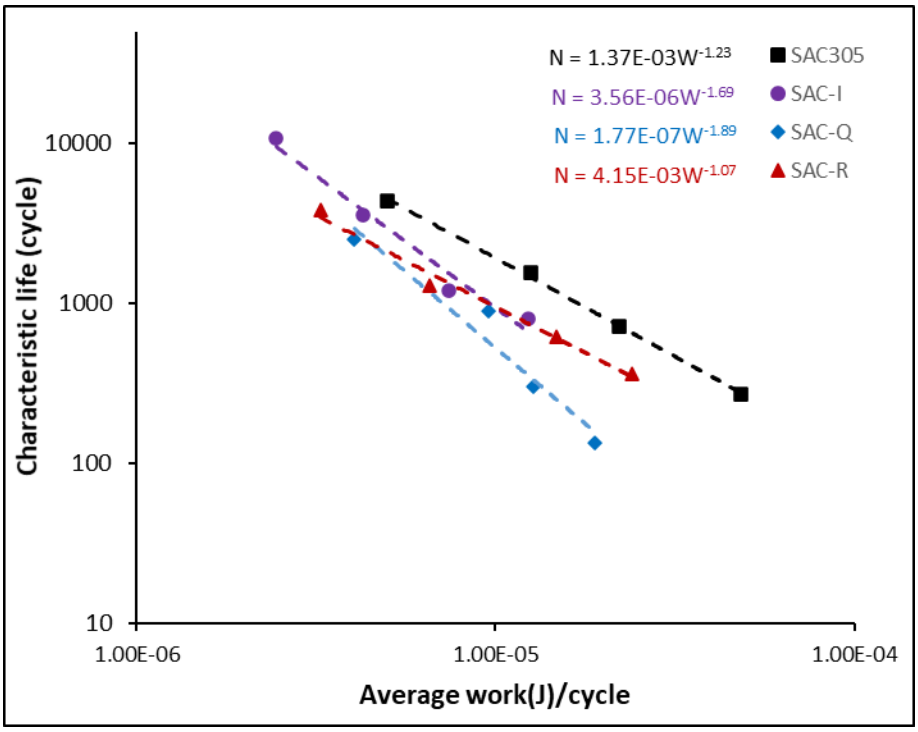

Figure 5-9 Fitted Curves of SAC305, SAC-I, SAC-Q, and SAC-R Using Morrow Energy Model

Table 5-2 Summary of the Morrow Energy Model's Coefficients

Alloy	fatigue ductility, *C*	fatigue exponent, *n*
SAC305	4.70E-03	0.813
SAC-I	5.97E-04	0.592
SAC-Q	2.68E-04	0.529
SAC-R	5.94E-04	0.935

Figure 5-10 shows a typical example of the plastic strain range per cycle evolution through the fatigue life (cycles) of SAC305 cycled at 16MPa stress amplitude. Three regions are detected in the plastic strain curve. In Region 1, the plastic strain will fall after several cycles because of the solder joint hardening. After that, the plastic strain will keep steady in Region 2, and it will dramatically increase until the complete failure in Region 3 because of crack initiation and growth. Figure 5-11 shows a comparison of the plastic strain range of SAC305 solder joints cycled at different stress levels. The plastic strain range per cycle in the steady region is higher for higher

stress amplitudes, which indicates more damage per cycle is generated under higher stress loads. Also, the number of cycles until complete failure is lower for higher stress amplitudes.

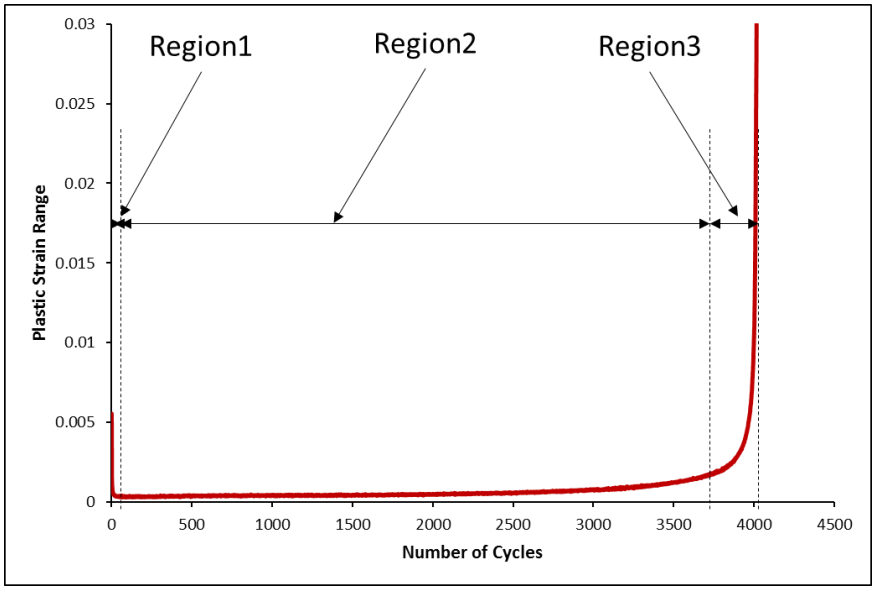

Figure 5-10 Evolution of the Plastic Strain Range through the Fatigue Life of a SAC305 Solder Joint Cycled under 16MPa

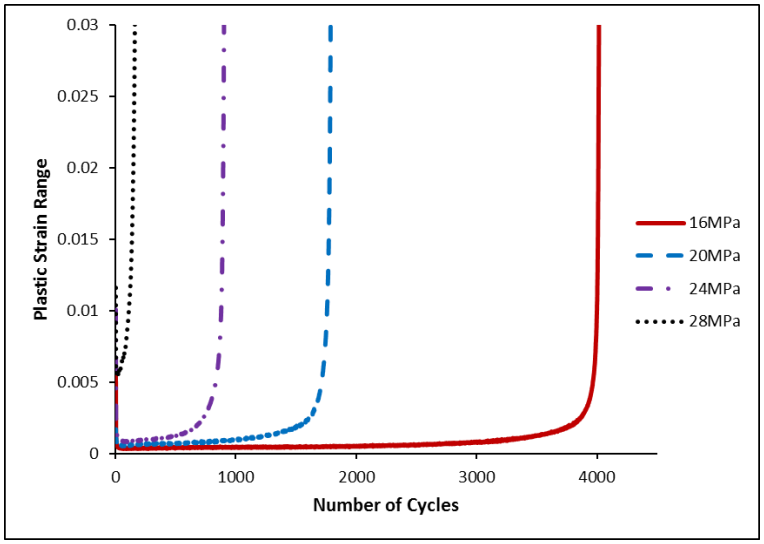

Figure 5-11 Plastic Strain Range Vs. Number of Cycles for SAC305 Solder Joints Cycled at Different Stress Levels

Figure 5-12 shows a comparison of the evolution in the plastic strain range per cycle of different solder alloys cycled at a fixed stress amplitude of 24MPa. The plastic strain range of the SAC305

and SAC-R are much higher than that for SAC-Q and SAC-I under the same stress level. The SAC-Q plastic strain under the steady stage is similar to SAC-I.

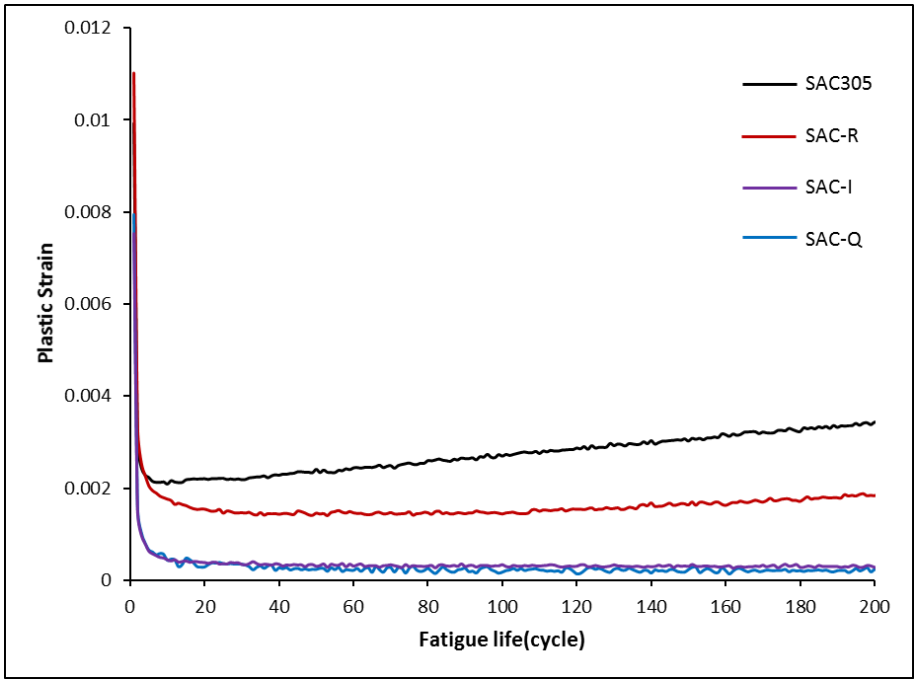

Figure 5-12 Comparison of the Plastic Strain Range Per Cycle of Different Solder Alloys Cycled at 24MPa

The Coffin-Manson fatigue model is commonly used in displacement control tests to fit the relationship between plastic strain range and fatigue life. The plastic strain range in this load-controlled experiment is not constant through the fatigue life; it evolves, as shown in Figure 5-11. However, most of the fatigue life is in the steady-state region, region 2, where it exhibits relatively constant plastic strain range. Thus, the correlation between the fatigue life of the solder joint in this experiment and the average plastic strain range in the steady-state region, region 2, can be defined using the Coffin-Manson model. Figure 5-13 shows the characteristic life (cycles) of the tested alloys as a function of the plastic strain range with Coffin-Manson fitted curves. Table 5-3 shows the constants, the fatigue ductility and fatigue exponent coefficients for all solder joints alloys. It is obvious that the fitted curves of SAC-Q and SAC-I are almost overlapped with very close Coffin-Manson constants.

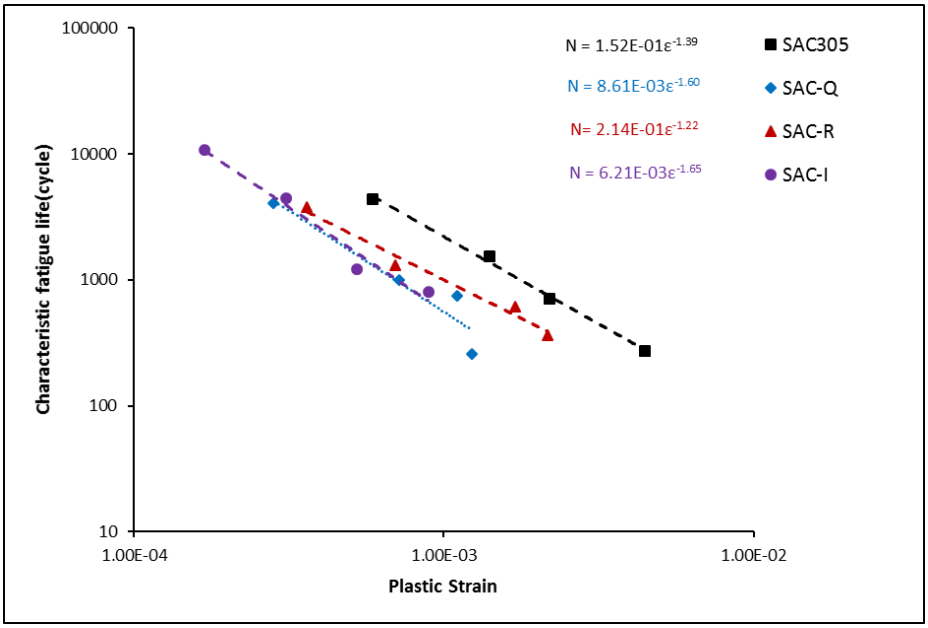

Figure 5-13 Coffin-Manson Fatigue Model Curves for All Solder Alloys

Table 5-3 Summary of the Coffin-Manson Model Coefficients

Alloy	Fatigue Ductility, θ	Fatigue Exponent, α
SAC305	0.258	0.719
SAC-Q	0.0512	0.625
SAC-R	0.283	0.820
SAC-I	0.0460	0.606

5.4 Microstructure and Failure Mode

Figure 5-14, Figure 5-15, and Figure 5-16 show the microstructure of SAC-Q, SAC-I, and SAC-R. Adding Bi to the SAC-alloy leads to an increase in the strength and fatigue resistance by solid solution hardening. SAC-I and SAC-Q have over 3% Bi. Bi can dissolve in the Sn crystalline matrix and causes distortion, thus decreases the creep rate, and improves the mechanical properties. However, the solubility of Bi in the Sn matrix is low at room temperature, around 1.8%. Thus, the additional Bi over the solubility limit will form a separate Bi-rich phase, which it appears

under the SEM as bright particles as shown in Figure 5-14 and Figure 5-15. For SAC-R, the Bi-rich phase was not detected in the SEM for the cross-section samples. SAC-R has around 2.4% Bi; thus, it is expected to have less Bi-rich particles comparing to SAC-Q and SAC-I. Also, the microstructure of SAC-R is different than SAC305. SAC-R has no Ag-Sn precipitates since it has no Ag content. However, from the mechanical performance, it appears that SAC-R is designed to have a similar mechanical performance to SAC305 by replacing the 3% Ag with 2.4% Bi.

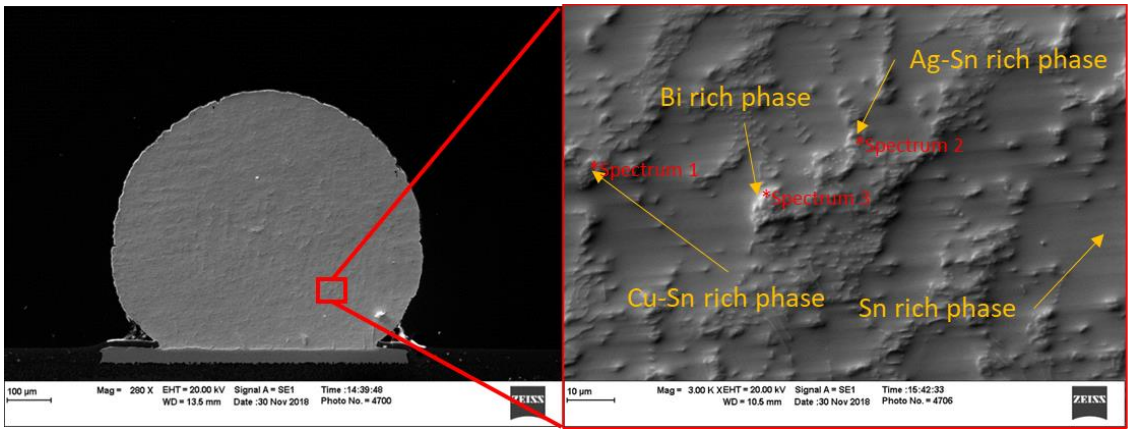

Figure 5-14 Morphology and Microstructure of SAC-Q Using SEM

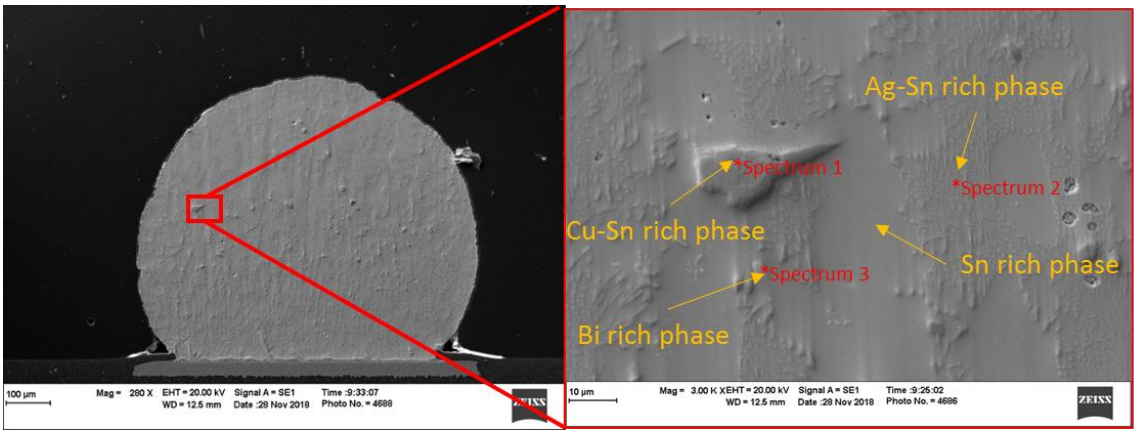

Figure 5-15 Morphology and Microstructure of SAC-I Using SEM

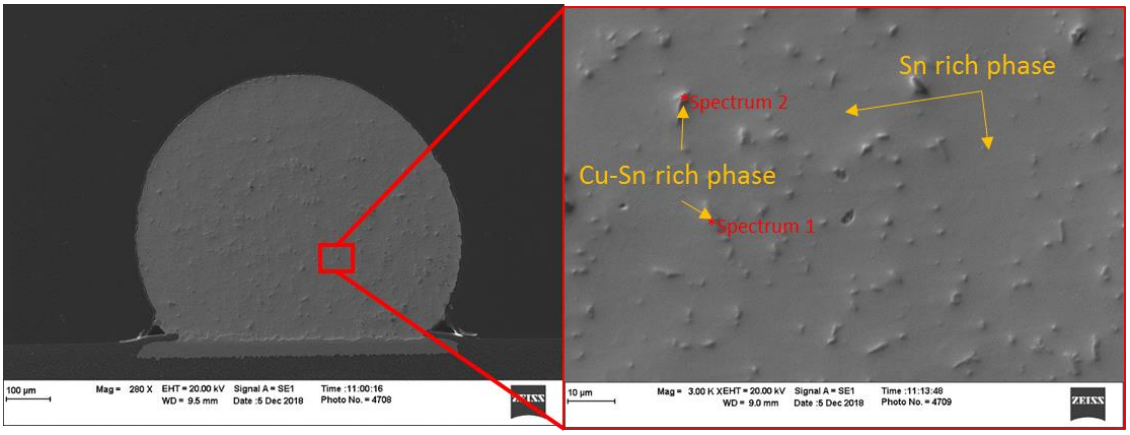

Figure 5-16 Morphology and Microstructure of SAC-R Using SEM

Figure 5-17, Figure 5-18, and Figure 5-19 show the EDS spectrum analysis of some typical precipitates that exist in SAC-Q, SAC-I, and SAC-R. Basically, there exists much solid solutions and precipitates uniformly distributed in solder ball, such as Sn-rich phase, Ag-Sn-rich phase, Cu-Sn-rich phase and Bi-rich phase.

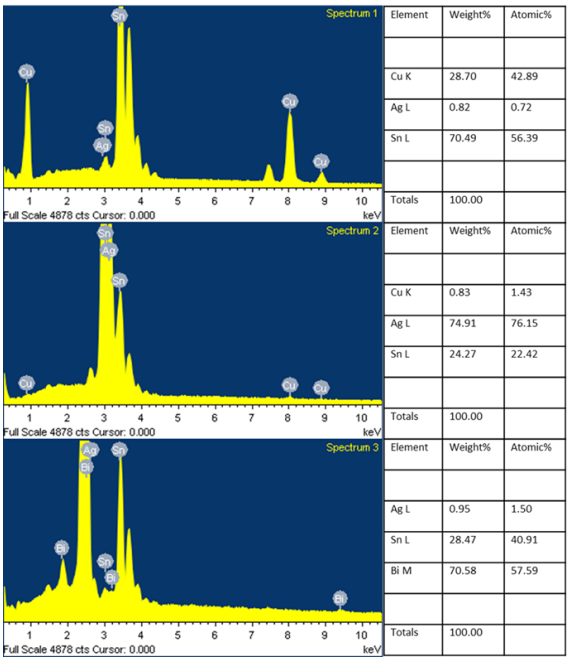

Element	Weight%	Atomic%
Cu K	28.70	42.89
Ag L	0.82	0.72
Sn L	70.49	56.39
Totals	100.00	

Element	Weight%	Atomic%
Cu K	0.83	1.43
Ag L	74.91	76.15
Sn L	24.27	22.42
Totals	100.00	

Element	Weight%	Atomic%
Ag L	0.95	1.50
Sn L	28.47	40.91
Bi M	70.58	57.59
Totals	100.00	

Figure 5-17 EDS Spectrum Analysis of SAC-Q

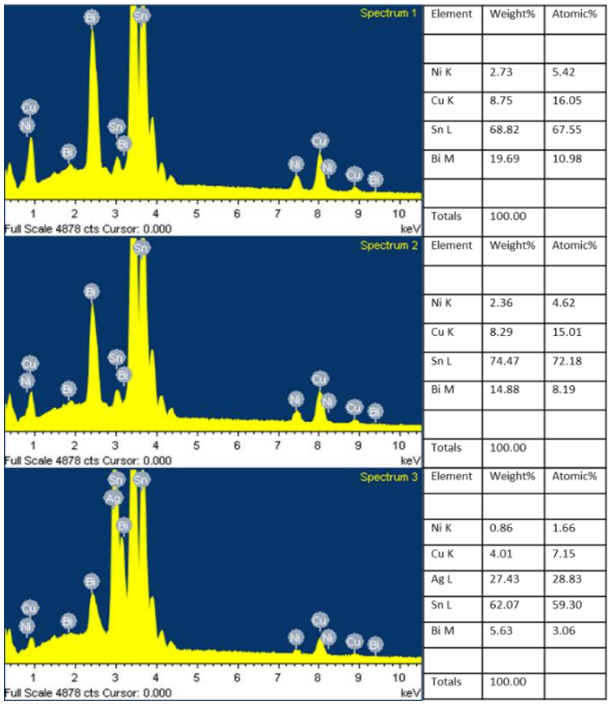

Element	Weight%	Atomic%
Ni K	2.73	5.42
Cu K	8.75	16.05
Sn L	68.82	67.55
Bi M	19.69	10.98
Totals	100.00	

Element	Weight%	Atomic%
Ni K	2.36	4.62
Cu K	8.29	15.01
Sn L	74.47	72.18
Bi M	14.88	8.19
Totals	100.00	

Element	Weight%	Atomic%
Ni K	0.86	1.66
Cu K	4.01	7.15
Ag L	27.43	28.83
Sn L	62.07	59.30
Bi M	5.63	3.06
Totals	100.00	

Figure 5-18 EDS Spectrum Analysis of SAC-I

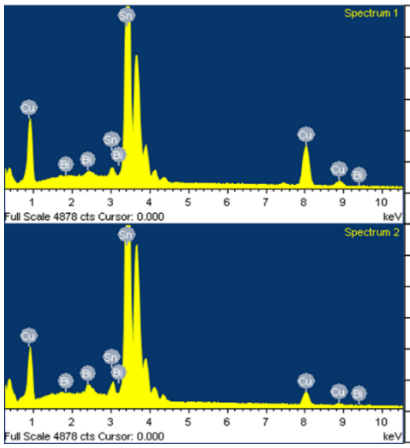

Element	Weight%	Atomic%
Cu K	20.60	32.80
Sn L	78.09	66.56
Bi M	1.30	0.63
Totals	100.00	

Element	Weight%	Atomic%
Cu K	6.46	11.53
Sn L	91.19	87.19
Bi M	2.36	1.28
Totals	100.00	

Figure 5-19 EDS Spectrum Analysis of SAC-R

5.5 Conclusions

The fatigue test of 4 kinds of individual solder joints including SAC305, SAC-Q, SAC-I, and SAC-R were done in this paper. Meanwhile, the fatigue performance of the 4 kinds of solder alloys were compared based on the analysis of the characteristic fatigue life and hysteresis loop. Also, the Morrow Energy model and the Coffin-Manson model were well-fitted to associate the characteristic fatigue life with the inelastic work and plastic strain, respectively. In total, the SAC-Q and SAC-I are expected to have better fatigue resistances than the SAC305 and SAC-R, based on the fatigue life analysis. Also, Comparing SAC-Q to SAC-I, the addition of Ni and Sb in SAC-I did not affect mechanical fatigue performance. Thus, the bismuth can be considered as the main reason for the superior fatigue performance of the SAC-Q and SAC-I, when compared with SAC305 and SAC-R. The main mechanism is that the added bismuth goes into the crystalline lattice and prevents the plastic deformation by more difficult dislocations. This work created a baseline to investigate the effect of varying stress and aging condition on the fatigue performance of individual solder joints. For the next study, we will discuss how the SAC-Bi solder alloys perform under varying stress amplitude condition.

Chapter 6 Fatigue Performance of SAC-Bi Solder Joint under Varying Stress Cycling

6.1 Introduction

A single solder joint's fatigue under realistic service life is typically the bottleneck of reliability of electronic assemblies. Fatigue life prediction of solder joints relies on the result of accelerated test, but it may be misleading regardless of loading history. Limited research work has investigated the SAC-Bi solder alloys' fatigue under varying stress amplitude cycling. In this study, three types of individual SAC-Bi solder joints (SAC305, SAC-Q, and SAC-R) would be tested under varying stress amplitude cycling. Basically, the stress keeps alternating between mild stress and harsh stress. The hysteresis loop (Inelastic work and loading slope) was investigated and compared under varying stress amplitude cycling, and a "Step-up" phenomenon of inelastic work was observed under varying stress amplitude cycling. Table 6-1 shows the summary of mild stress and harsh stress for all SAC-Bi solder alloys in varying stress amplitude test. In this section, we would focus on SAC-Bi solder joints' fatigue under varying stress amplitude, and we would also compare the fatigue among various SAC-Bi solder alloys.

Table 6-1 Mild and Harsh Stress Amplitude for SAC305, SAC-Q, and SAC-R

Alloy	Stress Amplitude	
	Mild Stress	Harsh Stress
SAC305	18MPa	27.6MPa
SAC-Q	24MPa	32MPa
SAC-R	17.5MPa	28.9MPa

6.2 SAC305

Based on the result of single stress amplitude test (Figure 4-11), we can figure out the characteristic life (cycles) of SAC305 under 4 single stress amplitudes test. Figure 6-1 shows the fitted equations of characteristic life (cycles) of SAC305 under 4 stress amplitude in a log-log scale graph. Using the fitted power equation, we can estimate the stress amplitude associated with any specific characteristic life (cycles). Typically, we can know that the characteristic life (cycles) of SAC305 under 18MPa can reach 2500 cycles and the characteristic life (cycles) of SAC305 under 27.6MPa can reach 300 cycles. Therefore, it provides us a reference to look for the mild and harsh stress amplitude for each solder alloy. One of the most important tasks in single stress amplitude is to figure out the mild and harsh stress amplitudes associated with 2500 and 300 characteristic life (cycles).

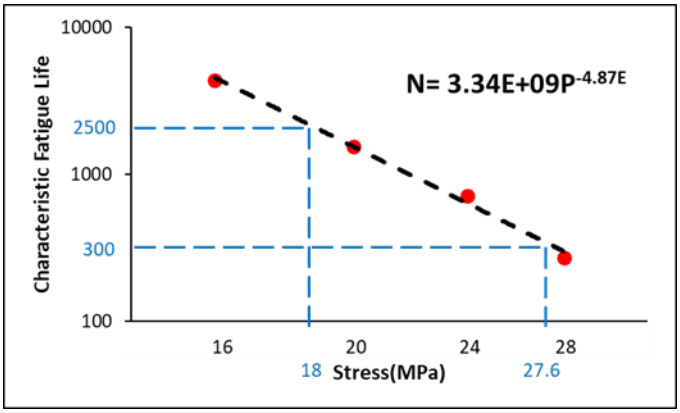

Figure 6-1 Fitted Power Equation of Characteristic Life (Cycles) versus Stress (MPa) for SAC305

Figure 6-2 shows the verification test result of SAC305 under 18MPa and 27.6MPa, respectively. At least 7 replicates were done under the estimated mild and harsh stress amplitudes. And the fatigue life (cycles) of new replications were fitted with Weibull distribution to verify the

characteristic life (cycles) are truly 2500 cycles and 300 cycles associated with the mild and harsh stress amplitude. According to the definition of scale parameters, the scale parameter (2568) typically represents that 63.2% of solder joints are expected to fail before this characteristic life (2568 cycles) under the stress amplitude 18MPa. And the scale parameter (301) typically represents that 63.2% of solder joints are expected to fail before this characteristic life (301 cycles) under the stress amplitude 27.6MPa. Based on the verification test, we were sure that the characteristic life (cycles) of SAC305 under 18MPa can reach 2500 cycles and the characteristic life (cycles) of SAC305 under 27.6MPa can reach 300 cycles.

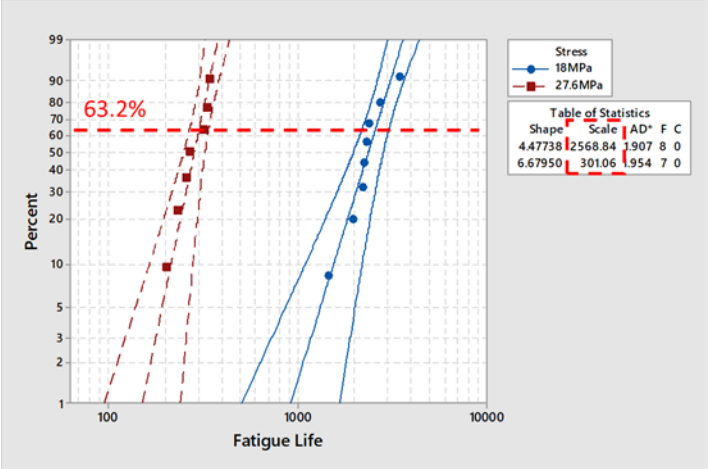

Figure 6-2 Fitted Weibull Distribution of SAC305 Solder Joints under 18MPa and 27.6MPa

The Instron System will record the information of stress and strain for each cycle during the test, which is known as the hysteresis loop. Figure 6-3 shows a typical example of hysteresis loops of SAC305 under 18MPa and 27.6MPa in a stress-strain graph. The hysteresis loop generally records the inelastic work and loading slope per cycle. Inelastic work is defined as the area enclosed within the loop, which can be considered as “damage” accumulated per cycle. In Figure 6-3, the loop area of 27.6MPa stress amplitude is larger than that of 18MPa stress amplitude. It makes sense since

harsh stress amplitude cycles are supposed to generate more “damage” on the solder joint than mild stress amplitude cycles. And the loading slope is defined as the initial slope of the hysteresis loop, which is an empirical measure of effective stiffness of solder joint in the plane of stress. Although the stress amplitude applied on solder joint is different, the loading slope of 18MPa stress amplitude is close to that of 27.6MPa stress amplitude. Therefore, the loading slope is supposed to be independent to stress amplitude applied on solder joint.

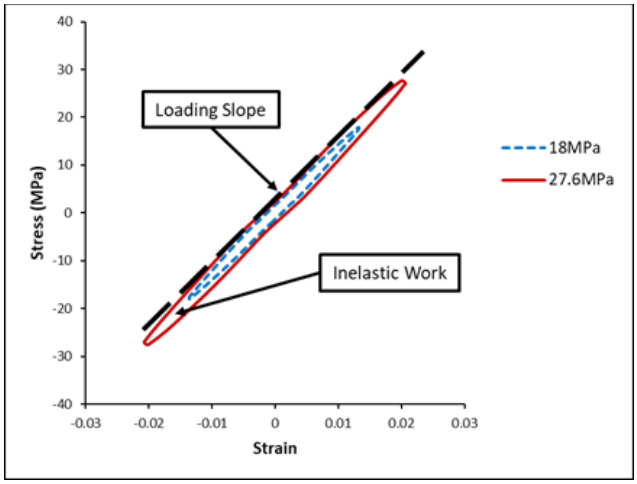

Figure 6-3 Hysteresis Loop Example of SAC305 under 18MPa and 27.6MPa

Figure 6-4 shows a typical example of a SAC305 solder joint’s loading slope in varying stress amplitude test (18MPa-27.6MPa). During the first 25 cycles of 18MPa, the loading slope initially increases in first several cycles and keeps steady around 44.2. However, after alternating from 3 cycles of 27.6MPa, the loading slope stabilizes around 44, which cannot return to the same level before alternating. After the next alternating, the average loading slope of 18MPa stress amplitude cycles has dropped around 43.8. In total, the loading slope steps down after every alternating from harsh stress amplitude to mild stress amplitude under varying stress amplitude test. It seems like solder joint becomes softer after every alternating under varying stress amplitude condition.

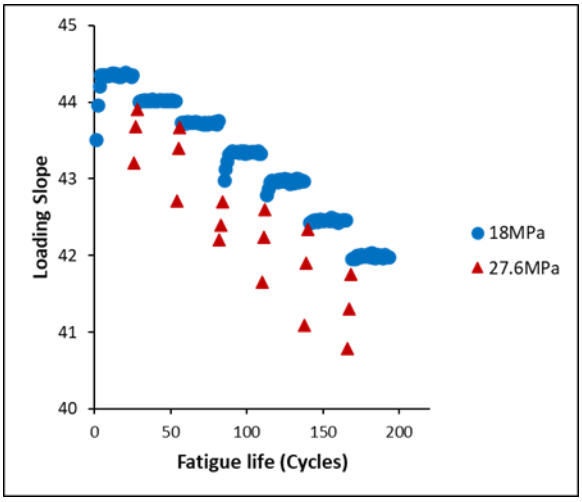

Figure 6-4 Loading Slope Example of SAC305 under Varying Stress Amplitude (18MPa-27.6MPa)

Figure 6-5 shows an example of one SAC305 solder joint's inelastic work in varying stress amplitude test (18MPa-27.6MPa). Typically, the inelastic work of 18MPa stress amplitude rises after alternating from 27.6MPa stress amplitude cycles. At the beginning of varying stress amplitude test, the inelastic work evolves into steady stage soon after several cycles. After 3 cycles of 27.6MPa stress amplitude, the inelastic work tends to stabilize slightly higher than that before alternating. And the rise of average inelastic work of 18MPa stress amplitude cycles are continuously observed after every alternating from 27.6MPa stress amplitude cycles. Since the inelastic work per cycle quantifies "damage" accumulated per cycle, the observed "Step-Up" phenomena of inelastic work indicate that the damage accumulated by each cycle is increased after every alternating from harsh stress amplitude.

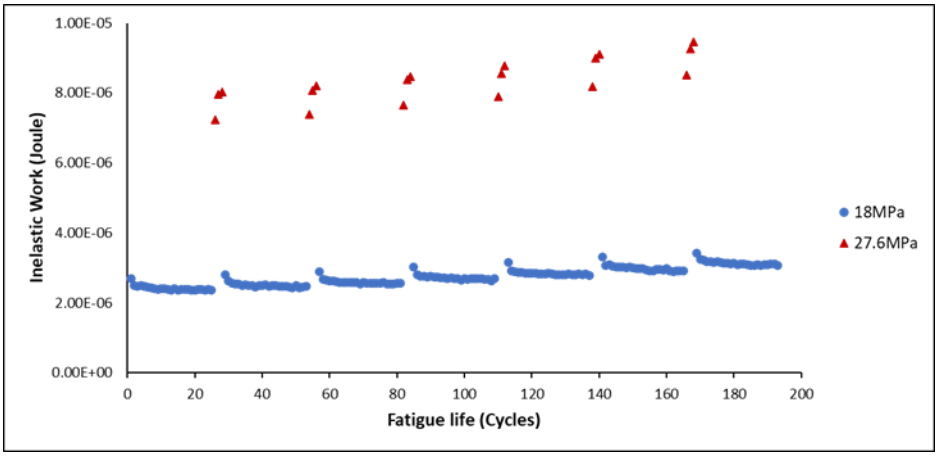

Figure 6-5 Inelastic Work Example of SAC305 under Varying Stress Amplitude (18MPa-27.6MPa)

6.3 SAC-Q

Figure 6-6 shows the fitted equations of characteristic life (cycles) of SAC-Q under 4 stress amplitude in a log-log scale graph. Using the fitted power equation, we can estimate the stress amplitude associated with any specific characteristic life (cycles). Typically, we can know that the characteristic life (cycles) of SAC305 under 24MPa can reach 2500 cycles and the characteristic life (cycles) of SAC305 under 32MPa can reach 300 cycles. Because SAC305 and SAC-Q solder alloys have different contents, and their strengths are different. As it is shown, SAC305 and SAC-Q's stress levels associated with same 2500 and 300 characteristic life (cycles) are different. But we can still use the equation to estimate any characteristic life (cycles) of SAC-Q under any stress amplitudes.

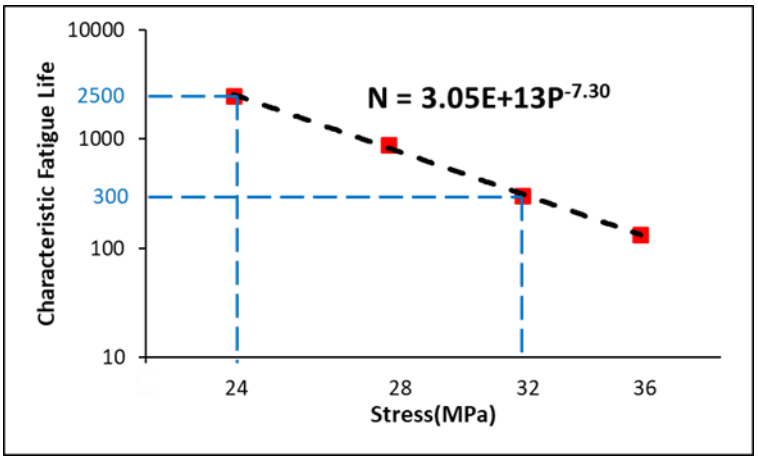

Figure 6-6 Fitted Power Equation of Characteristic Life (Cycles) versus Stress (MPa) for SAC-Q

Figure 6-7 shows the verification test result of SAC-Q under 24MPa and 32MPa, respectively. At least 7 replicates were done under the estimated mild and harsh stress amplitudes. Based on the verification test, we were sure that the characteristic life (cycles) of SAC305 under 18MPa can reach 2500 cycles and the characteristic life (cycles) of SAC305 under 27.6MPa can reach 300 cycles.

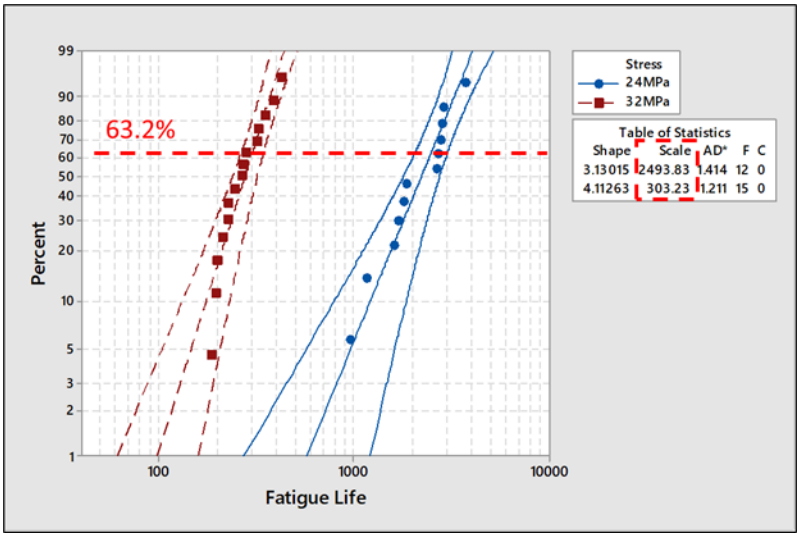

Figure 6-7 Fitted Weibull Distribution of SAC-Q Solder Joints under 24MPa and 32MPa

Similar as SAC305, we plot stress-strain information of one mild cycle and one harsh cycle within one switching interval in a log-log scale graph, shown in Figure 6-8. Red line is the hysteresis loop of harsh cycles and blue line is the hysteresis loop of mild cycles. The area within harsh cycles' hysteresis loop is significantly larger than that within mild cycles' hysteresis loop. It indicates that the inelastic work per harsh cycle is larger than the inelastic work per mild cycle. Same as we observed in the case of SAC305.

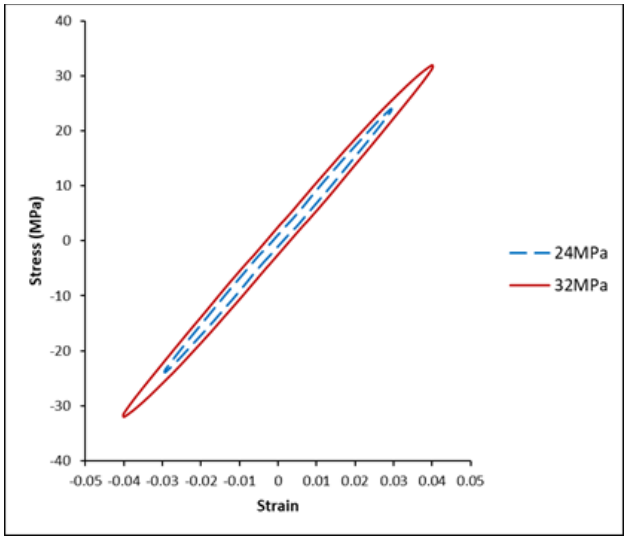

Figure 6-8 Hysteresis Loop Example of SAC-Q under 24MPa and 32MPa

Figure 6-9 shows a typical example of a SAC-Q solder joint's loading slope in varying stress amplitude test (24MPa-32MPa). After that, it keeps steady and we observed that it stays around 45.4 before switching to harsh stress amplitude 32MPa. After the solder joint is cycled 3 times with the harsh stress amplitude 32MPa (Red point), the loading slope of mild stress amplitude cycles (Blue point) falls. After every switch to harsh stress amplitude 32MPa, the loading slope of mild stress amplitude cycles falls, which is same with the loading slope performance of SAC305 under varying stress amplitude condition. Additionally, we notice that the average loading slope

of SAC-Q in the first 25 cycles is higher than that of SAC305 and it is possible because of different composition in both solder joint. The doped Bi may probably be the key to improve the solder joint's stiffness because there is Bi in SAC-Q and no Bi in SAC305.

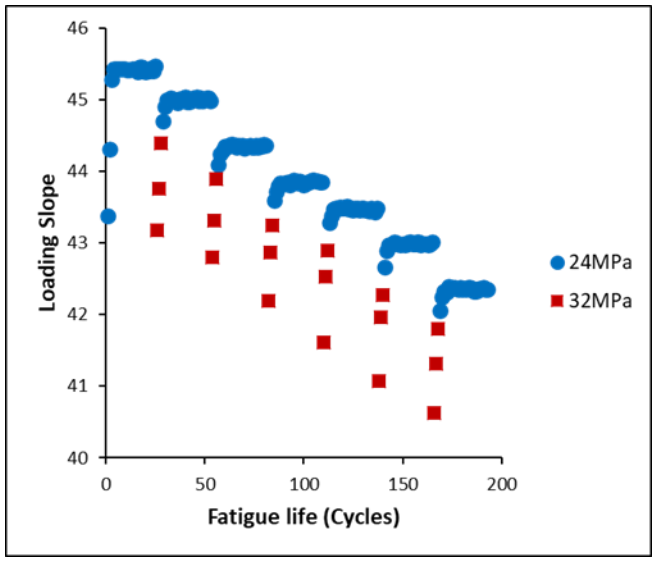

Figure 6-9 Loading Slope Example of SAC-Q under Varying Stress Amplitude (24MPa-32MPa)

Figure 6-10 shows an enlarged view of inelastic work of SAC-Q under varying 24MPa-32MPa test. The SAC-Q solder joint will be first cycled 25 times with mild stress amplitude 24MPa and then 3 times with harsh stress amplitude 32MPa. The inelastic work of mild stress amplitude cycles should fall in several cycles and keep steady until total failure if no switch, which is supposed to be similar with what we discussed in single stress amplitude test. However, in the varying amplitude test, after switching to the harsh stress amplitude 32MPa, the inelastic work of next 25 mild stress amplitude (cycle 29-53) will increase slightly compared with the mild stress amplitude before that switch. And that step-up of inelastic work is observed after every switch from harsh stress amplitude cycles to mild stress amplitude cycles in Figure 6-10.

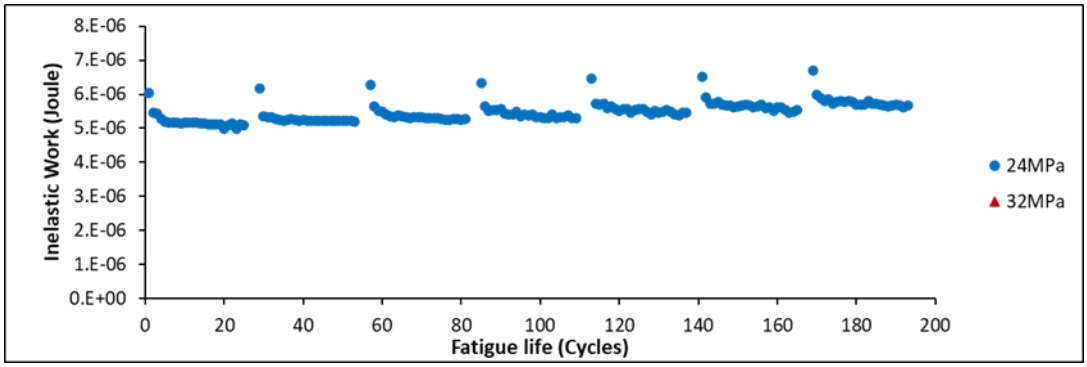

Figure 6-10 Inelastic Work Example of SAC-Q under Varying Stress Amplitude (24MPa-32MPa)

6.4 SAC-R

Figure 6-11 shows the fitted equations of characteristic life (cycles) versus stress (MPa) of SAC-R in a log-log scale graph. As it is estimated, we can know that the characteristic life (cycles) of SAC-R under 17.5MPa can reach 2500 cycles and the characteristic life (cycles) of SAC-R under 28.9MPa can reach 300 cycles. The estimated mild and harsh stress amplitudes of SAC-R is lower than that of SAC-Q, but similar with SAC305, for same characteristic life (cycles). The possible reason is, there exists Bi instead of silver in SAC-R. Also, we need a verification test for the characteristic life (cycles) under 17.5MPa and 28.9MPa.

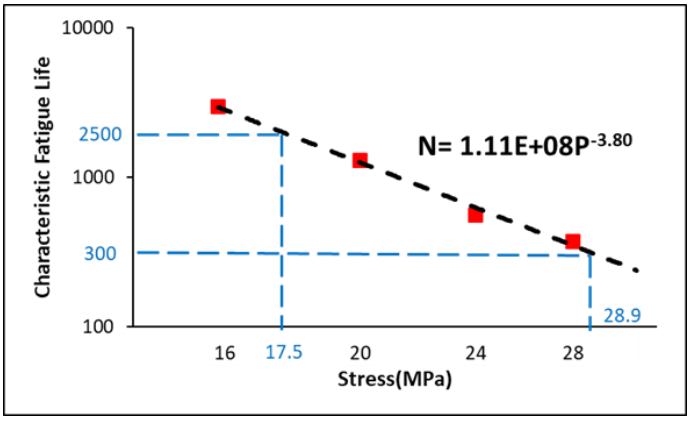

Figure 6-11 Fitted Power Equation of Characteristic Life (Cycles) versus Stress (MPa) for SAC-R

At least 7 replicates were conducted under these two stress amplitudes. Figure 6-12 shows the fitted Weibull distribution of SAC-R under 17.5MPa and 28.9MPa, respectively. And the scale parameter of Weibull distribution represents the characteristic life (cycles) when 63.2% of individual solder joint is expected to fail. It proves that the stress amplitudes 17.5MPa and 28.9MPa are the true value that associated with 2500 and 300 characteristic life (cycles). Figure 6-13 shows hysteresis loop example of SAC-R under 17.5MPa and 28.9MPa, respectively. It is similar with what we observed in SAC305 and SAC-Q.

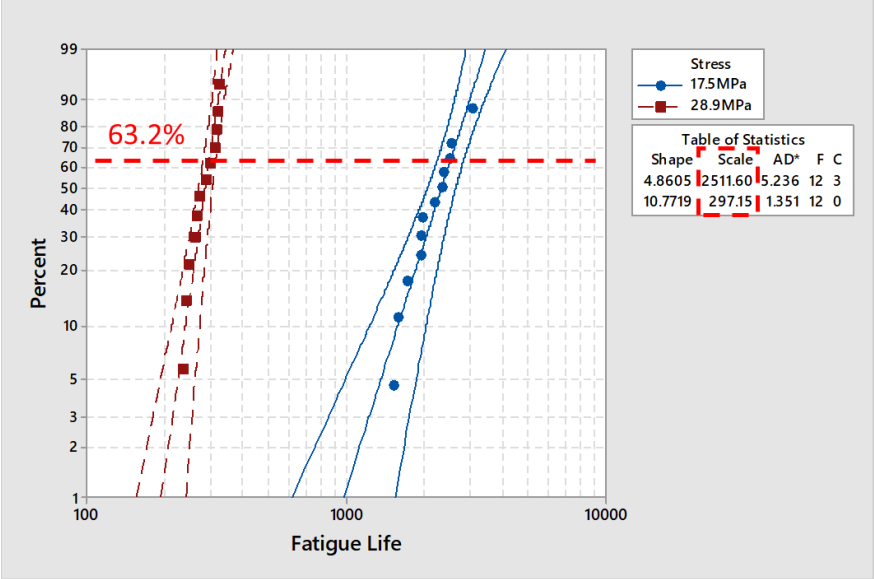

Figure 6-12 Fitted Weibull Distribution of SAC-Q Solder Joints under 17.5MPa and 28.9MPa

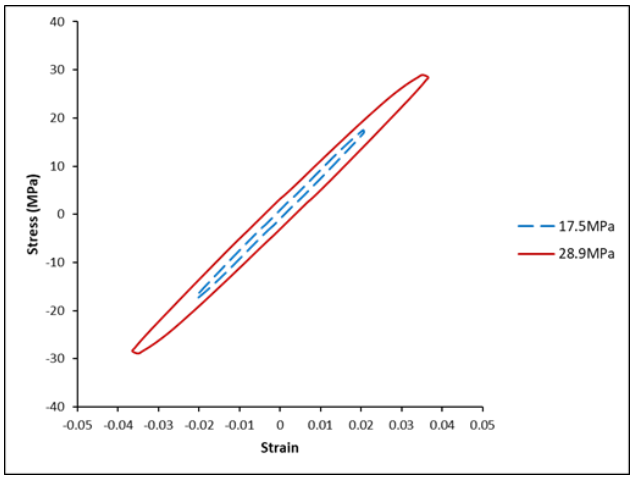

Figure 6-13 Hysteresis Loop Example of SAC-R under 17.5MPa and 28.9MPa

Figure 6-14 shows an example of loading slope of SAC-R under varying 17.5MPa-28.9MPa test. The average loading slope of mild stress amplitude cycles drops down after every switch, which is similar with what we observed in the varying stress amplitude test of SAC305 and SAC-Q. As it is shown, the loading slope increases in the first several cycles with mild stress amplitude 17.5MPa. After that, it keeps steady above 44 until switching to harsh stress amplitude 28.9MPa. After 3 harsh stress amplitude cycles, the average loading slope of mild stress amplitude drops below 44 and never comes back to the previous level before these 3 harsh stress amplitude cycles. As illustrated before, the loading slopes are independent on the stress amplitudes in single stress test. Thus, it indicates that we can compare the initial 25 cycles' loading slope despite of applying different stresses. It is worth noting that, the average loading slope of SAC-R in the first 25 stress amplitude cycles is similar with that of SAC305, but much less than that of SAC-Q. It indicates that the SAC-Q solder joint's is initially harder than SAC-R and SAC305. In SAC-R, there is Bi but no Ag. Thus, it is believed that doped Bi in SAC-R cannot significantly improve the effective stiffness of the solder joint without Ag. And that is why the loading slope of SAC-R is lower than that of SAC-Q.

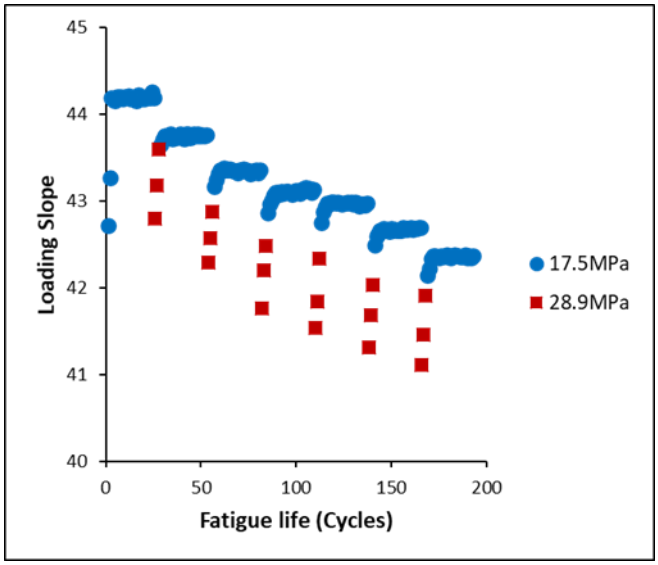

Figure 6-14 Loading Slope Example of SAC-R under Varying Stress Amplitude (17.5MPa-28.9MPa)

Figure 6-15 shows an enlarged view of inelastic work of SAC-R under varying 17.5MPa-28.9MPa test. Also, the inelastic work of mild stress amplitude cycles is increased after every switch from harsh stress amplitude cycles to mild stress amplitude cycles. Thus, all the results indicate that the inelastic work, or "damage", is accumulated more with the same stress amplitude after harsh stress amplitude cycles. And there exists a significant effect of harsh stress amplitude cycles on mild stress amplitude cycles.

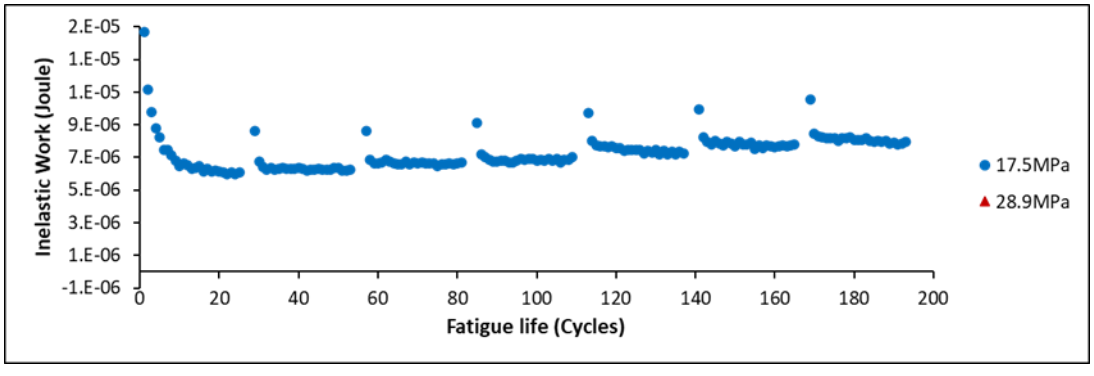

Figure 6-15 Inelastic Work Example of SAC-R under Varying Stress Amplitude (17.5MPa-28.9MPa)

6.5 Fatigue life (Intervals) Comparison

Figure 6-16 shows the fatigue life (Intervals) summary of SAC305, SAC-Q and SAC-R fitted with Weibull distribution in varying stress amplitude test. Each point represents the fatigue life (Intervals) of SAC305 (Blue), SAC-Q (Red), and SAC-R (Green). Note that we are using "Intervals" instead of "cycles" to account fatigue life. One interval indicates one loop of alternating mild stress amplitude to harsh stress amplitude. In other words, one interval includes 25 mild stress cycles and 3 harsh stress cycles. Although the mild stress amplitude and harsh stress amplitude are different for SAC305, SAC-Q and SAC-R, the characteristic life (cycles) associated with the mild stress amplitude and harsh stress amplitude of these solder alloys are about 2500 cycles and 300 cycles. Based on Miner's rule, there will be 1% damage accumulated by cycling the solder joint 25 times with mild stress amplitude, and another 1% damage accumulated by cycling the solder joint 3 times with harsh stress amplitude. Therefore, all the samples supposed to fail after similar cycles (28*2%/100%=1400 cycles), though the alloys have different compositions. In other words, 2% damage are accumulated per interval (28 cycles) and all the individual solder joint are expected to fail around 50 intervals. However, all the samples fail before 50 intervals in Figure 6-16, which indicates that the Miner's rule overestimates the fatigue life of SAC305, SAC-Q and SAC-R in varying stress amplitude test. In this test, the sample variance of group SAC305 seems larger than the other two groups. Meanwhile, SAC-Q's characteristic life (Intervals) is significantly higher than the other two groups. Thus, it is reasonable to believe that SAC-Q shows better fatigue resistance than SAC305 and SAC-R in varying stress amplitude test.

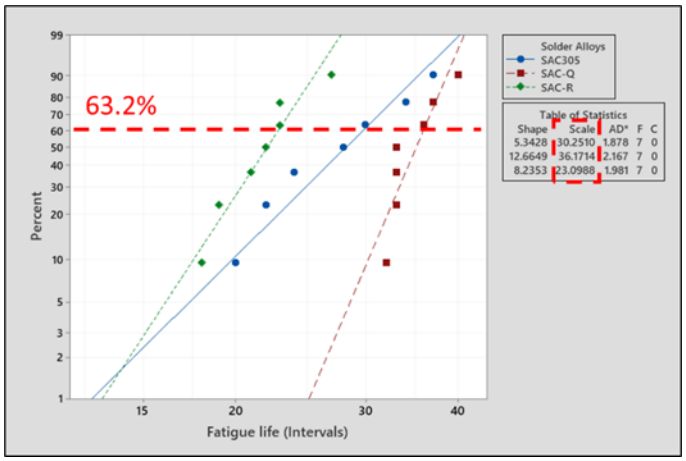

Figure 6-16 Fitted Weibull Distribution of SAC305, SAC-Q, and SAC-R Solder Joints in Varying Stress Cycling

6.6 Conclusion

In this study, SAC-Q shows better fatigue resistance than SAC305 and SAC-R in varying stress amplitude cycling test. Both loading slope and inelastic work in varying stress amplitude cycling test are significant different from these in single stress amplitude test. On one hand, the loading slope, which represents effective stiffness of the material, was not recovering to the original level after switching from harsh to mild stress. On the other hand, inelastic work per cycle of mild stress cycling, which is considered as the "damage" per cycle, is becoming larger after each switch from harsh to mild stress, though same stress amplitude was applied. The test result indicates varying stress amplitude cycling leads to damage acceleration and thus significant less fatigue life (Intervals) for all SAC based alloys with Bi-doped. And common damage accumulation model fails in varying amplitude cycling. Besides, we are interested in the performance of aged SAC305, SAC-Q, and SAC-R in varying stress amplitude test, which will be our next topic. Additionally, the common damage accumulation model failed to estimate the fatigue life of SAC-Bi solder joint

under varying stress amplitude condition. Therefore, it is essential to propose a new model to estimate the damage accumulation when varying stress cycling of individual solder joint.

Chapter 7 Fatigue Performance of Aged SAC-Bi Solder Joint under Single and Varying Stress Cycling

7.1 Introduction

In realist service life of electronic packaging, solder joints are not only going through a varying stress cycling condition but affected by aging simultaneously. Limited research has been done about the effect of aging and varying cycling on fatigue of SAC-Bi solder joint. According to previous chapter, it was observed that SAC-Bi solder joint failed earlier than expected under varying stress cycling condition. Inelastic work per cycle was observed to level up after each alternating from mild stress cycling to harsh stress cycling. However, it is still not clear of the fatigue of aged SAC-Bi solder joint under varying stress cycling. Individual SAC-Bi solder joints were aged for 10hours and 1000hours under 125℃, and they were cycled until total failure under single and varying stress cycling condition. The test results and comparisons were discussed to investigate the aging effect on individual solder joints' fatigue in single stress cycling and varying stress cycling.

7.2 Single Stress Amplitude Cycling

In this study, single stress amplitude tests of SAC305, SAC-Q, and SAC-R were completed and their characteristic life (cycles) under each stress amplitude were shown in Table 7-1. Typically, at least 7 individual solder joints were cycled until total failure under each single stress amplitude. For example, the characteristic life of 0hour aged SAC305 under 16MPa is 4639 cycles after fitting the 7 individual solder joints' fatigue life with Weibull distribution. Basically, SAC-Q has more fatigue resistance than SAC305 and SAC-R since the characteristic life of SAC-Q is significantly

larger. It can be also seen that characteristic life is decreasing as the stress amplitude increase for same solder alloy and same aging time. And characteristic life is decreasing as the aging time increase for same solder alloy.

Table 7-1 Characteristic Life (Cycles) Of Aged SAC305, SAC-Q and SAC-R

	Aging Time	Stress Amplitudes					
		16 MPa	20 MPa	24 MPa	28 MPa	32 MPa	36 MPa
SAC305	0hour	4369	1551	713	271	-	-
	10hour	2501	785	392	161	-	-
	1000hour	1350	559	276	107	-	-
SAC-Q	0hour	-	-	2493	888	303	133
	10hour	-	-	2259	851	290	129
	1000hour	-	-	2099	835	278	122
SAC-R	0hour	2965	1308	560	375	-	-
	10hour	2762	1189	538	356	-	-
	1000hour	2656	1092	511	304	-	-

7.2.1 SAC305

If 0hour aged SAC305's characteristic life (cycles) is considered as baseline, we can calculate the ratio of 10hours and 1000hours aged SAC305's characteristic life (cycles) over baseline under each stress amplitude. Figure 7-1 is a bar chart to show the drop rate of characteristic life (cycles) of 10hours (yellow) aged case and 1000hours (red) aged case over 0hour aging case (blue) for SAC305. It can be seen that the characteristic life of 10hour aged SAC305 are only about 50%-

60% of that of 0hour aged SAC305. And it only has 30%-40% after 1000 hours aging. It indicates that aging time has significant effect on the fatigue resistance of SAC305. Under 125℃ aging condition, SAC305 shows less fatigue resistance as aging time increases.

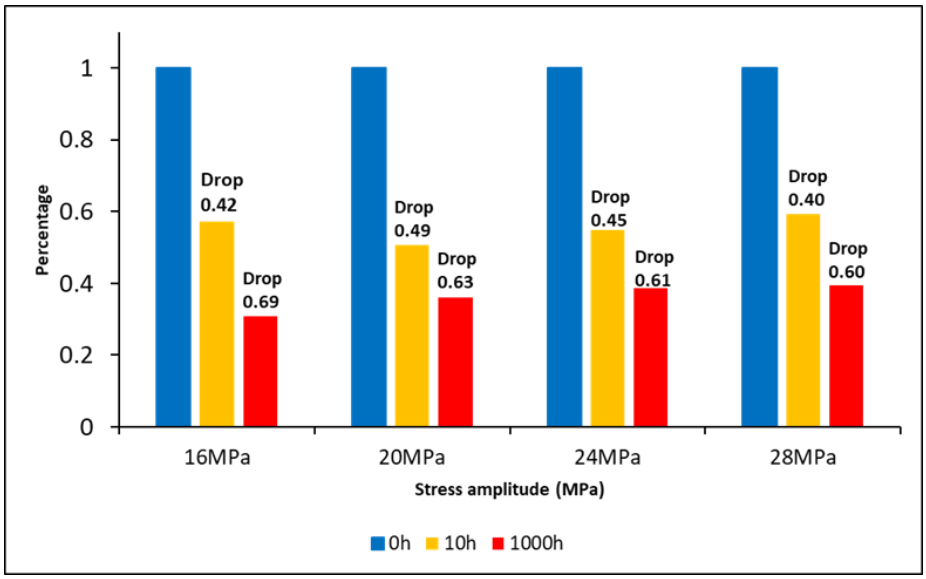

Figure 7-1 Characteristic Life (Cycles) of 0hour, 10hours, and 1000hours Aged SAC305 Solder Joints

Figure 7-2 shows 0hour, 10hours, 1000hours aged SAC305s' fitted power equations of characteristic life (cycles) versus stress amplitude (MPa) in a log-log scale graph. Based on the equations, we can figure out the mild and harsh stress amplitude associated with 2500 cycles and 300 cycles. The summary of mild and harsh stress amplitude is summarized in Table 7-2. Because SAC305 degrade after aging, the characteristic life (cycles) is reducing as aging time increase. Therefore, it is reasonable for aged SAC305 to have less stress amplitude associated with same characteristic life (cycles).

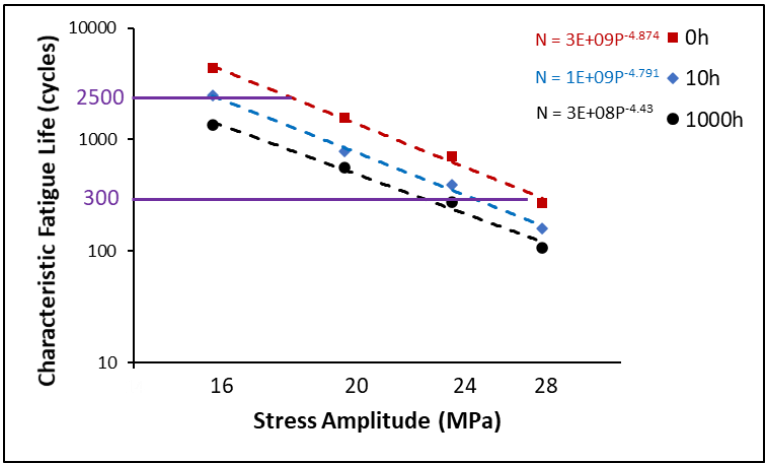

Figure 7-2 Fitted Power Equation of Characteristic Fatigue Life (Cycles) versus Stress Amplitude for 0hour, 10hours and 1000hours Aged SAC305

Table 7-2 Mild and Harsh Stress Amplitude of Aged SAC305

Alloy	Aging Time	Stress Amplitude	
		Mild Stress	Harsh Stress
SAC305	0h	18MPa	27.6MPa
	10h	16MPa	24.8MPa
	1000h	14.4MPa	23.48MPa

The verification tests were conducted to confirm the above estimation. At least 7 replicates were done under stress amplitude condition. Figure 7-3 and Figure 7-4 show the fitted Weibull distribution of 10hours and 1000hours aged SAC305 under their mild and harsh stress amplitudes. The scale parameter in table of statistics is approaching to 2500 cycles and 300 cycles, which verified our estimation. And we were considering these stress amplitudes as the mild and harsh stress amplitude in varying stress amplitude test.

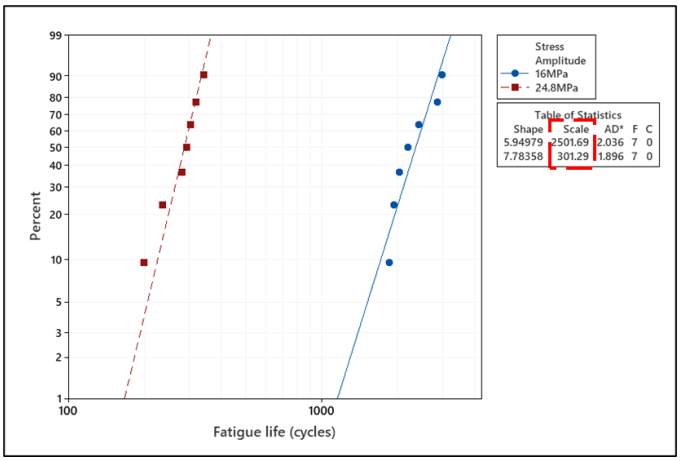

Figure 7-3 Fitted Weibull Distribution of SAC305 Solder Joints under 16MPa and 24.8MPa

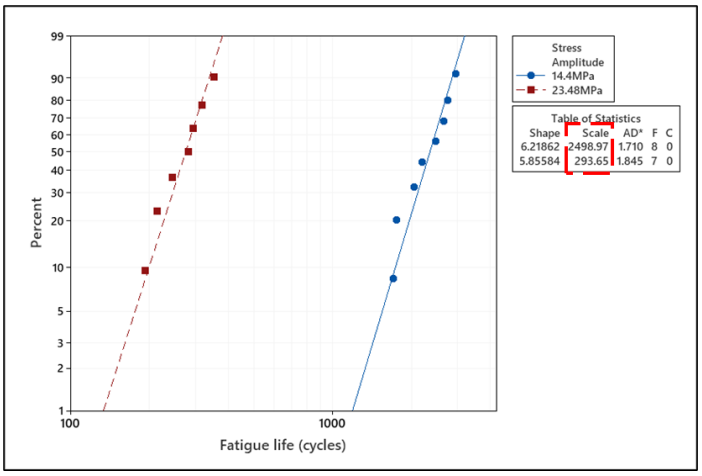

Figure 7-4 Fitted Weibull Distribution of SAC305 Solder Joints under 14.4MPa and 23.48MPa

7.2.2 SAC-Q

However, SAC-Q shows more aging resistance than SAC305. Figure 7-5 shows characteristic life drop of SAC-Q after 10hours and 1000hours aging comparing with 0hour aging case. The characteristic life (cycles) of aged SAC-Q was reduced after aging, but SAC-Q does not degrade that much (only about 10% drop of characteristic life). It illustrates that aged SAC-Q will degrade under single stress amplitude test. Furthermore, the fatigue of SAC-Q is less affected by aging

time, comparing with SAC305. Since there is Bi in SAC-Q and no Bi in SAC305, we believe that Bi is the main reason to improve the fatigue resistance of aged SAC-Q under single stress amplitude test.

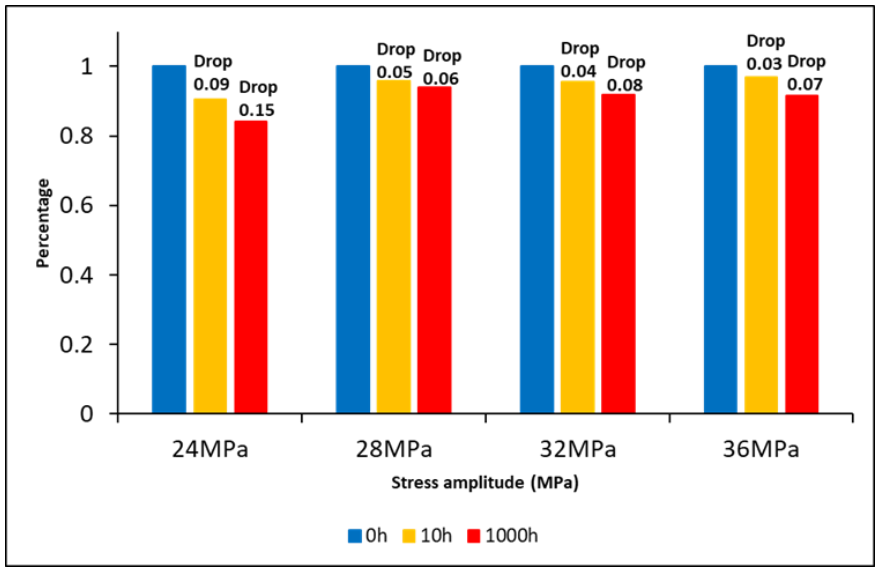

Figure 7-5 Characteristic Life (Cycles) of 0hour, 10hours, and 1000hours Aged SAC-Q Solder Joints

Based on the characteristic life (cycles) under single stress amplitude, we can figure out 0hour, 10hours, 1000hours aged SAC-Qs' fitted power equations of characteristic life (cycles) versus stress amplitude (MPa). According to the fitted equations, we can estimate the mild and harsh stress amplitude associated with 2500 and 300 characteristic life (cycles). Table 7-3 shows the summary of mild and harsh stress amplitude for 0hour, 10hours, 1000hours aged SAC-Q. As it is shown, the estimated mild stress and harsh stress of 10hours and 1000hours aged SAC-Q are close to that of 0hour aged SAC-Q because SAC-Q shows better aging resistance in single stress amplitude test.

Table 7-3 Mild and Harsh Stress Amplitude of Aged SAC-Q

Alloy	Aging Time	Stress Amplitude	
		Mild Stress	Harsh Stress
SAC-Q	0h	24MPa	32MPa
	10h	23.8MPa	31.88MPa
	1000h	23.6MPa	31.72MPa

Same as what we did for SAC305. Verification tests were done to ensure the mild and harsh stress are associated with 2500 and 300 characteristic life (cycles). Figure 7-6 and Figure 7-7 show the fitted Weibull distribution of 10hours and 1000hours aged SAC-Q under their mild and harsh stress amplitudes. The scale parameter in table of statistics is approaching to 2500 cycles and 300 cycles, which verified our estimation. And we were considering these stress amplitudes as the mild and harsh stress amplitude in varying stress amplitude test.

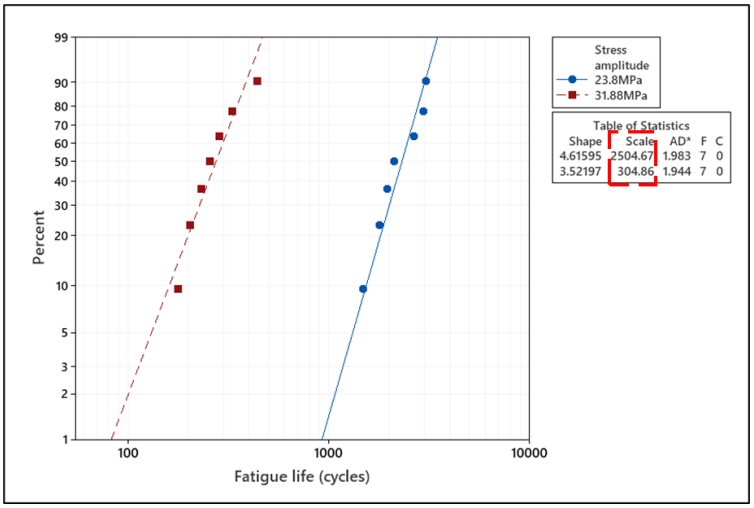

Figure 7-6 Fitted Weibull Distribution of SAC-Q Solder Joints under 23.8MPa and 31.88MPa

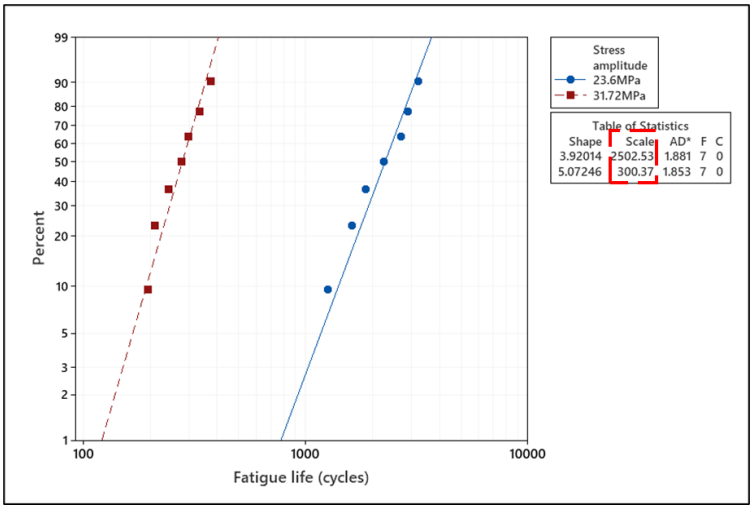

Figure 7-7 Fitted Weibull Distribution of SAC-Q Solder Joints under 23.8MPa and 31.88MPa

7.2.3 SAC-R

SAC-R also shows better aging resistance compared with SAC305. Figure 7-8 shows characteristic life drop of SAC-R after 10hours and 1000hours aging comparing with 0hour aging case. The characteristic life (cycles) of SAC-R drops less than 10% in 10hours case and less than 20% in 1000hours case. Typically, all the SAC-Bi individual solder joints degrade after 10hours and 1000hours aging under 125℃. However, the fatigue of SAC-Q and SAC-R under single stress amplitude condition are less affected by aging time, comparing with SAC305.

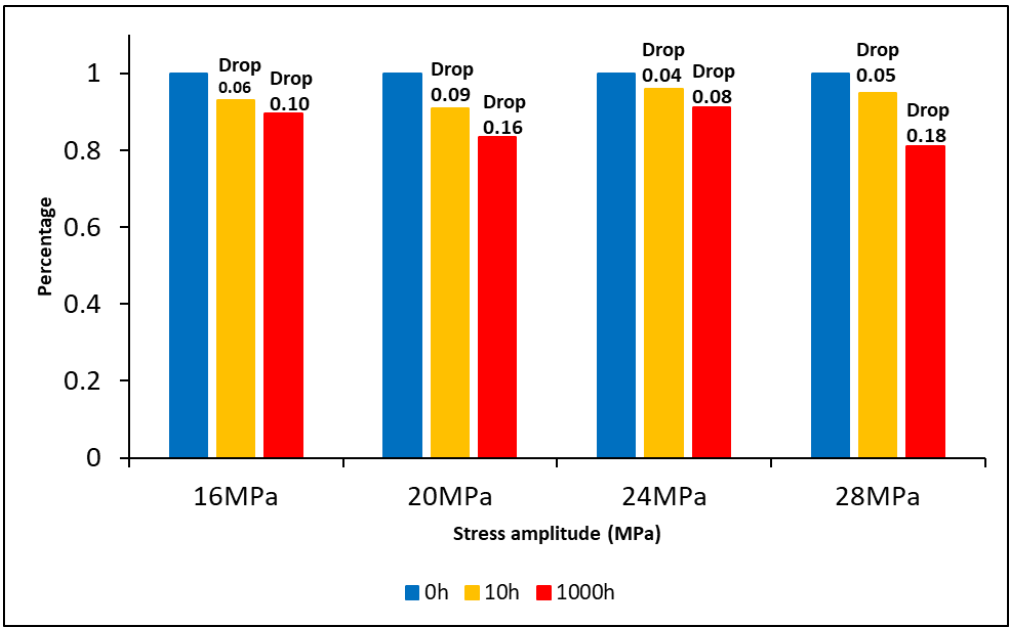

Figure 7-8 Characteristic Life (Cycles) of 0hour, 10hours, and 1000hours Aged SAC-R Solder Joints

Similar as what we did for SAC305 and SAC-Q, we can figure out the fitted power equation using characteristic life (cycles) and stress amplitude (MPa). The estimated mild and harsh stress amplitude associated with 2500 and 300 characteristic life (cycles) can be found according to that fitted power equation. And the mild stress and harsh stress were summarized in Table 7-4.

Table 7-4 Mild and Harsh Stress Amplitude of Aged SAC-R

Alloy	Aging Time	Stress Amplitude	
		Mild Stress	Harsh Stress
SAC-R	0h	17.5MPa	28.9MPa
	10h	17.08MPa	28.48MPa
	1000h	16.8MPa	28MPa

Also, verification tests of aged SAC-R were conducted under found mild stress and harsh stress amplitude conditions. At least 7 replicates were done for each case. Figure 7-9 are the fitted

Weibull distribution of 10hours aged SAC-R under mild stress amplitude (Blue) and harsh stress amplitude (Red). Figure 7-10 are the fitted Weibull distribution of 1000hours aged SAC-R under mild stress amplitude (Blue) and harsh stress amplitude (Red). The scale parameter of mild stress and harsh stress amplitude in both graphs are close to 2500 and 300 cycles.

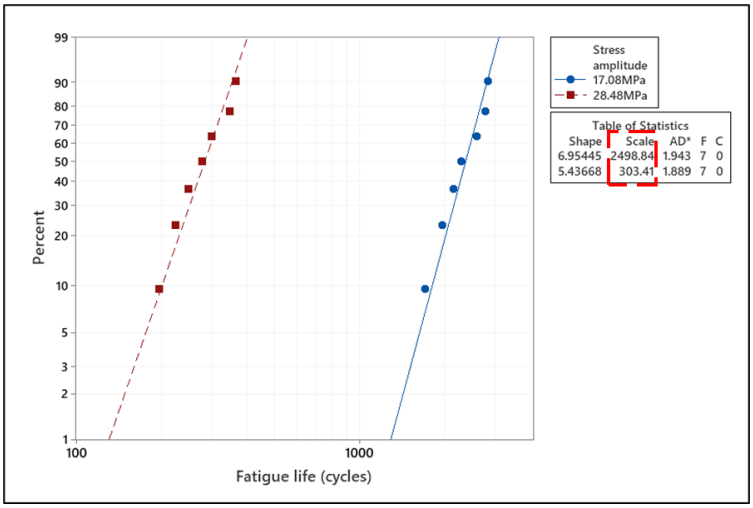

Figure 7-9 Fitted Weibull Distribution of SAC-R Solder Joints under 17.08MPa and 28.48MPa

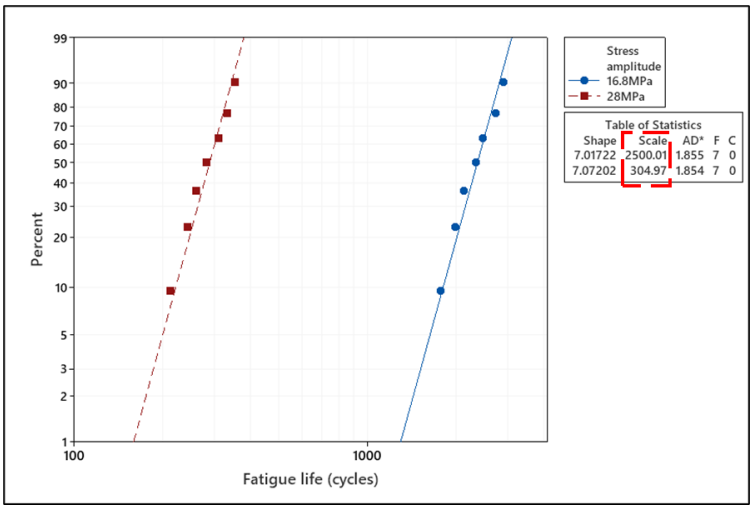

Figure 7-10 Fitted Weibull Distribution of SAC-R Solder Joints under 16.8MPa and 28MPa

7.3 Varying Stress Amplitude Cycling

7.3.1 Fatigue Life Comparisons

According to the stress amplitudes from single stress amplitude test (Table 7-2, Table 7-3, and Table 7-4), at least 7 replicates of non-aged and aged solder joints were conduct until total failure under varying stress amplitude cycling. Their fatigue life (intervals) and stress-strain information were recorded. In the following comparisons of fatigue life, the unit of fatigue life was intervals rather than cycles. Each interval represents 25 mild stress cycles and 3 harsh stress cycles. Because the mild stress and harsh stress are associated with 2500 and 300 characteristic life, the expected damage accumulated in one interval will be $25/2500 + 3/300 = 2\%$. In the other words, we expected individual solder joint will fail at about 50 intervals.

Figure 7-11 shows fitted Weibull plots of 0hour, 10hours, and 1000hours aged SAC305 under varying stress amplitude test. As it is shown, all the samples of SAC305 were failed before 50 intervals. It indicates that more damage was accumulated than expected under varying stress amplitude test and thus the SAC305 individual solder joint failed earlier. Meanwhile, the Weibull plot of SAC305 is significantly separated by aging time, and the characteristic life (Intervals) were significantly different according to the test of equal scale parameter. It can be seen that the characteristic life (Intervals) is decreasing while aging time is increasing. It proves that SAC305 also degraded after aging under varying stress amplitude test. We are not surprised about this phenomenon because SAC305 shows not much aging resistance in single stress amplitude.

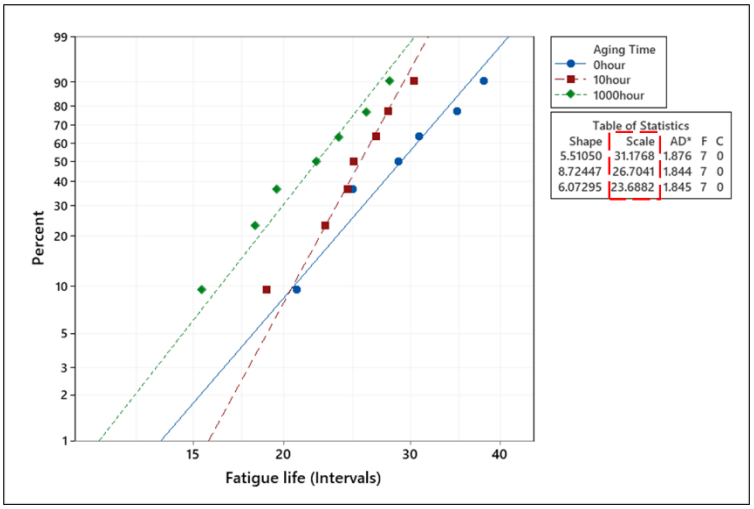

Figure 7-11 Fitted Weibull Distribution and the Characteristic Fatigue Life (Intervals) of Aged SAC305 in Varying Stress Cycling

We observed similar degrading of SAC-Q, which is shown in Figure 7-12. P-value in Test of equal scale parameter is less than 0.05 and thus we are 95% confident that the characteristic life (Intervals) of 0hour, 10hours, and 1000hour aged SAC-Q are different. Also, the characteristic life (Intervals) of SAC-Q under varying stress amplitude test is decreasing with aging time increasing.

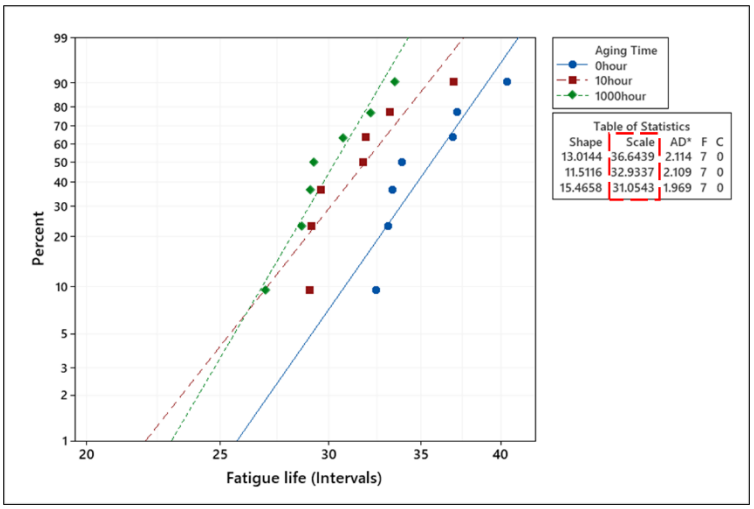

Figure 7-12 Fitted Weibull Distribution and the Characteristic Fatigue Life (Intervals) of Aged SAC-Q in Varying Stress Cycling

However, the scale parameter is not significantly different in the case of SAC-R. Figure 7-13 shows fitted Weibull plots of 0hour, 10hours, and 1000hours aged SAC-R under varying stress amplitude test. It can be seen that the fitted Weibull plots of aged SAC-R were not significantly separated in the graph, and the characteristic life (Intervals) was close to each other. A decreasing trend of characteristic life (Intervals) can be observed, though it is not significant.

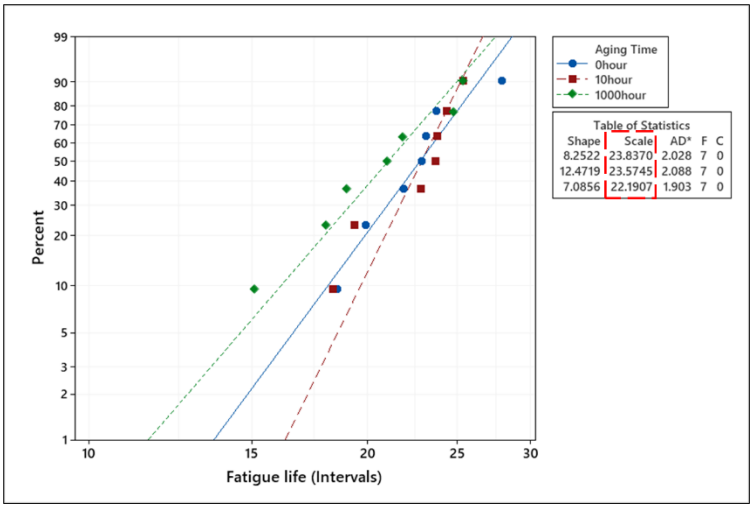

Figure 7-13 Fitted Weibull Distribution and the Characteristic Fatigue Life (Intervals) of Aged SAC-R in Varying Stress Cycling

Figure 7-14 shows the effect of aging on different solder alloys' characteristic life (Intervals) under varying stress amplitude cycling. If we consider the characteristic life (Intervals) of 0hour aged solder joint as baseline, we can calculate the drop percentage of 10hours and 1000hours aged solder joint's characteristic life (Intervals) comparing with the baseline. As it is shown, SAC305 shows the worst aging resistance under varying stress amplitude test, since its characteristic life (Intervals) has the largest drop rate after aging. SAC-Q shows better aging resistance in varying stress cycling comparing with SAC305. Remember that, SAC-Q has best aging resistance in single stress cycling. However, it is surprise for us that the characteristic life (Intervals) of 10hours and

1000hours aged SAC-R only drop 2% and 7% of 0hour aged SAC-R's characteristic life (Intervals).

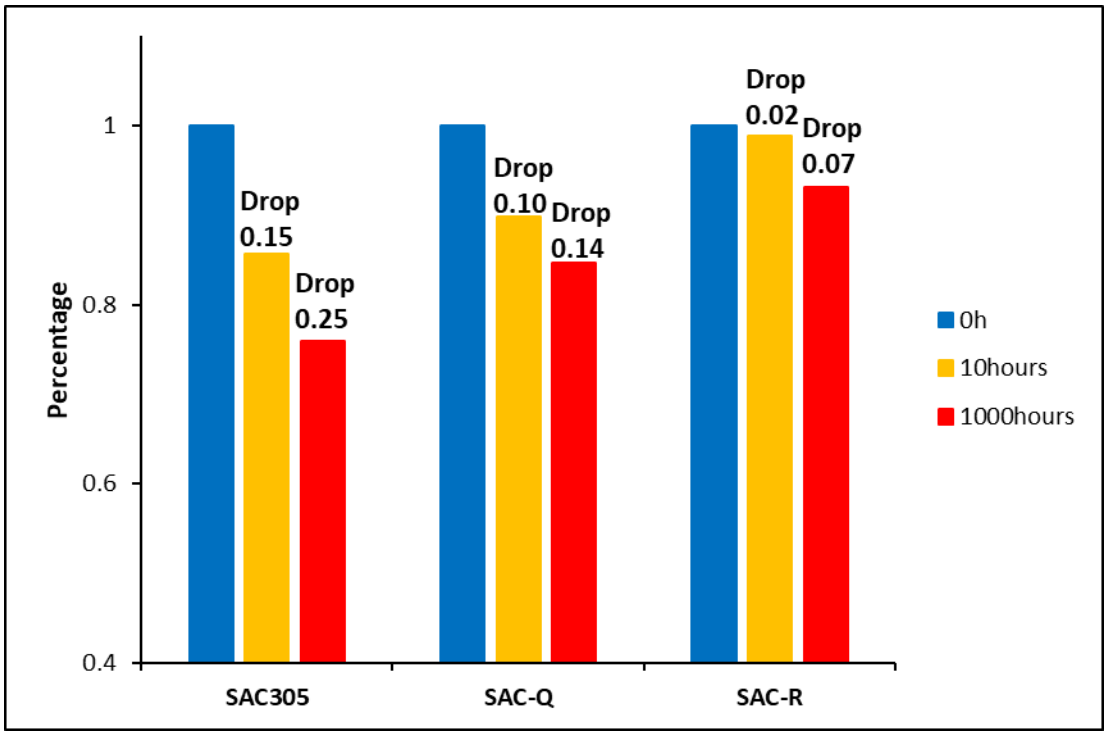

Figure 7-14 Characteristic Life (Cycles) of Aged SAC305, SAC-Q and SAC-R Solder Joints

7.3.2 Loading Slope

We observed similar loading slope performance of 10hours and 1000hours aged SAC305, comparing with non-aged SAC305. Figure 7-15 shows an example of 10hours aged SAC305's loading slope performance under varying 16MPa-24.8MPa cycling. Basically, the loading slope initially increase and stabilize around 45 in first 25 mild cycles. It drops to around 44.2 after switching from harsh cycles to mild cycles. And the drop occurs after every switch until total failure and the loading slope never return to the previous level. Remember that loading slope

represents the stiffness of solder alloy. However, the process of switching seems to degrade the stiffness of solder alloy under varying stress cycling.

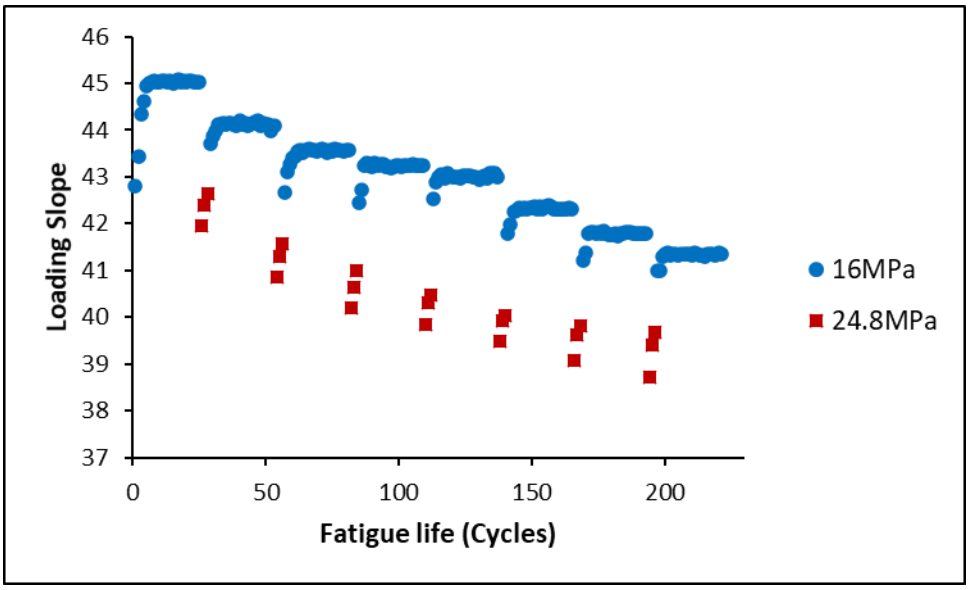

Figure 7-15 Loading Slope Example of 10hours Aged SAC305 under Varying Stress Amplitude (16MPa-24.8MPa)

Similar phenomena were observed in the case of aged SAC-Q and SAC-R. Figure 7-16 shows an example of 1000hours aged SAC-R's loading slope performance under varying 16.8MPa-28MPa cycling. Basically, the loading slope first increases because of solder ball flattening, and it stabilizes around 45.6. After switching from harsh to mild stress again, the solder joint is seen to harden again but the average of loading slope drops a little bit (stabilizes around 45.2). Repeated returns to harsh stress amplitude cycles are seen to further reduce the loading slope. We keep observing the drop of loading slope along the whole life of individual solder joint under varying stress amplitude cycling.

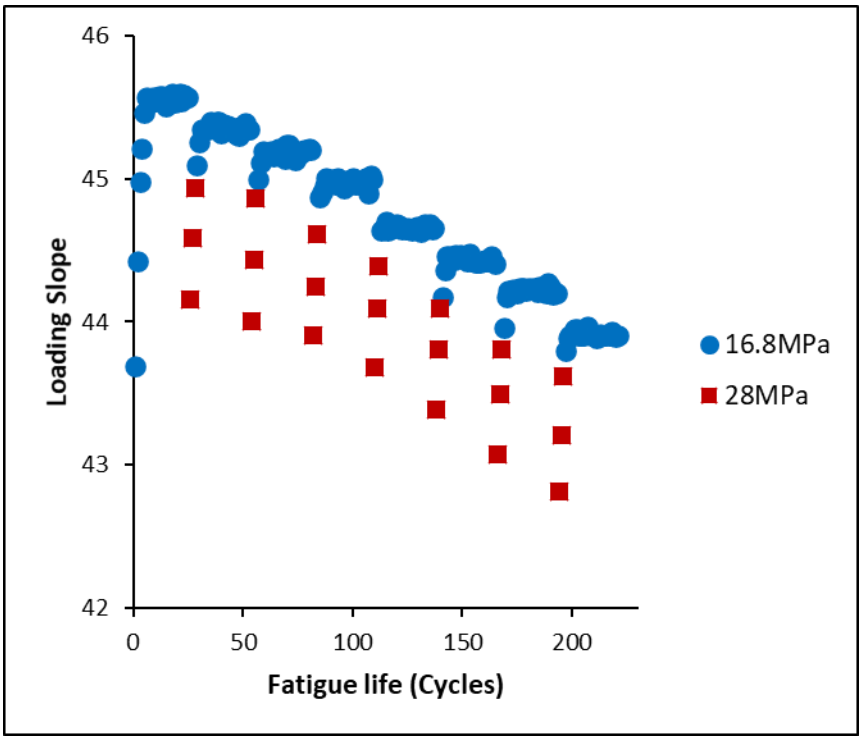

Figure 7-16 Loading Slope Example of 1000hours Aged SAC-R under Varying Stress Amplitude (16.8MPa-28MPa)

7.3.3 Inelastic work

We observed similar inelastic work performance of 10hours and 1000hours aged SAC305, comparing with non-aged SAC305. Figure 7-17 shows an example of 10hours aged SAC305's inelastic work performance under 16MPa-24.8MPa. The inelastic work initially drops due to initially flattening and hardening of solder joint, and it keeps steady in the first 25 mild cycles, but it can be seen that inelastic work of both mild and harsh cycles rises up after every switch between mild and harsh cycles. And it never drops back to the previous level.

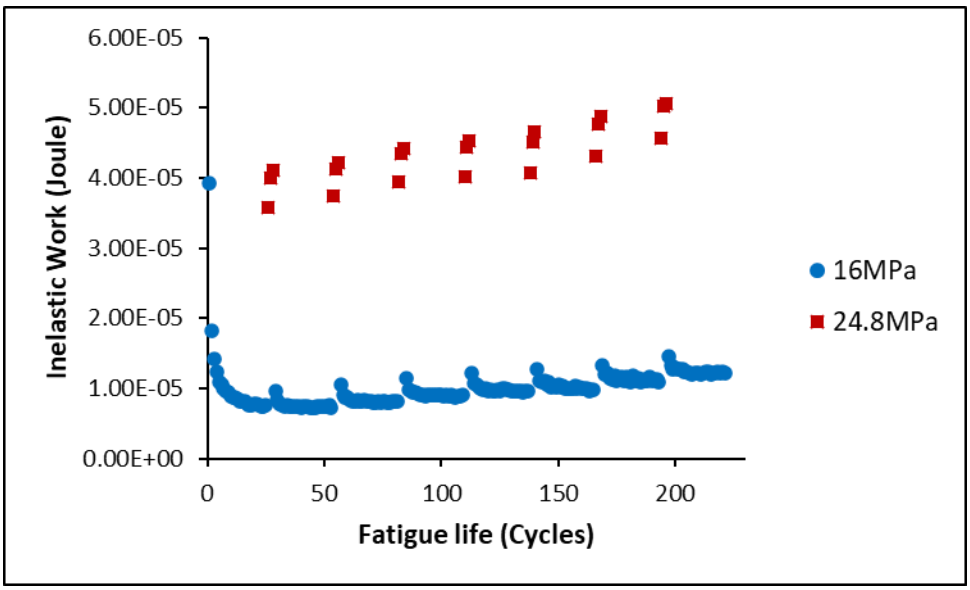

Figure 7-17 Inelastic Work Example of 10hours Aged SAC305 under Varying Stress Amplitude (16MPa-24.8MPa)

Similar phenomena were observed in the case of aged SAC-Q and SAC-R. Figure 7-18 shows an example of 10hours aged SAC-Q's inelastic work performance under varying 23.8MPa-31.88MPa cycling. The inelastic work will initially decrease and stay steady before first switching. Once the stress amplitude is changed from 23.8MPa to 31.88MPa, the inelastic work dramatically increases, and it is reasonable because harsh stress supposes to accumulate more damage per cycle. It agrees with what we observed from hysteresis loop in Figure 6-3. More important is, immediately after switching back to 23.8MPa, there is an amplification relative to the level established before the 31.88MPa cycles. And this amplification of inelastic work was observed along the whole life of individual solder joint under varying stress amplitude cycling.

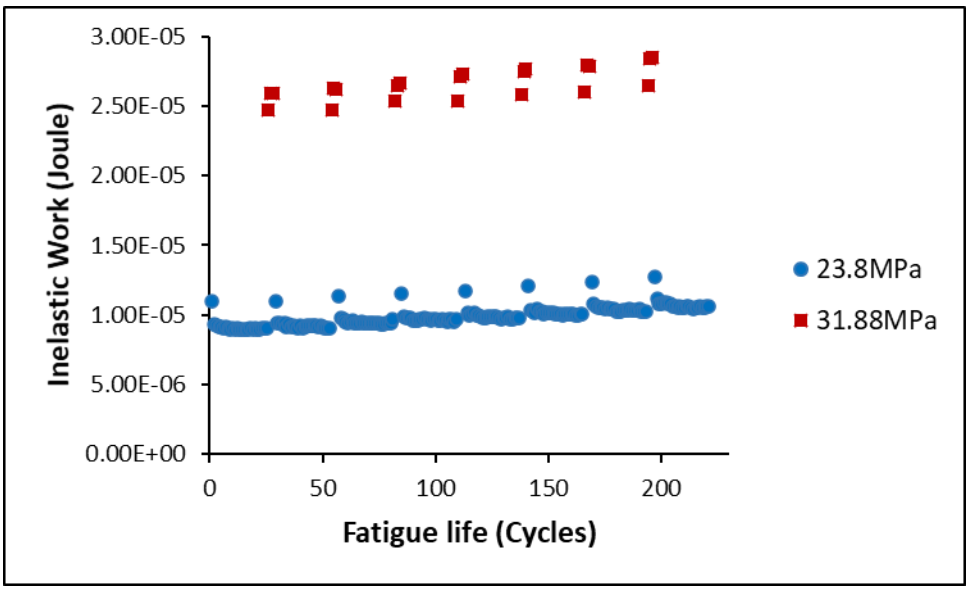

Figure 7-18 Inelastic Work Example of 10hours Aged SAC-Q under Varying Stress Amplitude (23.8MPa-31.88MPa)

7.4 Failure Mode

Figure 7-19 shows a typical brittle failure example of 0hour aged SAC-Q under single stress amplitude in (a) cross-section view and (b) top view. The failure occurs along the IMC layer and solder balls were totally separated from the copper pads, since the high contents of Bi and Ag in SAC-Q will contribute to high strength of solder alloy. Therefore, the IMC layer is becoming the "bottleneck" of the solder joint's strength. Same failure mode was commonly observed in the case of 10hours and 1000hours aged SAC-Q under varying stress amplitude cycling as well. Therefore, it seems that the failure mode of SAC-Q is not affected by the varying stress amplitude and aging condition.

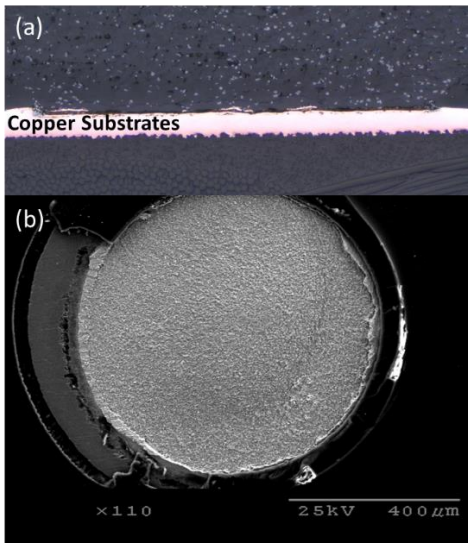

Figure 7-19 Brittle Failure Example of 0hour Aged SAC-Q under Single Stress Amplitude In (a) Cross-Section View (b) Top View

Figure 7-20 shows a typical ductile failure example of 0hour aged SAC-R under single stress amplitude in (a) cross-section view and (b) top view. In contrast to brittle failure mode, most of solder alloys were separated due to shear fatigue but there will be some portion of solder alloys left on the copper substrates. The crack propagates within the solder alloys. The ductile failure mode was also observed in the case of 10hours aged and 1000hours aged SAC-R under varying stress amplitude cycling. For 0hour aged, 10hours aged, 1000hours aged SAC305, we observed similar failure mode under single stress amplitude and varying stress amplitude cycling.

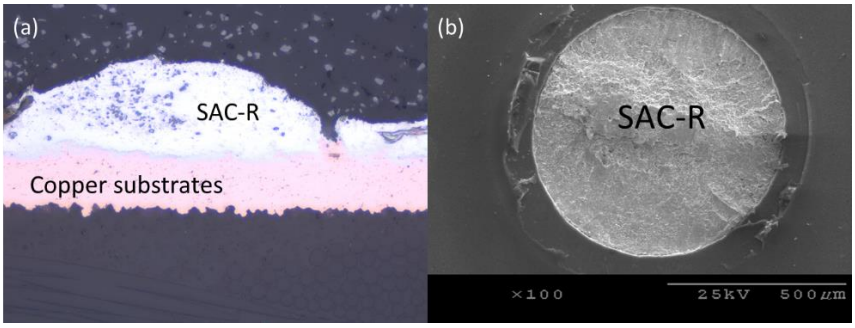

Figure 7-20 Ductile Failure Example of 0hour Aged SAC-R under Single Stress Amplitude In (a) Cross-Section View (b) Top View

7.5 Conclusion

In this chapter, the fatigue performances of aged SAC305, SAC-Q, and SAC-R under both single and varying stress cycling were investigated. In single stress amplitude cycling, we figured out the characteristic life (cycles) of aged SAC305, SAC-Q and SAC-R. The comparison results showed that SAC-Q and SAC-R had aging resistance comparing with SAC305 in the single stress amplitude cycling. The possible reason is Bi in SAC-Q and SAC-R. Also, we were able to estimate the stress amplitudes associated with 2500 and 300 characteristic life (cycles) for different aged solder alloys based on the single stress amplitude test. Using the verified stress amplitude, we conduct the varying stress amplitude test for aged SAC305, SAC-Q, and SAC-R. It showed that aging process degraded SAC305 and SAC-Q solder alloy under varying stress amplitude cycling. And SAC-R shows better aging resistance compared with SAC305 and SAC-R under varying stress amplitude cycling. More important is, we observed similar “drop-down” of loading slope and “step-up” of inelastic work for aged SAC305, SAC-Q, and SAC-R under varying stress amplitude cycling. Besides, “brittle” and “ductile” failure modes of varying stress amplitude cycling were observed for aged SAC305, SAC-Q, and SAC-R. In the next chapter, we will discuss the fatigue modeling based on our observations.

Chapter 8 Fatigue Modeling of Aged SAC-Bi Solder Joint under Varying Stress Cycling

8.1 Introduction

SAC solder alloys have been widely used in electronic assembly, and its fatigue resistance under varying stress cycling is a critical factor that affects the reliability of electronics. The previous work has shown that the fatigue life of SAC-Bi solder joints is less than expected according to common damage accumulation model. It is essential to improve the fatigue life estimation of SAC-Bi solder joint under varying stress amplitude conditions. Additionally, inelastic work is observed to be amplified after every switch from harsh to mild cycles. Based on this phenomenon, a new damage accumulation model would be proposed to estimate fatigue life of SAC-Bi under varying stress amplitude conditions in this chapter.

8.2 Amplification of Inelastic Work

Figure 8-1 shows a typical example of inelastic work performance of one 0hour aged SAC305 individual solder joint in varying stress amplitude test. Red point represents the inelastic work of harsh (27.6MPa) cycles and blue point represents the inelastic work of mild (18MPa) cycles. Typically, the inelastic work of mild stress cycles is leveled up after every switch from harsh to mild cycles. For example, the inelastic work of cycle 160 is significantly higher than that of cycle 20, though the stress of cycle 160 and cycle 20 are same. Meanwhile, it can be seen that the average inelastic work of harsh stress cycles is increased after each switch, which is red cycled in the graph. It indicates that the inelastic work of both mild and harsh cycles is amplified after switch.

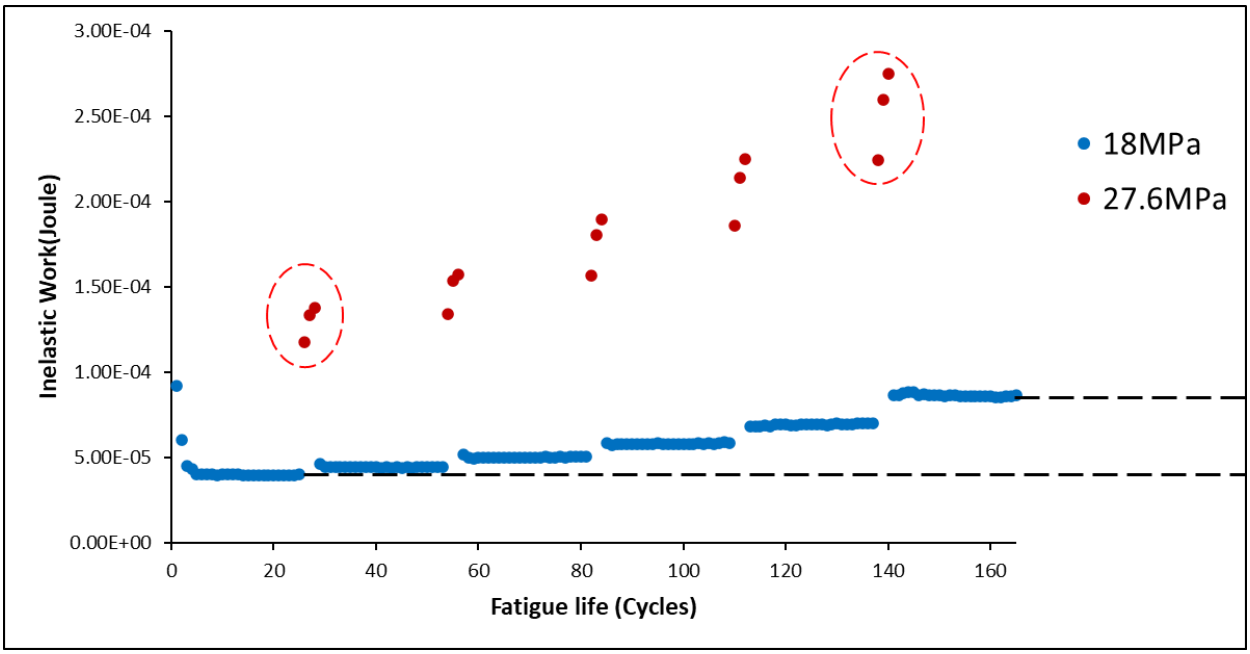

Figure 8-1 Inelastic Work of One 0hour Aged SAC305 Individual Soler Joint in Varying Stress Amplitude Test (18MPa-27.6MPa)

Figure 8-2 shows the average information of inelastic work of one 0hour aged SAC305 individual solder joint in varying stress amplitude test. To quantify the amplification phenomena, we collect the average inelastic work of harsh stress cycles (Red triangle) and mild stress cycles (Blue circle) in each switch. And we define the amplification factor as the ratio of each switch's inelastic work over the inelastic work before the first switch, which is shown in Figure 8-3. It can be seen that the amplification factor of both harsh and mild cycles can be well fitted with linear regression. Additionally, the slope of harsh stress cycles linear equation is less than that of mild stress cycles linear equation for same individual solder joint. It indicates that the inelastic work of mild stress cycles is increasing faster than that of harsh stress cycles in 0hour aged SAC305. It is observed for all the other cases.

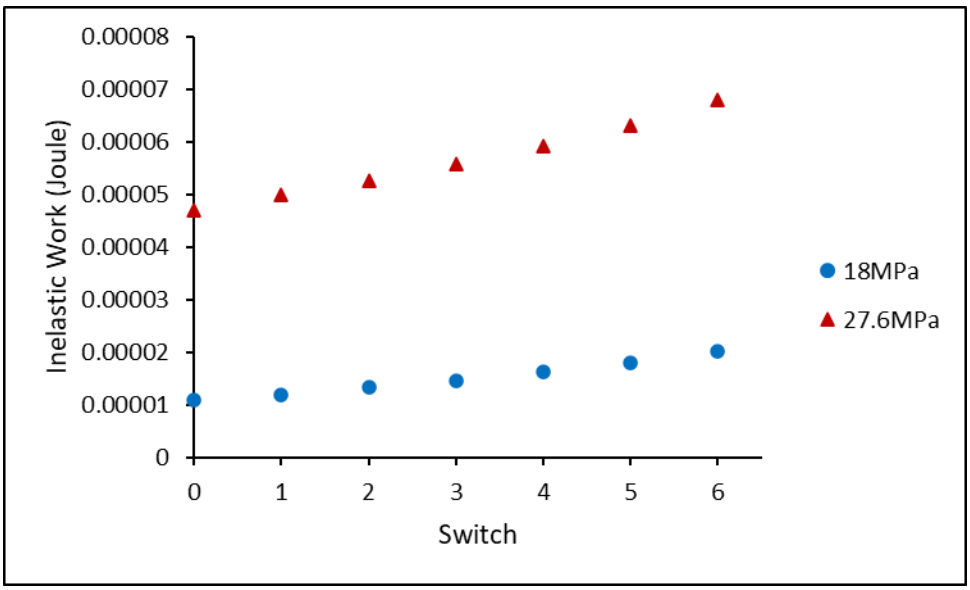

Figure 8-2 Average Inelastic Work of One 0hour Aged SAC305 Individual Soler Joint in Varying Stress Amplitude Test (18MPa-27.6MPa)

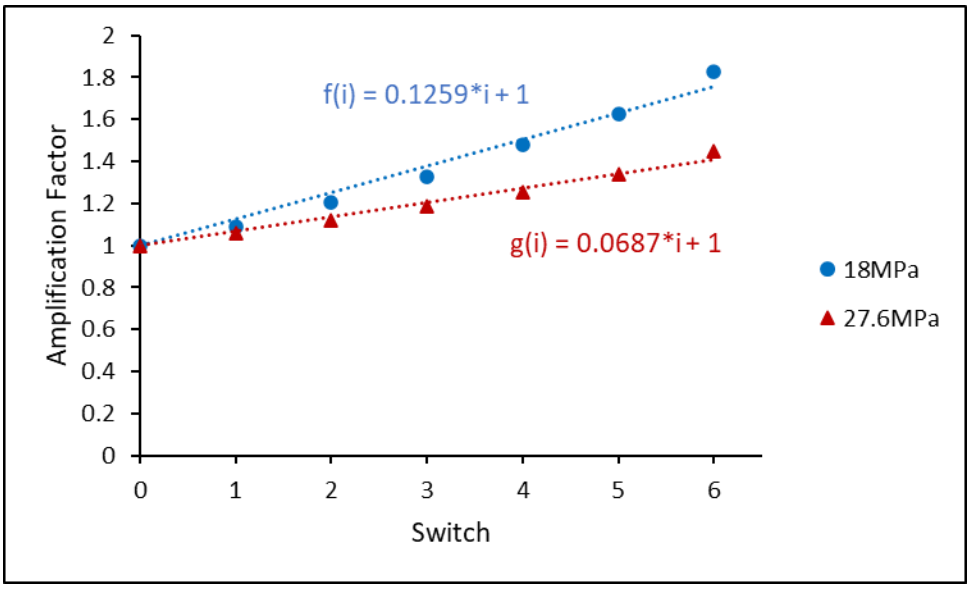

Figure 8-3 Amplification Factor of One 0hour Aged SAC305 Individual Soler Joint in Varying Stress Amplitude Test (18MPa-27.6MPa)

8.3 Analysis of Amplification Slope

Figure 8-4 shows the 95% confidence interval of mild amplification slope of 0hour aged, 10hour aged, and 1000hour aged SAC305 individual solder joint. Though there is no significant difference among 0hour, 10hour, and 1000hour aging condition, it can be seen that the average slope is decreasing as the aging time increases. So as the harsh amplification slope, which is shown in Figure 8-5. Basically, it indicates that the inelastic work of SAC305 is less amplified after aging.

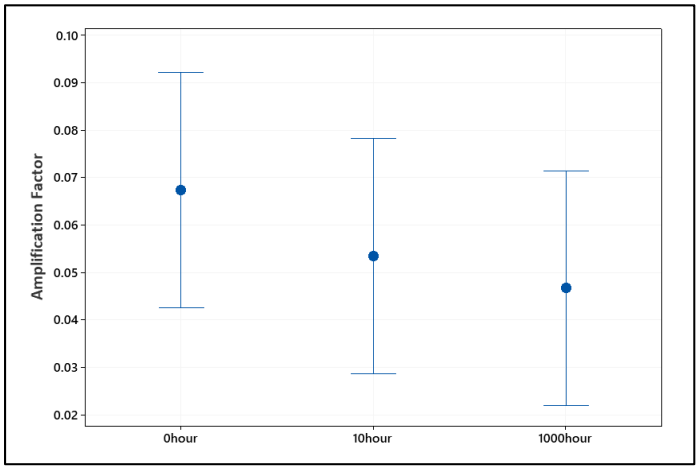

Figure 8-4 Confidence Interval of Mild Amplification Slope of 0hour Aged, 10hour Aged, and 1000hour Aged SAC305 Individual Solder Joint

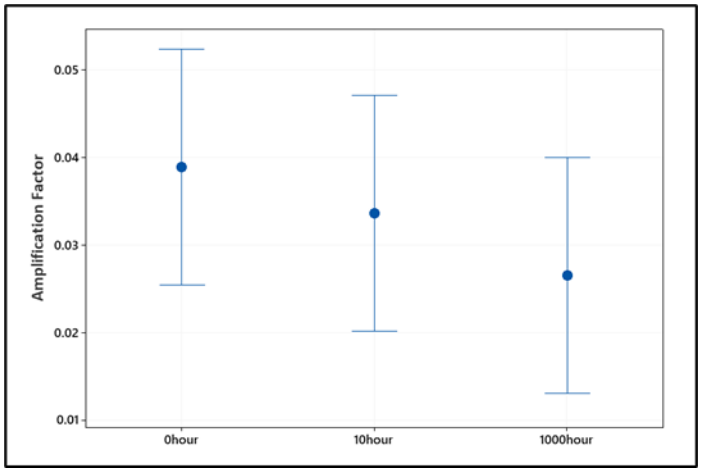

Figure 8-5 Confidence Interval of Harsh Amplification Slope of 0hour Aged, 10hour Aged, and 1000hour Aged SAC305 Individual Solder Joint

Figure 8-6 and Figure 8-7 show the power fit equations of average mild and harsh amplification slope versus aging time for SAC305, SAC-R, and SAC-Q. Generally, the mild amplification slope of SAC305 and SAC-R are much higher than SAC-Q. It means the inelastic work is amplified faster after each switch in the case of SAC305 and SAC-R.

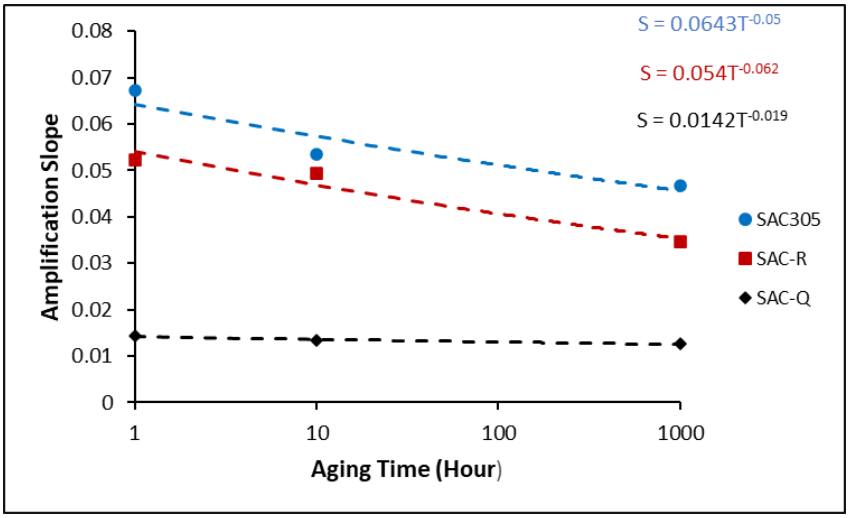

Figure 8-6 Power Fit Equation of Average Mild Amplification Slope versus Aging Time for SAC305, SAC-R, and SAC-Q

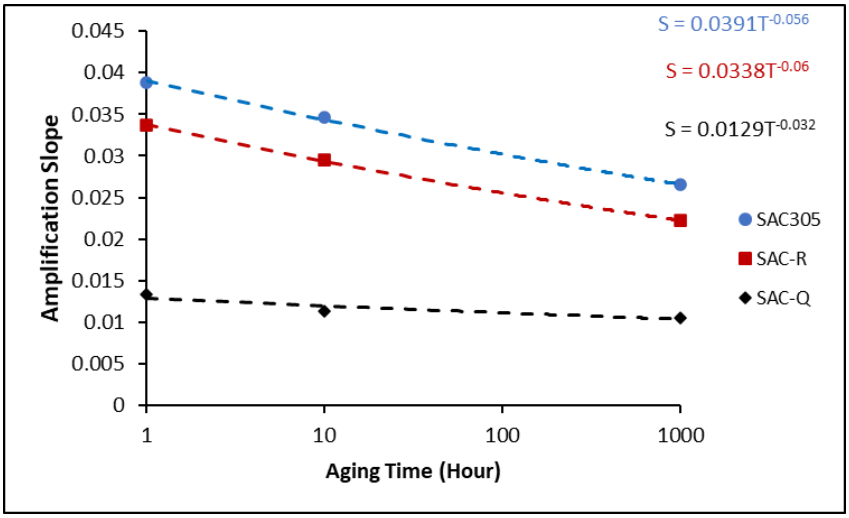

Figure 8-7 Power Fit Equation of Average Harsh Amplification Slope versus Aging Time for SAC305, SAC-R, and SAC-Q

Figure 8-8 shows the estimated CDI of each totally failed 0hour aged SAC305 individual solder joint in varying stress amplitude test. The blue circle represents the estimation using common cumulative damage model. It can be seen that all the estimated CDI is far from 1 and the average is only about 55%, while all the samples are totally failed, and CDI should be approaching to 1. The black triangle represents the estimation considering the amplification of mild cycle's inelastic work. The estimated accumulated damage is improved to 0.75. When we take both mild and harsh amplification effect into consideration, the average estimated CDI is 0.88 approaching to 1. However, there exists some gap to reach 1, which indicates that we can make more progress.

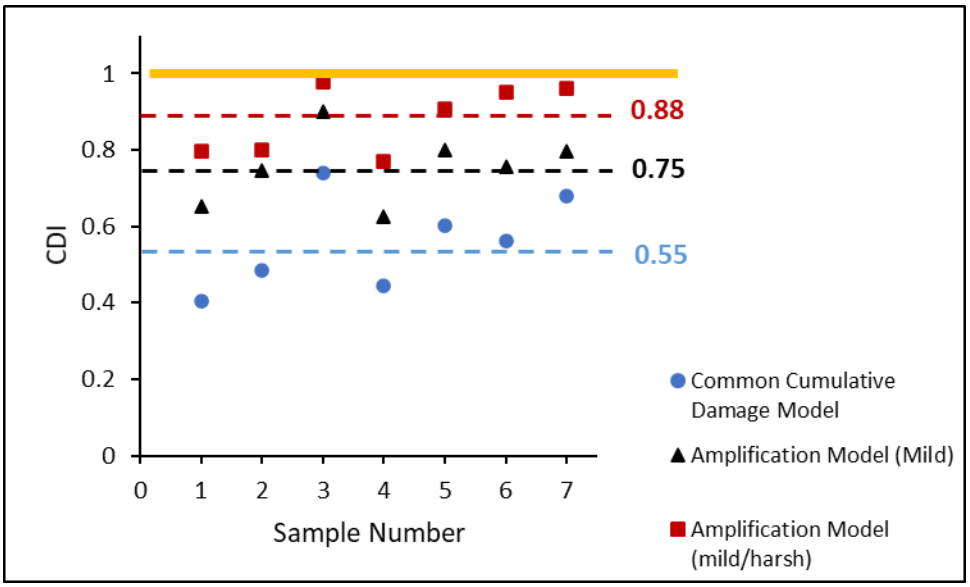

Figure 8-8 CDI of Each Totally Failed 0hour Aged SAC305 Individual Solder Joint in Varying Stress Amplitude Test

8.4 Piecewise Function of Amplification Factor

Figure 8-9 and Figure 8-10 show the mild and harsh amplification factor of one 0hour aged SAC305 individual solder joint under varying stress amplitude condition. As it is shown, the inelastic work is linearly amplified after each switch in the early stage of fatigue test. However,

the inelastic work will dramatically increase after some point until total failure. Therefore, we will use a piecewise function to describe the inelastic work performance of individual solder joint until total failure under varying stress amplitude condition. In Figure 8-9 and Figure 8-10, linear regression equations (Black circle) are applied to estimate the damage accumulated before the 9th switch, while exponential equations (Red triangle) are used for after that until total failure.

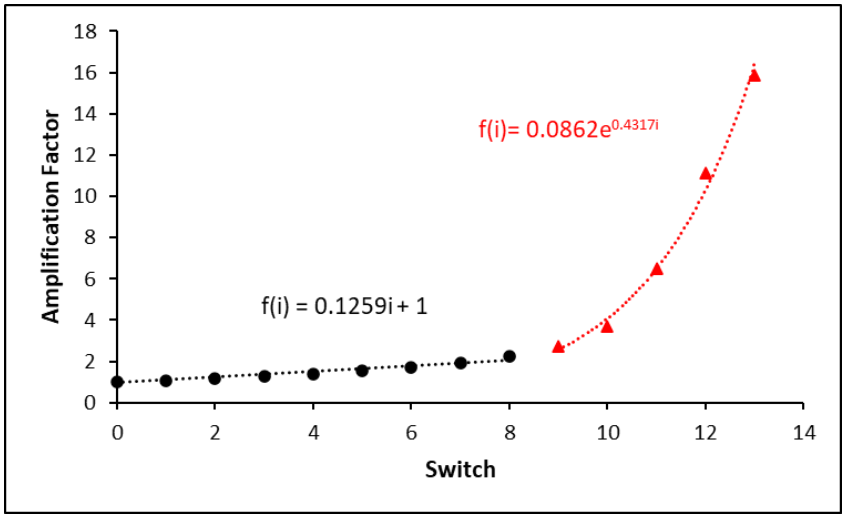

Figure 8-9 Mild Amplification Factor of One 0hour Aged SAC305 Individual Solder Joint in Varying Stress Amplitude Test

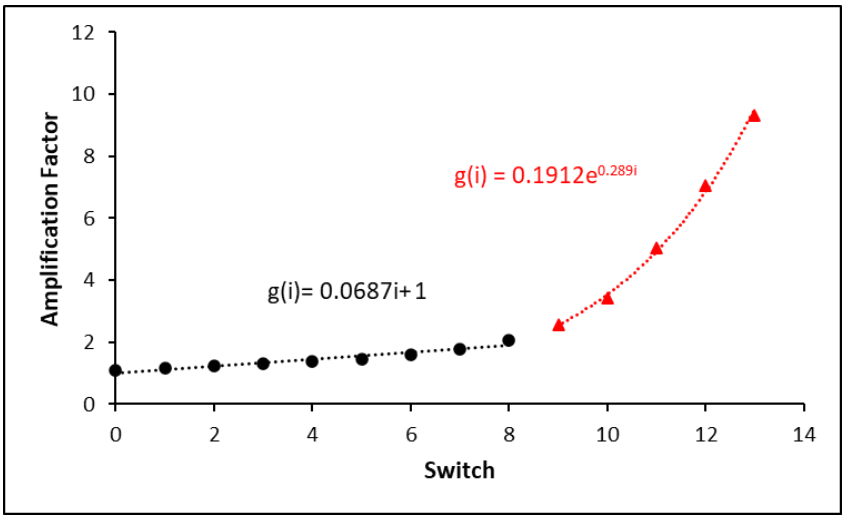

Figure 8-10 Harsh Amplification Factor of One 0hour Aged SAC305 Individual Solder Joint in Varying Stress Amplitude Test

Figure 8-11 shows a typical example of mild amplification factor of 0hour aged SAC-R individual solder joint under varying stress amplitude condition. Similar piecewise functions are fitted. In the previous proposed CDI calculation model, the damage accumulation is estimated using linear function for the whole life of individual solder joint under varying stress amplitude condition. However, the damage is amplified faster than expect in the last several switch and it is less estimated by the linear function from switch 8 to switch 14.

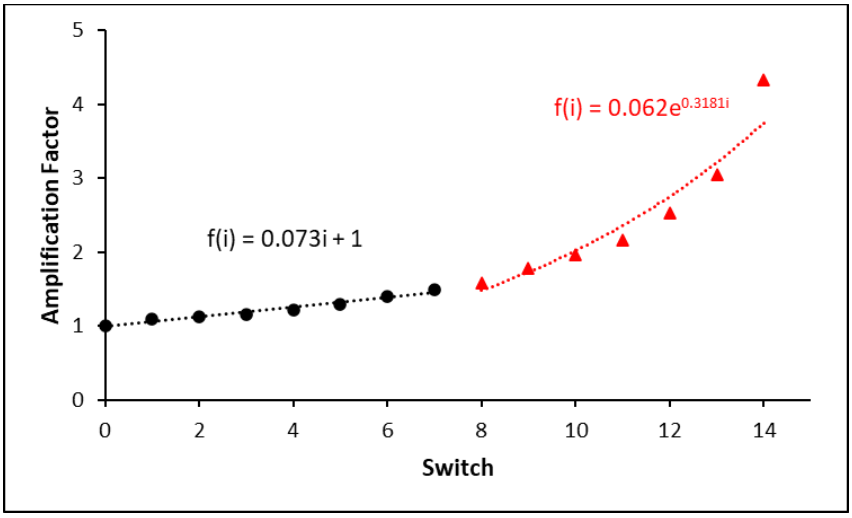

Figure 8-11 Mild Amplification Factor of One 0hour Aged SAC-R Individual Solder Joint in Varying Stress Amplitude Test

Figure 8-12 shows a typical example of harsh amplification factor of 0hour aged SAC-Q individual solder joint under varying stress amplitude condition. The amplification factor can be well fitted with similar piecewise function. However, the percentage of linear part is much higher than that in the case of SAC305 and SAC-R. And now the key is to define the cut-off point for different individual solder joints. Figure 8-13 shows a cut-off summary for 0hour aged, 10hours aged, and 1000hours aged SAC-Q individual solder joint. Basically, the cut-off here indicates the percent of linear amplification part. In the graph, it can be seen that the average cut-off points (Red) are

around 83%, which indicates that the inelastic work will linearly amplify around 83% of an individual solder joint's total life under varying stress amplitude condition. Then in the last 17% of its total life, the amplification factor will be exponentially increasing. With 5% significant level, there is no significant evidence that aging time will influence the cut-off points in the case of SAC-Q individual solder joint.

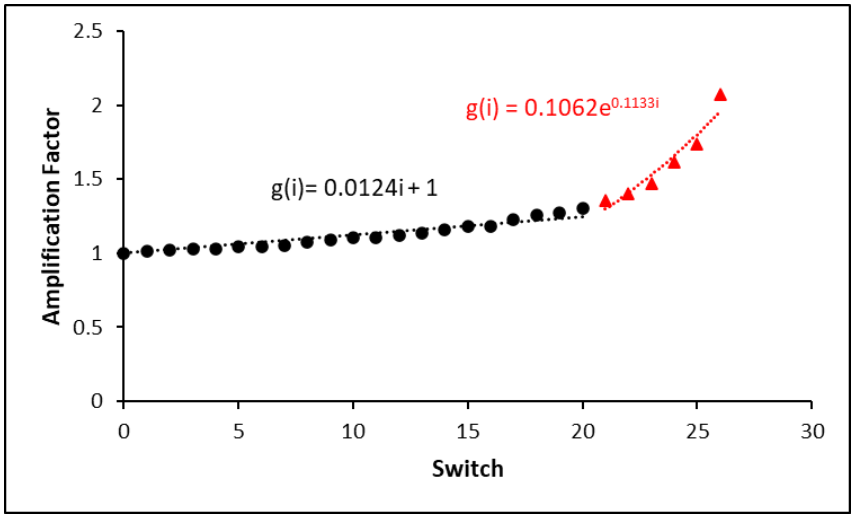

Figure 8-12 Harsh Amplification Factor of One 0hour Aged SAC-Q Individual Solder Joint in Varying Stress Amplitude Test

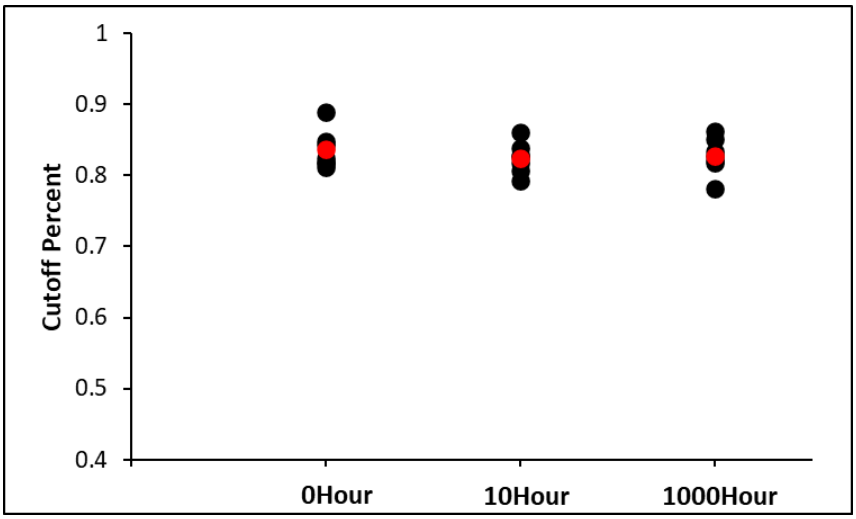

Figure 8-13 Cut-Off Summary for 0hour Aged, 10hours Aged, and 1000hours Aged SAC-Q Individual Solder Joint

Figure 8-14 and Figure 8-15 show the cut-off summary for 0hour aged, 10hours aged, and 1000hours aged SAC305 and SAC-R individual solder joint. Basically, the average linear cut-off percent of SAC305 and SAC-R are both less than that of SAC-Q. Similarly, there is no evidence to prove that the aging time will influence the cut-off points with 5% significant level.

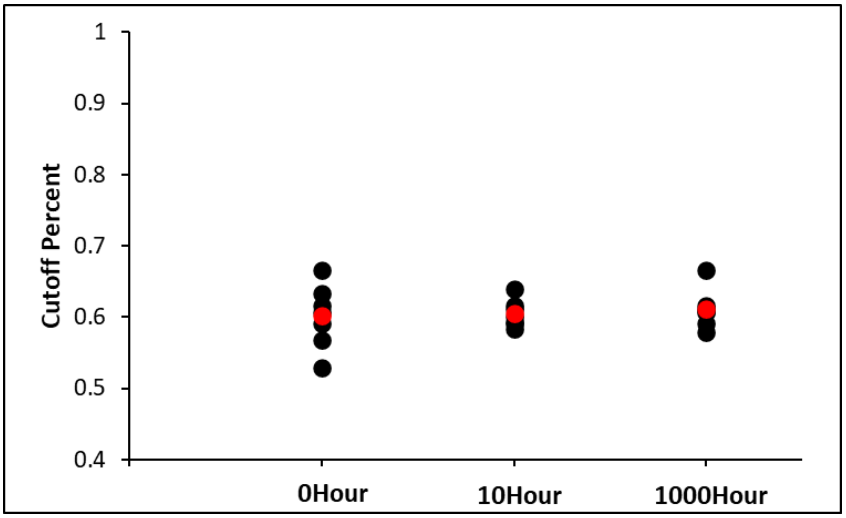

Figure 8-14 Cut-Off Summary for 0hour Aged, 10hours Aged, and 1000hours Aged SAC305 Individual Solder Joint

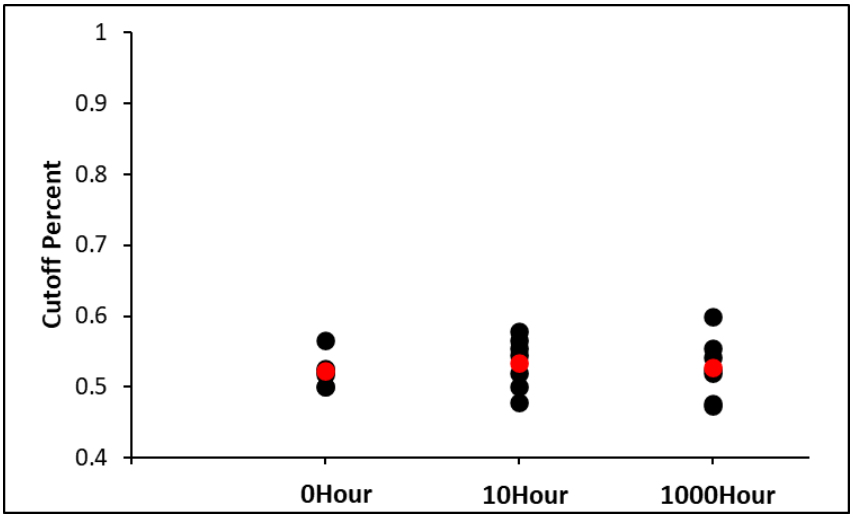

Figure 8-15 Cut-Off Summary for 0hour Aged, 10hours Aged, and 1000hours Aged SAC-R Individual Solder Joint

8.5 Final Proposed Model

According to all the analysis above, we propose our final damage accumulative model as following:

$$CDI = \sum_{i} f(i)\frac{n_m}{N_m} + g(i)\frac{n_h}{N_h} \tag{8.1}$$

where n_m is the number of cycles under mild stress amplitude, N_m is the number of cycles when failure happens under mild stress amplitude, n_h is the number of cycles under harsh stress amplitude, N_h is the number of cycles when failure happens under harsh stress amplitude, $f(i)$ and $g(i)$ are the amplification functions, which represent the effect of switch on the inelastic work amplification for mild stress cycles and harsh stress cycles. Additionally, the amplification function is defined by a piecewise function that consists of linear function and exponential function.

Figure 8-16 shows comparisons of damage accumulative models in the case of 0hour aged SAC305 individual solder joint in varying stress amplitude test. The blue circles represent the estimated CDI of each 0hour aged SAC305 individual solder joint using the common cumulative damage model. The black triangles represent the estimated CDI considering the amplification function (linear function) of mild stress cycles. The red squares represent the estimated CDI considering the amplification function (linear function) of mild and harsh stress cycles. The yellow diamonds represent the estimated CDI considering the amplification function (Piecewise function) of mild and harsh stress cycles. It can be seen that the average CDI of proposed model is very close to 1 compared to the other models.

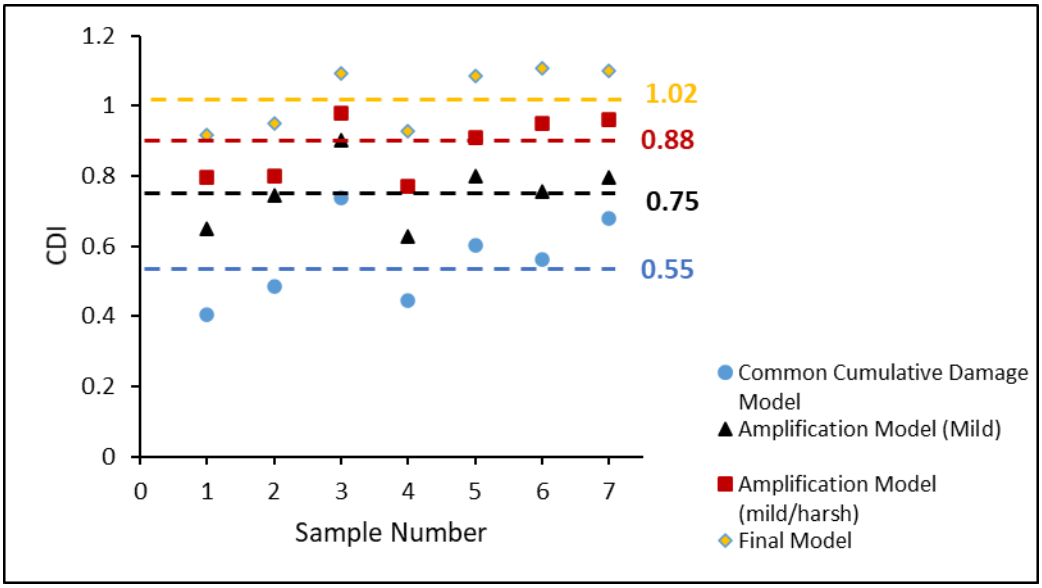

Figure 8-16 CDI Comparison of 0hour Aged SAC305 Individual Solder Joint in Varying Stress Amplitude Test

8.6 Conclusion

A new damage accumulation model is proposed to estimate CDI of SAC-Bi individual solder joint in varying stress amplitude test. The amplification of inelastic work after each switch between mild and harsh stress cycles, is observed for all the solder joints and aging time condition. The work focuses on the study of amplification function for different solder alloys under aging conditions. It can be seen that the inelastic work is linearly amplified in the early stage, but it will be exponentially amplified after some cut-off point. The slope of linear amplification function is compared for different solder alloy and aging condition. And the results indicate that SAC305 and SAC-R individual solder joints intend to enter the exponential region earlier than SAC-Q. The new proposed model (Piecewise function) is compared with the other models and it is proved to better estimate the CDI of aged SAC-Bi individual solder joint under varying stress amplitude condition.

Chapter 9 Conclusions and Future Work

9.1 Results and Conclusions

Prediction of SAC-Bi individual solder joint's service life under varying stress amplitude cycling can be misleading according to common damage accumulation model. This dissertation focuses on the study of fatigue performance of SAC-Bi individual solder joint under single and varying stress amplitude cycling. Under single stress amplitude condition, at least 7 individual solder joints (SAC305, SAC-Q, SAC-I, and SAC-R) were cycled until total failure. Additionally, SAC305, SAC-Q and SAC-R were aged for 10hours and 1000hours under 125℃ for varying stress amplitude cycling test. At least 7 individual solder joints (Aged and non-Aged SAC305, SAC-Q, and SAC-R) were cycled under varying stress amplitude condition until total failure. Their fatigue performances were compared through the characteristic life, hysteresis loop, inelastic work, plastic strain, etc. Optical microscope, SEM, and EDS were used to identify the participate, failure mode, and IMC layers. A new damage accumulate model was proposed to predict the service life of SAC-Bi individual solder joint under varying stress amplitude cycling. The conclusions of this dissertation can be summarized as following:

1) Two-parameter Weibull distribution was used to fit with the fatigue life of SAC305, SAC-Q, SAC-I, and SAC-R under single stress amplitude cycling. Characteristic fatigue life of SAC305, SAC-Q, SAC-I, and SAC-R is fitted with stress levels using power function. SAC-I and SAC-Q show better fatigue resistance than SAC305 and SAC-R. It is believed that Bi is the main reason to enhance the fatigue resistance of SAC individual soler joint.

2) The inelastic work intends to be higher and the hysteresis loops will be larger when stress level is higher under single stress amplitude cycling. Additionally, SAC-I and SAC-Q intend to have less inelastic work and hysteresis loop than that of SAC305 and SAC-R. Based on the fitted Morrow Energy model, it can be seen that the fatigue ductility of SAC305 is significantly different from the other solder alloys, because of the exist of Bi in SAC-Q, SAC-I, and SAC-R.
3) Plastic strain shows consistent behavior comparing with inelastic work in the case of SAC-Bi individual solder joint. It basically evolves into 3 stages until total failure occurs. SAC-Q and SAC-I show less plastic strain compared with SAC305 and SAC-R in the stage 2. Coffin-Manson fatigue model for all solder alloys is fitted. SAC-Q and SAC-I have similar fatigue ductility in Coffin-Manson fatigue model.
4) Comparing SAC-Q to SAC-I, the addition of Ni and Sb in SAC-I did not affect mechanical fatigue performance. Thus, the bismuth can be considered as the main reason for the superior fatigue performance of the SAC-Q and SAC-I, when compared with SAC305 and SAC-R. The main mechanism is that the added bismuth goes into the crystalline lattice and prevents the plastic deformation by more difficult dislocations.
5) The characteristic life of 10hours and 1000hours aged individual solder joint less than that of non-aged individual solder joint under the same stress level. The characteristic life of 10hour aged SAC305 are only about 50%-60% of that of 0hour aged SAC305. And it only has 30%-40% after 1000 hours aging. It indicates that aging time has significant effect on the fatigue resistance of SAC305. But The characteristic life (cycles) of aged SAC-Q and SAC-R do not degrade that much (only about 10% drop). Since there is Bi in SAC-Q and SAC-R and no Bi

in SAC305, we believe that Bi is the main reason to improve the fatigue resistance of SAC-Q and SAC-R after aging under single stress amplitude test.

6) SAC305, SAC-Q, and SAC-R failed earlier than expected by common cumulative damage model in varying stress amplitude test. After 10hour and 1000hour aging, the characteristic life of SAC305, SAC-Q, and SAC-R is decreasing. In addition, SAC-Q shows better fatigue resistance than SAC305 and SAC-R in varying stress amplitude test. Ductile failure mode was commonly seen in both single and varying stress test of SAC305 and SAC-R. Brittle failure mode was commonly seen in both single and varying stress test SAC-Q. And aging time will not change the failure mode of individual solder joint in both single and varying stress amplitude test.
7) In single stress amplitude test, the loading slope of SAC-Q is higher than that of SAC305 and SAC-R, which indicates that SAC-Q has higher stiffness. A “step-down” phenomena of loading slope after switching between mild and harsh stress cycles was observed in varying stress amplitude test.
8) A “raise-up” phenomena of inelastic work after switching between mild and harsh stress cycles was observed in varying stress amplitude test. The inelastic work of same stress cycles is amplified by switching. Therefore, the amplification factor is proposed in the cumulative damage model. The amplification slope of harsh stress cycles was generally less than that of mild stress cycles. And a decreasing trend of amplification slope can be seen when the individual solder joint is aged for longer time.
9) The amplification factor is linearly increasing in the early stage of cycling, and it will dramatically increase after some point. Therefore, a piecewise function was proposed to quantify the amplification of inelastic work. The cut-off percentage for SAC305, SAC-Q, and

SAC-R were analyzed. Basically, the amplification factor of SAC305 and SAC-R is linearly increase until 50%-60% of their fatigue life. After that, it starts to exponential increase until total failure. But the cut-off percent of SAC-Q can be 80%-90% of its fatigue life. Additionally, the aging time does not influence the cut-off percent much with 5% significant level.

10) A new damage accumulative model was proposed to estimate the CDI of SAC-Bi individual solder joint in varying stress amplitude test. It was compared with the other cumulative damage model, and it is proved that it can gain the best estimation of CDI among the candidate models.

9.2 Future Work

The mechanical and fatigue performance vary a lot for each SAC individual solder joint because of precipitate distributions and grain orientations. It is very hard to assess its reliability under realistic service condition and it is essential to evaluate its reliability from various aspects. Therefore, the following topic is suggested for future work:

1) Study the effect of Bi's percentage on SAC individual solder joint's fatigue.
2) Study the fatigue of SAC-Bi individual solder joint under complex (three) stress amplitudes switching condition, since current research is focusing on the fatigue under two stress amplitudes switching condition.
3) Develop a global fatigue model for complex stress amplitudes switching conditions.
4) Study the effect of varying amplitude cycling on creep properties of SAC-Bi individual solder joints.
5) Study the fatigue of SAC-Bi individual solder joint in an elevated working temperature.

6) Study the fatigue of SAC-Bi individual solder joint combined with vibration test and thermocycling test.

References

[1] H. C., Electronic packaging and interconnection handbook, McGraw-Hill, Inc., 2004.

[2] P. L. J. C. S. James W. Dally, Mechanical Design of Electronic System, College House Enterprises, 2008.

[3] IPC-A-610, "Acceptability of Electronic Assemblies," *IPC Standard,* 2005.

[4] R. Prasad, Surface mount technology: principles and practice, Springer Science & Business Media, 2013.

[5] J.-W. a. S.-B. J. Kim, "Experimental and finite element analysis of the shear speed effects on the Sn–Ag and Sn–Ag–Cu BGA solder joints," *Materials Science and Engineering,* pp. 371(1-2): 267-276, 2004.

[6] B. K. Judd M, Soldering in electronics assembly, Elsevier, 1999.

[7] S. J. C. Ma H, "A review of mechanical properties of lead-free solders for electronic packaging," *Journal of materials science,* pp. 44(5): 1141-1158, 2009.

[8] K. B. Shangtong G, "Modern Electronic Packaging Technology," *Semiconductor Information,* p. 35(2): 9, 1998.

[9] L. W. B. Sa'd Hamasha, "Statistical Variations of Solder Joint Fatigue Life Under Realistic Service Conditions," *IEEE Transactions on Components, Packaging and Manufacturing Technology,* pp. 5(9): 1284-1291, 2015.

[10] H. P. D. M. S. H. Kotadia H R, "A review: On the development of low melting temperature Pb-free solders," *Microelectronics Reliability,* pp. 54(6-7): 1253-1273, 2014.

[11] C. Y. C. Li Y, "Effect of silver (Ag) nanoparticle size on the microstructure and mechanical properties of Sn58Bi–Ag composite solders," *Journal of Alloys and compounds,* pp. 645: 566-576, 2015.

[12] T. K. N. Zhang L, "Structure and properties of lead-free solders bearing micro and nano particles," *Materials Science and Engineering: R: Reports,* pp. 82: 1-32, 2014.

[13] X. S. B. Z. G. e. a. Zhang L, "Interface reaction between SnAgCu/SnAgCuCe solders and Cu substrate subjected to thermal cycling and isothermal aging," *Journal of Alloys and Compounds,* pp. 510(1): 38-45, 2012.

[14] F. X. H. C. e. a. Zhang L, "Intermetallic compound layer growth between SnAgCu solder and Cu substrate in electronic packaging," *Journal of Materials Science: Materials in Electronics,* pp. 24(9): 3249-3254, 2013.

[15] E. S. N. A. V. L. He M, "Microstructure and creep deformation of Sn-Ag-Cu-Bi/Cu solder joints," *Journal of Electronic Materials,* pp. 37(3): 300-306, 2008.

[16] R. J. A. Vianco P T, "Properties of ternary Sn-Ag-Bi solder alloys: Part I—Thermal properties and microstructural analysis," *Journal of electronic materials,* pp. 28(10): 1127-1137., 1999.

[17] V. S. G. G. e. a. Loomans M E, "Investigation of multi-component lead-free solders," *Journal of Electronic Materials,* pp. 23(8): 741-746, 1994.

[18] L. Z. L. J. e. a. Andersson C, " Comparison of isothermal mechanical fatigue properties of lead-free solder joints and bulk solders," *Materials Science and Engineering,* pp. 394(1-2): 20-27, 2005.

[19] Y. J. Q. O. B. Sa'd Hamasha, "Assessment of Solder Joint Fatigue Life Under Realistic Service Conditions," *Journal of Electronic Materials,* pp. 43(12): 4472-4484., 2014.

[20] K. K. Mookam N, "Evolution of intermetallic compounds between Sn-0.3 Ag-0.7 Cu low-silver lead-free solder and Cu substrate during thermal aging," *Journal of Materials Science & Technology,* pp. 28(1): 53-59, 2012.

[21] B. P., "Effects of strain rate and amplitude variations on solder joint fatigue life in isothermal cycling," *Journal of Electronic Packaging,* p. 138(2): 021002, 2016.

[22] A. F. D. A. e. a. Su S, "Solder joint reliability in isothermal varying load cycling," in *2017 16th IEEE Intersociety Conference on Thermal and Thermomechanical Phenomena in Electronic Systems (ITherm)*, 2017.

[23] H. H. Z. Z. S. P. e. a. Lv Z, "A modified nonlinear fatigue damage accumulation model," *International Journal of Damage Mechanics,* pp. 24(2): 168-181, 2015.

[24] M. M. A., "Cumulative fatigue damage," *Journal of applied mechanics,* pp. 12(3): A159-A164, 1945.

[25] A. Q. Y. J. P. B. Sa'd Hamasha, "Correlation Between Solder Joint Fatigue Life and Accumulated Work in Isothermal Cycling," *IEEE Transactions on Components, Packaging and Manufacturing Technology,* pp. 5(9): 1292-1299, 2015.

[26] C. J. O. J. E. e. a. Jaradat Y, "Effects of variable amplitude loading on lead-free solder joint propoerties and damage accumulation," in *13th InterSociety Conference on Thermal and Thermomechanical Phenomena in Electronic Systems*, 2012.

[27] F. A. S. R. R. e. a. Stephens R I, Metal fatigue in engineering, John Wiley & Sons, 2000.

[28] K. P. C. W. M. A. Klutke G A, "A critical look at the bathtub curve," *IEEE Transactions on reliability,* pp. 52(1): 125-129, 2003.

[29] X. Y. S. K. Maalekian M, Effect of Bi content on properties of low silver SAC solders, AIM Metals & Alloys, Montreal., 2016.

[30] P. R. A. B. e. a. Coyle R, "The effect of nickel microalloying on thermal fatigue reliability and microstructure of SAC105 and SAC205 solders," in *2014 IEEE 64th Electronic Components and Technology Conference (ECTC)*, 2014.

[31] L. B. G. V. R. e. a. Pandher R S, "Drop shock reliability of lead-free alloys-effect of micro-additives," in *2007 Proceedings 57th Electronic Components and Technology Conference*, 2007.

[32] L. Z. H. L. J. e. a. Ye L, "Microstructure investigation of Sn-0.5 Cu-3.5 Ag and Sn-3.5 Ag-0.5 Cu-0.5 B lead-free solders," *Soldering & Surface Mount Technology,* pp. 13(3): 16-20, 2001.

[33] S. M. F. M. B. I. A. Shnawah D A, "The Limited Reliability of Board-Level SAC Solder Joints under both Mechanical and Thermo-mechanical Loads," *INFORMACIJE MIDEM-JOURNAL OF MICROELECTRONICS ELECTRONIC COMPONENTS AND MATERIALS*, pp. 42(1): 3-10, 2012.

[34] F. B. M. S. M. A. B. I. e. a. Abdul Ameer Shnawah D, "A review on effect of minor alloying elements on thermal cycling and drop impact reliability of low-Ag Sn-Ag-Cu solder joints," *Microelectronics International,* pp. 29(1): 47-57, 2012.

[35] S. M. F. M. S. D. A. e. a. Mahdavifard M H, "The effect of iron and bismuth addition on the microstructural, mechanical, and thermal properties of Sn–1Ag–0.5 Cu solder alloy," *Microelectronics Reliability,* pp. 55(9-10): 1886-1890, 2015.

[36] F. M. S. M. A. B. I. e. a. Abdul-Ameer Shnawah D, "The bulk alloy microstructure and tensile properties of Sn-1Ag-0.5 Cu-x Al lead-free solder alloys (x= 0, 1, 1.5 and 2 wt.%)," *Microelectronics International,* pp. 29(2): 108-116, 2012.

[37] F. T. C. Y. C. e. a. Gain A K, "The influence of addition of Al nano-particles on the microstructure and shear strength of eutectic Sn–Ag–Cu solder on Au/Ni metallized Cu pads," *Journal of Alloys and Compounds,* pp. 506(1): 216-223, 2010.

[38] Z. Q. S. W. Z. G. e. a. Song H Y, "Effects of Zn addition on microstructure and tensile properties of Sn–1Ag–0.5 Cu alloy," *Materials Science and Engineering: A,* pp. 527(6): 1343-1350, 2010.

[39] P. M. L. E. e. a. Hodúlová E, "Kinetics of intermetallic phase formation at the interface of Sn–Ag–Cu–X (X= Bi, In) solders with Cu substrate," *Journal of Alloys and Compounds,* pp. 509(25): 7052-7059, 2011.

[40] S. M. F. M. B. I. A. e. a. Shnawah D A, "Effect of Ag content and the minor alloying element Fe on the mechanical properties and microstructural stability of Sn-Ag-Cu solder alloy under high-temperature annealing," *Journal of electronic materials,* pp. 42(3): 470-484, 2013.

[41] K. R. Kanlayasiri K, "Property alterations of Sn-0.6 Cu-0.05 Ni-Ge lead-free solder by Ag, Bi, In and Sb addition," *Transactions of Nonferrous Metals Society of China,* pp. 28(6): 1166-1175, 2018.

[42] C. B. L. S. X. Q. e. a. Li G Y, "Effects of Sb addition on tensile strength of Sn–3.5 Ag–0.7 Cu solder alloy and joint," *Thin Solid Films,* pp. 504(1-2): 421-425, 2006.

[43] H. A. E. A.-G. G. S. e. a. El-Daly A A, "Influence of Zn addition on the microstructure, melt properties and creep behavior of low Ag-content Sn–Ag–Cu lead-free solders," *Materials Science and Engineering: A,* pp. 608: 130-138, 2014.

[44] Q. L. W. X. e. a. Zhao J, "Influence of Bi on microstructures evolution and mechanical properties in Sn–Ag–Cu lead-free solder," *Journal of Alloys and Compounds,* pp. 375(1-2): 196-201, 2004.

[45] X. S. Z. L. e. a. Gao L, "Effect of alloying elements on properties and microstructures of SnAgCu solders," *Microelectronic Engineering,* pp. 87(11): 2025-2034, 2010.

[46] M. Y. M. Y. e. a. Zhao J, "Fatigue crack-growth behavior of Sn-Ag-Cu and Sn-Ag-Cu-Bi lead-free solders," *Journal of Electronic Materials,* pp. 31(8): 879-886, 2002.

[47] O. M. Kariya Y, "Effect of bismuth on the isothermal fatigue properties of Sn-3.5 mass% Ag solder alloy," *Journal of Electronic Materials,* pp. 27(7): 866-870, 1998.

[48] M. Y. M. Y. Kanchanomai C, "Low-cycle fatigue behavior of Sn-Ag, Sn-Ag-Cu, and Sn-Ag-Cu-Bi lead-free solders," *Journal of Electronic Materials,* pp. 31(5): 456-465, 2002.

[49] H. L. D. O. Torres A, "Effect of Antimony Additions on Corrosion and Mechanical Properties of Sn-Bi Eutectic Lead-Free Solder Alloy," *Materials Sciences and Applications,* vol. 3, no. 6, p. 355, 2012.

[50] C. C. Q. L. e. a. Zhao J, "Kinetics of intermetallic compound layers and shear strength in Bi-bearing SnAgCu/Cu soldering couples," *Journal of Alloys and Compounds,* pp. 473(1-2): 382-388, 2009.

[51] E.-T. A. M. G. S. El-Daly A A, "Development of new multicomponent Sn–Ag–Cu–Bi lead-free solders for low-cost commercial electronic assembly," *Journal of Alloys and Compounds,* pp. 627: 268-275, 2015.

[52] C. J. L. F., "A study of the effects of cyclic thermal stresses on a ductile metal," *Transactions of the American Society of Mechanical Engineers,* vol. 76, pp. 931-950, 1954.

[53] P. H. L. J. Z. W. e. a. Shi X Q, "Low cycle fatigue analysis of temperature and frequency effects in eutectic solder alloy," *International Journal of fatigue,* pp. 22(3): 217-228, 2000.

[54] L. N. C. P. A. e. a. Liu W, "Achieving high reliability low cost lead-free SAC solder joints via Mn or Ce doping," in *2009 59th Electronic Components and Technology Conference*, 2009.

[55] C. Y. C. B. C. e. a. Rizvi M J, "Effect of adding 1 wt% Bi into the Sn–2.8 Ag–0.5 Cu solder alloy on the intermetallic formations with Cu-substrate during soldering and isothermal aging," *Journal of Alloys and Compounds,* pp. 407(1-2): 208-214, 2006.

[56] M. J. D, Cyclic plastic strain energy and fatigue of metals, Internal friction, damping, and cyclic plasticity ASTM International, 1965.

[57] T. E. D. Solomon H D, "Energy approach to the fatigue of 60/40 solder: Part I—Influence of temperature and cycle frequency," *Journal of Electronic Packaging,* pp. 117(2): 130-135, 1995.

[58] H. H. Z. L. Y. e. a. Zhu S P, "A practical method for determining the Corten-Dolan exponent and its application to fatigue life prediction," *Int. J. Turbo Jet-Engines,* pp. 29(2): 79-87, 2012.

[59] H. S. W. L. e. a. Borgesen P, "Interpreting accelerated test results for lead free solder joints," in *2016 Pan Pacific Microelectronics Symposium (Pan Pacific),* 2016.

[60] H. S. O. M. e. a. Borgesen P, "Solder joint reliability under realistic service conditions," *Microelectronics Reliability,* pp. 53(9-11): 1587-1591, 2013.

[61] H. S. J. Y. e. a. Obaidat M, "Effects of varying amplitudes on the fatigue life of lead free solder joints," in *2013 IEEE 63rd Electronic Components and Technology Conference.*, 2013.

[62] S. S. A. H. e. a. Akkara F, "Effect of Cycling Amplitude Variations on SnAgCu Solder Joint Fatigue Life," *IEEE Transactions on Components, Packaging and Manufacturing Technology,* pp. (99): 1-9, 2018.

[63] H. Grover, "An Observation Concerning the Cycle Ratio in Cumulative Damage," *ASTM International,* p. 124, 1960.

[64] H. S. N. D. Y. X. B. Z. Z. Tong YanTee, "Board level solder joint reliability modeling and testing of TFBGA packages for telecommunication applications," *Microelectronics Reliability,* vol. 43, no. 7, pp. 1117-1123, July 2003.